8-2020

Influence of Living Plant Roots and Mycorrhizal Hyphae on Soil Hydraulic Properties

Katelyn M. Marcacci
University of Tennessee, Knoxville, kmarcacc@vols.utk.edu

To the Graduate Council:

I am submitting herewith a thesis written by Katelyn M. Marcacci entitled "Influence of Living Plant Roots and Mycorrhizal Hyphae on Soil Hydraulic Properties." I have examined the final electronic copy of this thesis for form and content and recommend that it be accepted in partial fulfillment of the requirements for the degree of Master of Science, with a major in Geology.

Edmund Perfect, Major Professor

We have read this thesis and recommend its acceptance:

Jeff Warren, Larry McKay

Accepted for the Council:
Dixie L. Thompson

Vice Provost and Dean of the Graduate School

(Original signatures are on file with official student records.)

Influence of Living Plant Roots and Mycorrhizal Hyphae on Soil Hydraulic Properties

A Thesis Presented for the
Master of Science
Degree
The University of Tennessee, Knoxville

Katelyn Marie Marcacci
August 2020

Acknowledgments

I would first like to thank the Department of Earth and Planetary Sciences, Oak Ridge National Laboratory (ORNL), and the METER Group (Grant A. Harris Fellowship) for funding this research opportunity. I would like to express my great appreciation to Drs. Ed Perfect and Jeff Warren for their immeasurable guidance and encouragement during this process. I am also grateful to Dr. Jessy Labbe for advice and assistance in the preparation and care of mycorrhizal fungi. I would like to thank Willie Coleman for creative insights and assistance in the production of digital graphics. I am thankful for the support provided by various ORNL lab technicians and interns in the preparation and care of plants used in this study. Furthermore, I am grateful to my family, friends, and colleagues, without whom this thesis would not have been possible.

ABSTRACT

The interrelationships between vegetation, soil, and water are fundamental in evaluating the projected impacts of global climate change. Many predictive models require soil hydraulic parameters as inputs. As most hydraulic parameter datasets are for repacked soil, the influence of vegetation on hydraulic parameters is not thoroughly understood. Living roots and mycorrhizal fungi cause physicochemical alterations in soils. Quantifying how vegetation influences soil hydraulic parameters is necessary to more accurately simulate soil water dynamics in climate models.

Laboratory experiments were conducted to test if the presence of roots and roots inoculated with mycorrhizal fungi have a significant effect on the saturated and unsaturated hydraulic conductivity, and water retention properties of two soils with contrasting textures: Flint sand and Hamblen silt loam soil. Cores were seeded with Switchgrass (*Panicum virgatum*) and grown in a greenhouse over three separate growth periods. *Serendipita indica* was injected as liquid inoculant into designated mycorrhizal cores. In both soil types, the presence of roots with mycorrhizal fungi increased total biomass.

Saturated hydraulic conductivity measurements were obtained with a soil permeameter using the constant head method. Analysis of variance (ANOVA) revealed that saturated hydraulic conductivity was reduced (due to pore clogging) by the presence of plant roots when grown under nutrient-deficient conditions in comparison to bare soil. In contrast, no significant differences were found between treatments for unsaturated hydraulic conductivity curve parameters obtained using the evaporation method. Soil water retention curves were also obtained using the evaporation method,

and supplemented at the dry end for the Hamblen silt loam by water activity meter data. Retention curve parameters were obtained by fitting the van Genuchten equation to the resulting measurements. ANOVA indicated the presence of roots changed the shape of the water retention curve in two ways: (i) by increasing water content at saturation, and (ii) and by reducing the slope of the curve. These changes suggested roots created additional porosity and broadened the pore size distribution. The presence of mycorrhizal fungi further accentuated these effects.

Future research should investigate the effect of root-mycorrhizal interactions on soil hydraulic parameters for more soil types, plant-fungal associates, and time periods.

Table of Contents

LIST OF TABLES

LIST OF FIGURES

INTRODUCTION AND LITERATURE REVIEW

1.1 Introduction

Research into the unique hydraulic properties of vegetated soil can provide a better understanding of the relationship between soil and climatic conditions. Soil near roots and fungal hyphae has quite different hydraulic properties than the surrounding bulk soil (Carminati et al., 2010; Querejeta, 2017). However, it is difficult to separate the impact of roots on hydraulic properties from that due to mycorrhizal fungi because of the complexity of their mutualistic relationship (Gehring, 2017). This study compares the hydraulic properties of root-permeated soils, with and without mycorrhizal fungi, to quantify the relationship between fungal root symbionts and soil hydraulic properties.

1.2 Motivation

1.2.1 Soil Water Atmospheric Continuum

When studying soil-plant-water relations, it is essential to consider all components of the field environment as part of a dynamic system (Scott, 2000). Evaluating the relationship between vegetation, soil, and water is critical in understanding changes in climate. Climate models account for the relationship between plant physiology and hydraulic modeling, where transpiration and photosynthesis influence the soil-plant-atmospheric-continuum (Seneviratne et al., 2010). The atmosphere and soil are connected through root water uptake, a process by which soil water is absorbed by roots and exits through plant leaves via stomatal conductance and evapotranspiration (Feddes et al., 2001).

1.2.2 Climate Models

Although considered a fundamental climate variable, the influence of soil moisture on climate is difficult to capture (Robinson et al., 2019). A lack of quantitative data concerning soil physical characteristics has resulted in conflicting climate predictions. There is a need for the quantitative characterization of biophysical processes and validation of soil moisture-vegetation relationships (Seneviratne et al., 2010). The inability of hydraulic models to consider soil structure, land use, and climate factors when estimating hydraulic parameters further compounds predictive error (Jarvis et al., 2013). Continuous soil alteration by vegetation poses another difficulty in the procurement of soil moisture variables. The biological feedback between soil and vegetation makes it challenging to apply static variables to climate models (Robinson et al., 2019). By measuring soil hydraulic properties in the presence of roots and fungal mycorrhizae, this thesis seeks to provide more meaningful hydraulic parameters for inclusion in predictive climate models.

1.3 Previous Research

1.3.1 Plant Roots and the Rhizosphere

Roots play an essential role in the water balance, where soil-vegetation hydrological feedback is dependent upon water availability and depth of infiltration (Oswald et al., 2008). Roots alter soil hydraulic properties by changing the pore size distribution, with vegetated soil favoring the creation of macropores (Rachman et al., 2004). Changes in pore space geometry, when compared to bulk soil, are due to: (i) the presence of roots in soil pores, (ii) root water retention, and (iii) root exudates (Leung et

al., 2015a). The impact of roots on a soil system is also dependent on the age and physical characteristics of the root system. Younger, finer, roots have higher water uptake per surface area, but older roots have higher water uptake overall due to larger root diameter (Dhiman et al., 2018)

Water flow from bulk soil to the roots, in mycorrhizal-free soil, is dependent upon the rhizosphere, a soil region directly surrounding roots (Carminati et al., 2010). Water is drawn from the bulk soil into the rhizosphere by gradients in water potential (Moradi et al., 2011). The flow of water from bulk soil to roots is controlled by two aspects: (i) the ability of roots to absorb water, and (ii) how fast the soil replaces water that has been absorbed (Carminati et al., 2010).

The rhizosphere has been shown to have a higher water content than bulk soil due to the enhanced water holding capacity of root mucilage (Dhiman et al., 2018). There is also evidence that, due to root mucilage, the water content in the rhizosphere is inversely related to that of the bulk soil (Carminati et al., 2010). Root mucilage is a root exudate that causes chemical, physical, and biological changes in the soil. The water holding capacity of the rhizosphere is governed by the pore-size distribution, the chemical composition of root mucilage, and the previous wetting and drying history of the soil (Czarnes et al., 2000).

1.3.2 Mycorrhizal Fungi

Mycorrhizal fungi play a significant ecological role in soils, but little is known about the quantitative effects they have on soil and climate relations (Brito et al., 2009). There is a symbiotic relationship between roots and mycorrhizal fungi, whereby mycorrhizal hyphae provide water and nutrients in return for root assimilates (Van Der

Heijden et al., 2006). Mycorrhizal fungi improve rhizosphere root-hydraulic properties by redistributing water and nutrients from bulk soil to roots along preferential flow paths created by fungal hyphae (Augé et al., 2001).

Mycorrhizal fungi are known to change soil hydraulic properties by enmeshing soil particles with hyphae, promoting the formation of aggregates, and increasing aggregate stability. Soil aggregate formation increases the creation of macropores, thereby changing the pore-size distribution and reducing bulk density. Fungal hyphae exudates increase soil water retention leading to more water availability in soils during drying (Augé et al., 2001). These characteristics increase soil water retention and transmissive capacity (Querejeta, 2017).

1.3.3 Influence of Plant Roots and Fungal Hyphae on Soil Hydraulic Properties

Soils are created through complex physical and chemical interactions via living and non-living factors. Coined as the “five-factor model,” interactions between climate, parent material, topography, time, and living organisms, shape soil characteristics (Johnson and Lehmann, 2006). As living organisms within soils, roots, and their associated mycorrhizal fungi, influence soil development.

Roots and mycorrhizal fungi alter the structural and hydraulic properties of soils (Augé et al., 2001; Scanlan and Hinz, 2010). Differences in soil structure produce variations in hydraulic properties among soils of the same texture. This causes disparities when comparing results from disturbed soils, that were packed in a laboratory setting, to undisturbed soils characteristic of natural environments.

Soil structure differs between disturbed and undisturbed soils, in that undisturbed soils have a higher prevalence of macropores. Increasing capillary pressure head

causes larger pore spaces to drain before smaller pore spaces (Scott, 2000). Disturbed soils have a fewer macropores and therefore have higher water contents at any given capillary pressure head, near saturation, than undisturbed soils (Tuli et al., 2005). Differences in soil water retention between disturbed and undisturbed soils are generally only evident at relatively low capillary pressure heads near saturation. This is due to the inverse relationship between pore size and water retention (Scott, 2000).

1.3.3.1 Porosity and Saturated Water Content

The porosity (ϕ) is defined as $\phi = V_p/V_t$, where V_p is the volume of pores, and V_t is the total soil volume. The volumetric water content (θ) is defined as $\theta = V_w/V_t$, where V_w is the volume of water. When the soil is fully saturated with water, $V_w = V_p$, and the saturated volumetric water θ_s, is equivalent to the porosity ϕ. Laboratory methods for measuring ϕ and θ_s include calculation from bulk and particle densities, gravimetric measurements at saturation, and gas pycnometry (Dane and Topp, 2002).

A growing root can radially deform the surrounding soil by cylindrical expansion. Dexter (1987) developed a simplified model for this compaction process based on the assumption that the volume occupied by the root is accommodated by the loss of an equal volume of porosity in the rhizosphere. Whalley et al. (2005) found that the extent of root-induced compaction depends upon the particular plant species investigated. Aravena et al. (2011, 2014) and Daly et al. (2015) were able to observe localized root-induced compaction within the rhizosphere using x-ray computed tomography. Jotisankasa and Sirirattanachat (2017) report a highly significant inverse linear relationship between soil porosity and increasing root biomass.

Several studies have investigated the influence of roots on θ_s. Daly et al. (2015) found that θ_s is higher in the non-rhizosphere soil than in the rhizosphere. Alternatively, Powis et al. (2003), Carminati et al. (2010), Leung et al. (2015b), and Yan et al. (2018), suggested that soil with roots has a higher θ_s than unrooted soil. Bodner et al. (2014) found that θ_s has a positive logistical relationship to root density, while Shao et al. (2017) accounted for a higher θ_s in densely-rooted soil when formulating a dual-permeability model. Scanlan (2009) found that although wheat roots had a radius large enough to influence porosity, there was no difference in θ_s in the 0-20 cm capillary head range. The trends reported by the above studies demonstrate that the influence of plant roots on ϕ is plant and time specific where associated root density and compaction are key factors in influencing θ_s.

The effects of mycorrhizal hyphae on ϕ and/or θ_s have been investigated in several studies involving controlled pot experiments. The results varied depending upon the conditions of the particular study, such as the soil substrate used, and the plant / fungus combination. Thomas et al. (1986) looked at onion (*Allium cepa* L.) roots, not-inoculated, or inoculated with *Glomus macrocarpum*, grown in a silty clay loam soil. They found that soil containing roots and mycorrhizal hyphae significantly increased ϕ compared to soil containing just roots. Akhzari et al. (2015) and Samaei et al. (2015), working with *Medicago polymorpha* L. and barley (*Hordeum vulgare* L.), respectively, also observed increased porosity in the presence of mycorrhizal hyphae compared to uninoculated controls. In contrast, Daynes et al. (2013) found no effect of mycorrhizal hyphae on ϕ in a study involving one grass and two woody species, combined with different levels of compost applied to coal mine spoil. Most recently, a negative effect of

mycorrhizal hyphae on ϕ has been reported by Bitterlich et al. (2018). These authors grew tomato (*Solanum lycopersicum*), with and without a commercial inoculum containing *Rhizoglomus irregular*, in a mixture of natural sandy soil, fine sand, and vermiculite. Both ϕ and θ_s were significantly reduced within the mycorrhizal substrates, as compared to those containing roots alone.

1.3.3.2 Soil Water Retention Curve

The soil water retention curve, $\theta(h)$, is a non-linear function describing the relationship between volumetric water content (θ) and capillary pressure head (h). This relationship depends upon texture, organic matter, and structure, and therefore requires characterization for each soil type of interest. Soils are affected by hysteresis, whereby the $\theta(h)$ varies depending upon the history of wetting and drying (Scott, 2000). In the laboratory, $\theta(h)$ is commonly measured during monotonic drying using the hanging water column, pressure plate extractor, suction table and/or evaporation methods (Dane and Topp, 2002; Peters and Durner, 2008).

The $\theta(h)$ characterizes the static hydraulic properties of the soil; it does not describe the dynamics of soil water flow (Scott, 2000). It provides a measure of water availability and is largely dependent upon the pore-size distribution. In fully-saturated soil, at atmospheric pressure, the volumetric water content of the soil is equal to the porosity (Hillel, 2004). As the soil dries, the capillary pressure increases, and eventually, a critical pressure head is reached at which the largest pores drain. This critical value of h is known as air-entry pressure. Coarse-textured soils have air-entry pressures close to zero cm, while fine-textured soils can have very large air entry values.

The water retention curve is commonly parameterized by fitting a mathematical function to the experimental data (Dane and Topp, 2002). Such an approach makes data interpolation possible and provides hydraulic parameters for inputs to numerical models, or for comparative purposes. Numerous functions have been used to fit soil water retention data. Those that have previously been employed in plant root and/or fungal mycorrhizal studies are defined and discussed below.

The van Genuchten model (van Genuchten, 1980) is given by:

$$S_e = [1 + (\alpha h)^n]^{-m} \quad (1)$$

where $S_e = \frac{\theta - \theta_r}{\theta_s - \theta_r}$ is the effective saturation, θ_r is the residual water content, and α, n, and m are fitting parameters that control the shape of the curve. The θ_r represents the volume fraction of water that remains in the soil after drainage at very high capillary pressure head values. The α parameter is inversely related to the air entry pressure and controls the point at which water content starts to decline rapidly with increasing pressure head. The n and m parameters are related to pore-size distribution and influence the slope and inflection point of the $\theta(h)$. The following relationship between m and n is often employed to reduce the number of fitting parameters: $m = 1 - \frac{1}{n}$ (van Genuchten, 1980).

The Kosugi model (Kosugi, 1996) is based on the log-normal frequency distribution and is given by:

$$S_e = 0.5 erfc\left(\frac{log\left(\frac{h}{h_m}\right)}{\sqrt{2\sigma}}\right) \quad (2)$$

where h_m represents the pressure head corresponding to the center of the effective saturation range, while σ parameter is related to the pore-size distribution, as manifested in the slope of the $\theta(h)$ curve.

The Gallipoli model (Gallipoli et al., 2003) was derived from Eq. [1] and assumes that θ_r = 0, so that $S_e = S = \frac{\theta}{\theta_s}$, where S is the relative saturation. It includes the void ratio, e, and has four fitting parameters, i.e.

$$S = \left[1 + \left(\frac{he^{\psi}}{\omega}\right)^{n}\right]^{-m} \quad (3)$$

where n and m are the van Genuchten parameters related to pore-size distribution, and ψ and ω are fitting parameters related to the van Genuchten α pressure head parameter by $\alpha = \frac{\omega}{e^{\psi}}$.

The $\theta(h)$ model proposed by Daynes et al. (2013) has two fitting parameters, χ and β, and is given by:

$$h = e^{\left[\chi + \left(\frac{\beta}{\theta}\right)\right]} \quad (4)$$

Ln-transforming this model and employing linear regression to estimate its parameters, yields χ as represented by the y-intercept, with β given by the slope.

Augé et al. (2001, 2004) used non-linear regression and broken line regression to fit data to the following power exponential function:

$$h = \lambda e^{[\mu\theta^{\delta}]} \quad (5)$$

where λ represents the y-intercept, μ is related to the pore-size distribution and is defined as the rate at which the curve approaches the asymptote, while δ is related to the sharpness of the curve. Together μ and δ determine the slope of the curve.

Durner et al. (1994) created an adaptation of the van Genuchten model (van Genuchten, 1980) for substrate mixes with bimodal pore size distributions. Their model is given by:

$$S_e(h) = \sum_{i=1}^{2} \nu \left(\frac{1}{1+(\alpha|h|)^n}\right)^{1-\frac{1}{n}} \quad (6)$$

where ν is the weighing factor of the mixture components.

Most of the above models contain θ_s and θ_r and various fitting parameters related in some way to a benchmark pressure head and pore-size distribution. The various pressure head and pore-size distribution parameters associated with the different mathematical models are summarized in Table 1.

Overall, Plant roots tend to increase θ values close to saturation. The influence of roots on θ_s has already been discussed in the porosity section, and will not be covered here.

In the literature, the effects of roots on θ_r have proven to be either inconsistent or unreported. Yan et al. (2014) found that lower density soils, generally associated with vegetation, desaturated more than bare soils. Daly et al. (2014) found that root-permeated soil drained to a lower θ_r than bare soil, but their imaging model for x-ray tomography greatly overestimated θ_r. Leung et al. (2015) found that θ_r was consistent across vegetated and bare soil. In contrast, Carminati et al. (2010) and Ng et al. (2016) found that θ_r was higher in vegetated soil due to root mucilage.

Powis et al. (2003) found that the presence of plant roots increased the water retention capability of the soil in comparison to the soil in which roots were absent. Ng et al. (2016) have proposed a simple model to account for the effect of roots on the

$\theta(h)$, based on a root-dependent void ratio term. These authors developed a modified void ratio to account for the change in root volume ratio in root-permeated soil, i.e.

$$e_r = \frac{e - R_v(1+e)}{1 + R_v(1+e)} \quad (7)$$

where e_r is the void ratio of root-permeated soil, e represents the void ratio of the same soil without roots, and R_v is the total volume of roots per unit volume of soil. The lower bound on R_v is $R_v = 0$, representing soil with no roots. The upper bound cannot exceed the total pore volume (Ng et al., 2016). Equation [7] can then be substituted into Eq. [3] to account for root-induced changes in the $\theta(h)$. This approach demonstrated that root occupation of soil pores changed the pressure head parameter values in Eq. [3].

Using analysis of variance and Eq. [2], Scholl et al. (2017) found that h_m, corresponding to the pressure head at 50% effective saturation, was not statistically different for $\theta(h)$'s from unrooted versus rooted soil. In contrast, root density has been shown to influence the α parameter, which accounts for the vertical break in the $\theta(h)$ at air entry, through time. Shao et al. (2017) found that the planting density of shrubs in a silty sand soil resulted in higher α values. In contrast, Leung et al. (2015) and Jotisankasa and Sirirattanachat (2017) found that α decreased with root density in young plants undergoing vegetative growth. Carminati et al. (2010) found that 3-weeks after germination α was lower in rhizosphere soil than in non-rhizosphere soil. Scanlan (2009) has proposed that soil hydraulic properties change when root density increases during reproductive growth.

Roots also influence the slope of the $\theta(h)$ which is characterized by the pore-size distribution parameters in Table 1. Yan et al. (2014), report that the slope of the $\theta(h)$ correlates with the permeability of the soil. Their study found that vegetation did not

influence the slope of the $\theta(h)$ in high permeability sandy soil but increased slope steepness in cemented low permeability soil due to evapotranspiration. This result is supported by Shao et al. (2017), who found that the slope became steeper with planting density. Daly et al. (2015) found that, although, $\theta(h)$'s derived from x-ray tomography data poorly estimated n, they were consistent in having higher n values and a steeper slope in root-permeated soil than in bare soil. Using analysis of variance, Scholl et al. (2014) found that the σ parameter was statistically higher in root-permeated soil compared to bare soil, but not different between plant groups. Leung et al. (2015b) found that n values were lower for vegetated soil than bulk soil during drying, indicating the slope of the $\theta(h)$ was less steep for the root-permeated soil. Ranchman et al. (2014), reported that the slope of the $\theta(h)$ became less steep as plant roots spread, and bulk density decreased. Carminati et al. (2010) found that n was lower, and the slope was less steep in root-permeated soil than in bulk soil, and attributed this to the water retention capacity of root mucilage.

The $\theta(h)$ provides a measure of water availability and is dependent mainly on pore-size distribution as influenced by soil texture, structure, and organic matter content. The ability of plants and mycorrhizal fungi to influence pore size distribution causes $\theta(h)$'s to differ between bare, root-permeated, and mycorrhizal-inoculated root-permeated soil. Vegetation and mycorrhizal fungi induced differences in the $\theta(h)$ are best understood by comparing parameters derived from curve-fitted data. However, there is limited literature available comparing $\theta(h)$ parameters between mycorrhizal and non-mycorrhizal samples. Only three mathematical models, Eqs. [3], [4] and [5], have been used to curve-fit mycorrhizal specific $\theta(h)$ data. The χ and λ parameters in Eq. [4]

and Eq. [5] can be thought of as air entry type parameters. The pressure head parameter, α, in Eq. [6] is inversely related to the air entry pressure and controls the point at which water content starts to decline rapidly with increasing pressure head. The α, is closely related to porosity due to the inverse relationship with air entry pressure. Soils with larger pore spaces, like sands, have larger α values. Using Eq. [6] for bimodal porosity, Hosseini et al. (2016) found that α was lower in endophyte-fungi inoculated plants when compared to non-inoculated plants. Similarly, while statistically comparing parameters derived from Eq. [6], Bitterlich et al. (2018) found that total porosity was significantly lower in the inoculated samples. The mycorrhizal-derived porosity reduction appeared to be two-fold in origin: mycorrhizal fungi were believed to reduce porosity through an increase in fungal biomass, thereby clogging pore spaces, as well as through the production of water-repellent root exudates. The combination of these two factors resulted in an increased slope and shifted the $\theta(h)$ curves in mycorrhizal-inoculated samples (Bitterlich et al., 2018).

In Eq. [5], the pore size distribution parameter, μ, determines the slope of the $\theta(h)$ while δ determines the sharpness of the curve. When applying both parameters, Augé et al. (2001, 2004) found that root-permeated soil containing mycorrhizal fungi had more water loss during initial pressure head measurements than the non-mycorrhizal root-permeated soils. As the soil dried, more water was available in the mycorrhizal root-permeated soil than the untreated root-permeated soil. Similarly, Hosseini et al. (2016) found that n, the pore size distribution parameter in Eq. [6], was lower in fungi inoculated soil than in untreated samples. When using Eq. [4], Daynes et al. (2013) found that β was slightly lower for the mycorrhizal fungi plants. The $\theta(h)$ for fungi-

inoculated plants was slightly higher than the non-inoculated samples. However, no statistical significance was found, and additional results for nutrient enriched treatments showed no correlation.

1.3.3.3 Saturated Hydraulic Conductivity

The saturated hydraulic conductivity (K_{sat}) is the constant of proportionality in Darcy's equation and is defined in Equation [8].

$$K_{sat} = -q\frac{\Delta h}{\Delta z} \tag{8}$$

In Equation [8], q is the steady-state flow rate, and $\frac{\Delta h}{\Delta z}$ is the hydraulic gradient between inlet and outlet (Meter Group, 2017).

In the laboratory, K_{sat} is measured under fully saturated conditions generally using either the constant head or falling head methods (Dane and Topp, 2002).

The influence of plant roots on K_{sat} has been observed through multiple laboratory studies investigating vegetative effects on soil hydraulic properties. In root-permeated soil, K_{sat} is largely influenced by root density. Barley (1954) observed that the infiltration rate decreased in sandy soil due to pore blockage by roots. Leung et al. (2015a) found the K_{sat} of root-permeated soil was lower than that of the control soil without roots due to pore blockage. Jotisankasa and Siriattanachat (2017) reported that pore-clogging by roots was positively correlated to root biomass. As root density increased K_{sat} decreased. Shao et al. (2017) found that K_{sat} is dependent upon planting density, with a comparatively lower root density decreasing K_{sat}, and higher root density increasing K_{sat}.

Additionally, the relationship between K_{sat} and root mass appears to be age-dependent. Scanlan (2009) determined there was a noticeable, but not statistically significant, increase in K_{sat} when researching the changeover from vegetative to reproductive growth in 7-9-week-old wheat plants. Petersson et al. (1987) found a positive linear relationship between increased age and K_{sat} for older roots, while younger roots had a less direct, and negative relationship between increased root development and K_{sat}. These trends were supported by the work of Powis et al. (2003), who showed that K_{sat} decreased during root growth, but increased during root decay. Ni et al. (2018) modeled the relationship between root growth and decay in soil void space. The decay of structural roots from older plants increased macroporosity and thereby K_{sat}. Scholl et al. (2013) estimated K_{sat} inversely from cumulative outflow data and found an increase over time in planted soil columns as compared to unplanted columns.

K_{sat} is soil structure-dependent and is greatly influenced by the occurrence of macropores and water-stable aggregates. In a field study, Rachman et al. (2004) found a positive correlation between K_{sat} and macroporosity, with the highest abundance of macropores and water-stable soil aggregates occurring within the top 20-cm of switchgrass-planted soil. Aravena et al. (2010) found that soil aggregate contact area and pore connectivity increased due to root-induced radial compaction of the soil. The compaction of inter-aggregate pore-space increased K_{sat}.

Root-mycorrhizal symbiosis can stabilize soil aggregates through chemical and physical processes. Roots and mycorrhizal fungi bind soil into aggregates by excreting extracellular compounds, like proteins and polysaccharides (Querejeta, 2017). Strigolactones are a class of root exudate plant hormones that promote mycorrhizal

fungi establishment. Stimulated by these hormones, mycorrhizal fungi extend from the plant root into the soil matrix to access nutrients (Besserer et al., 2006). This process physically stabilizes the matrix through soil enmeshment by hyphal networks (Querejeta, 2017).

K_{sat} generally decreases with root growth and increases with root decay due to changes in total soil porosity and pore-size distribution. Rachman et al. (2004) found that a high incidence of inter-aggregate pore spaces (mesopores) corresponded to higher K_{sat} values in switchgrass-planted soil. In inoculated samples, the presence of mycorrhizal fungi was shown to decrease K_{sat}. Samaei et al. (2015) suggest that mycorrhizal hyphae reduce K_{sat} in dense soil by increasing intra-aggregate (micropore and mesopore) spaces. Their study found that mycorrhizal fungi increased stable aggregation by 201% and decreased K_{sat} by 88.2% when compared to non-mycorrhizal plants. Likewise, Bitterlich et al. (2018) found that K_{sat} was higher in non-mycorrhizal mutants at 1.18 x10^{-5} m/s when compared to inoculated samples with a K_{sat} of 9.40 x10^{-6} m/s. These differences in K_{sat} can be attributed to mycorrhizal derived changes in pore-size distribution, as well as the presence of significantly more water-stable aggregates in soils with mycorrhizal-plant symbiosis (Hallett et al., 2009).

1.3.3.4 Unsaturated Hydraulic Conductivity Curve

The functional relationship between hydraulic conductivity and volumetric water content for unsaturated soil, $K(\theta)$, is defined through Buckingham's extension of Darcy's equation shown in Equation [9].

$$K(\theta) = \frac{-q}{\frac{\Delta h}{\Delta z}} \quad (9)$$

In Equation [9] the water flux q at the center of the soil sample is divided by the average gradient $\Delta h/\Delta z$ of the hydraulic head to determine the unsaturated hydraulic conductivity (Pertassek et al., 2015). Measurement methods include steady-state centrifugation and the evaporation method as detailed in section 2.6 (Dane and Topp, 2002). The $K(\theta)$ function is also commonly calculated from the soil water retention curve (Dane and Topp, 2002).

The $K(\theta)$ is greatly influenced by pore space geometry due to Poiseuille's law. When applied to soil science, this law states that the water flux is proportional to the fourth power of the pore radius (Scott, 2000). As a result, larger pores will always conduct more water than smaller pores. In saturated flow, all pores are filled with water and conducting water. During unsaturated conditions, however, the largest pores are the first to desaturate and fill with air. Since macropores desaturate, water is confined to contact points between grains and intra-aggregate pores. The pockets of air between grains and aggregates become barriers to flow. This reduces the conductive portion of the soil as water is forced to flow within smaller pores (Hillel, 2004). The relationship between pore space geometry and flux causes $K(\theta)$ to decrease at a lower rate in fine-textured (micropore dominated) soils than in coarse-textured (macropore dominated) soils (Scott, 2000).

Nearly all soil-water interactions, including the supply of water to roots, take place in unsaturated soils (Hillel, 2004). However, relatively few studies have investigated the effects of plant roots on soil hydraulic conductivity under partially-saturated conditions. As mentioned in Section 1.3.3.1, roots change porosity and broaden pore-size distributions. Thus, in theory, the ability of root-permeated soils to

increase micropore abundance and clog macropores should lead to a higher unsaturated hydraulic conductivity when compared to bare soils.

When testing plants grown in a synthetic sand-clay mixture, Powis et al. (2003), did not observe any relationship between root volume or root length and $K(\theta)$. In contrast, Aravena et al. (2011) found that roots increased contact between aggregates, primarily through soil compaction. Cylindrical compaction of clay soil by roots reduced void spaces and resulted in higher $K(\theta)$ when compared to an unrooted control soil. Sedgley and Barley (1958), however, observed that a sandy loam planted with grass had lower $K(\theta)$ compared to control samples. The reduction in $K(\theta)$ was theorized to be the result of pore-clogging by fine roots and soil compaction by larger roots as well as hydrophobic root exudates. Macropores created by root decay were not considered an influencing factor because these samples were tested under conditions where larger pores would have already drained. The contradicting results between Aravena et al. (2011), and Sedgley and Barley (1958), could be related to the differences in soil type investigated (much like an interaction in analysis of variance). Unsaturated flow tends to be higher in clay soils than in coarse sands, suggesting that roots increase $K(\theta)$ under high flow conditions, and decrease them under low flow conditions. Further studies are needed to fully investigate the full range of root impacts on unsaturated flow.

Unsaturated flow is determined by the ability of water to move through soil pore spaces that retain water at h values greater than zero. When compared to non-mycorrhizal soils, soils inoculated with mycorrhizal fungi have been shown to have greater pore connectivity and flow during unsaturated conditions (Querejeta, 2017). Mycorrhizal fungi establishment in soil causes $K(\theta)$ to decrease with decreasing water

content at a lower rate compared to uninoculated soil. This effect is believed to be caused by a combination of three main factors.

Firstly, mycorrhizal fungi change the shape and organization of soil pores towards smaller pore spaces (Samaei et al., 2015). Pore-size distribution influences $K(\theta)$ due to the relationship between flux and pore space geometry. This relationship causes $K(\theta)$ to decrease more gradually in micropore dominated soil (Scott, 2000). Bitterlich et al. (2018) found that the presence of mycorrhizal fungi caused the shape and organization of pore systems to change and total porosity to decrease. This led to increased $K(\theta)$ at a given water content in a sand-clay soil occupied by mycorrhizal inoculated tomato plants.

Secondly, mycorrhizal fungi influence $K(\theta)$ by improving pore connectivity. Mycorrhizal fungi establish networks of preferential water flow along and within extraradical hyphae (Querejeta, 2017). Preferential flow through hyphal networks allows water transport between air-filled pore spaces (Bitterlich et al., 2018). Water flows around and within hyphae allows for greater redistribution of water when compared to non-mycorrhizal soils (Querejeta, 2017).

Thirdly, mycorrhizal fungi influence $K(\theta)$ through the exudation of organic compounds (Bitterlich et al., 2018). These compounds are strongly hydrophilic when wet and increase conductivity within water-filled pore spaces when compared to non-mycorrhizal soils (Hallet et al., 2008). The combination of these three factors can result in a “truly mycorrhizal” effect on $K(\theta)$ (Bitterlich et al. 2018).

Much like the soil water retention curve, unsaturated hydraulic conductivity data are often curve fitted using the capillary conductivity function from the Mualem pore bundle model (Mualem, 1976), i.e.

$$K = \left(K_{sat}{}^{-1}\theta\right)^{\tau}\left[\left(1-\left(K_{sat}{}^{-1}\theta\right)^{n}\right)^{\frac{1}{n}}\right]^{2} \quad (10)$$

In Equation [10], θ is the volumetric water content. The n parameter is related to pore-size distribution and is a fitting parameter for the van Genuchten equation detailed in section 1.3.3.2 (Peters and Durner, 2015). K_{sat}, is the saturated hydraulic conductivity, detailed in section 1.3.3.3.The other fitting parameter for this function is τ, an empirical parameter representing pore tortuosity and pore connectivity (Peters and Durner, 2015). To date, no studies have compared unsaturated hydraulic conductivity function parameters between bare, rooted, and mycorrhizal rooted soils.

1.4 Goal, Objectives, and Hypotheses

The purpose of this study is to investigate hydraulic parameters that can capture the influence of vegetation and mycorrhizal fungi on soil moisture. The overall goal of the research is to statistically analyze the impact of plant roots and mycorrhizal hyphae on soil hydraulic properties. There are two specific objectives: (i) in the laboratory, experimentally investigate how the presence and absence of mycorrhizal fungi, in conjunction with plant roots, impact soil hydraulic properties, and (ii) quantify total plant biomass and root volume in the presence and absence of fungal hyphae in order to seek statistical relationships between these biological parameters and soil hydraulic properties.

There are five hypotheses to be tested:

i. The presence of mycorrhizal fungi will promote growth and result in a greater biomass and root volume ratio than roots alone;

ii. the presence of roots and mycorrhizal fungi will partially fill macropores and therefore decrease the saturated hydraulic conductivity of the soil;

iii. presence of roots and mycorrhizal fungi will increase the water content at any given capillary pressure head near saturation, changing the shape of the soil water retention curve, relative to root/mycorrhizal free soil;

iv. The presence of roots and mycorrhizal fungi will increase pore connectivity during drying and therefore increase unsaturated hydraulic conductivity of the soil;

v. Roots alone will have less impact on soil hydraulic properties than roots with mycorrhizal fungi.

MATERIALS AND METHODS

2.1 Experimental Design

Bench-scale measurements of soil water retention and saturated and unsaturated hydraulic conductivity were performed in a laboratory setting using a total of 42 hand-packed cores. Two different soil types were used: Flint sand and Hamblen silt loam. The plant associate was *Panicum virgatum* “colony type” switchgrass, and the mycorrhizal inoculant was *Serendipita indica* (*Piriformospora indica*, ATCC 204458) (Verma et al., 1998; Weiß et al., 2016). The experimental design was as follows:

Flint Sand: 5 Treatments x 3 Replicates x 2 Growth Cycles = 30 Cores

Hamblen Silt Loam: 4 Treatments x 3 Replicates x 1 Growth Cycle = 12 Cores

The five treatments associated with Flint sand were: bare soil (control), soil + mycorrhizae, soil + roots, soil + roots + fertilizer, and soil + roots + mycorrhizae. The experimental design for Flint sand is illustrated schematically in Figure 1. This design was repeated over two separate growth cycles.

Only one growth cycle was investigated for the Hamblen silt loam soil because of the slow drainage of this soil type. Additionally, a fertilizer treatment was not included due to the presence of naturally-occurring nutrients in this soil with significant organic matter. Otherwise, the experimental design for the Hamblin silt loam was similar to that for the Flint sand (Figure 2).

2.2 Soils

Flint sand (Flint #13, U.S. Silica Company, Berkeley Springs, WV) was selected as an ideal porous medium for these experiments due to its predominately quartz

composition; negligible organic matter; high hydraulic conductivity; and rapid drainage time (Kang et al., 2013). Hamblen silt loam was selected to represent a naturally-occurring soil type within East Tennessee. The soil is considered ideal for agriculture and is formed from the watersheds of eroded limestone, sandstone, and shale (NRCS, 2019). The soil was sampled from the B horizon, air-dried, and passed through a 2 mm sieve. Selected physical and chemical properties of the two soils are summarized in Table 2 in Appendix 1-Tables.

2.3 Sample Preparation

2.3.1 Soil Protocols

First, the soils were autoclaved, a process in which steam permeates loosely packed soil killing microbial cells and spores. Both soils were autoclaved at 111.5 kPa and 121˚C for 30 min. After 24 hour they were autoclaved again to ensure the neutralization of resilient fungal spores (Brito et al., 2009). The autoclaved soils were subsequently oven-dried at 105˚C for 24 hours to remove any moisture before packing into sample containers.

The sample containers were stainless steel and cylindrical in shape with an inner diameter of 4 cm and a height of 5 cm (Meter Co, Munich, Germany). The bottoms of cylinders were fitted with 1 µm nylon mesh (ELKO Filtering Co, Miami, Florida) to contain the soil and prevent exterior root and hyphal growth. The sample containers and accompanying soil were autoclaved independently. As with the soil, the sample containers were autoclaved twice at 121 ˚C for 30 min to further neutralize any fungal spores (Brito et al., 2009). The sterilized oven-dried soil was weighed into equal parts

and packed into the sterilized sample containers by hand. Soil cores that were not selected for mycorrhizal inoculation were then wetted with DI water using a standing water table and seeded.

2.3.2 Mycorrhizae Protocols

After hand packing, a sub-set of soil cores were set aside for mycorrhizal inoculation. Prior to inoculation of the soil, *Serendipita indica* (*Piriformospora indica*, ATCC 204458) (Verma et al., 1998; Weiß et al., 2016) was grown from a 0.5-cm agar plug in 50 ml of 1x potato dextrose broth (Sigma Aldrich, USA) in the dark at 30 ˚C (120 rpm shaker) for two weeks. These liquid cultures were then filtered using sterile miracloth and rinsed twice with sterile water. The soil was re-autoclaved for 30 min at 121 ˚C. Stainless steel cylinders were UV sterilized for 30 min. The packed soil cylinders were saturated with sterile DI water from below. *S. indica* liquid inoculant was injected into the moistened soil to create a broad matrix of fungi.

2.3.3 Switchgrass Protocols

Soil cores were seeded with 3/8 teaspoon of *Panicum virgatum* “colony type” switchgrass seeds. The seeds were sprinkled uniformly on top of the soil surface. Immediately after application, the seeds were misted with DI water to promote germination. Germinated seedlings were counted 4 weeks after application of seeds to the soil cores. An average plant density of 1.75 seedlings per cm^2 was determined.

2.3.4 Plant Care and Growth

After seeding and/or inoculation, all the cylindrical containers for the benchtop experiments were placed in a greenhouse to promote growth. The plants were watered

daily with DI water by maintaining a standing water table and through spray bottle misting. The standing water table was gradually lowered as the plants matured. The plants grown in the Flint sand soil were harvested after 70 days, and the plants grown in the Hamblen silt loam were harvested after 80 days. Average greenhouse conditions during the growth cycles are summarized in Table 3.

2.4 Saturated Hydraulic Conductivity

Saturated hydraulic conductivity (K_{sat}) was measured using a Meter K_{sat} Permeameter (Meter Co, Munich, Germany); a device that uses a Mariotte bottle system and collects real-time data through a software application (Figure 3). Following harvesting of the above-ground biomass, the soil cores were saturated from below with a standing water table and then fitted into the permeameter.

The K_{sat} of the soil was determined using the constant head method. The constant head method uses gravitational differences in hydraulic head to determine K_{sat} (Scott, 2000). K_{sat} is determined mathematically using Darcy's Law shown in Equation [8] in section 1.3.3.3.

2.5 Soil Water Retention Curve

Following the saturated hydraulic conductivity measurements, the saturated soil cores were transferred to a Hyprop2 device (Meter Co, Munich, Germany) for soil water retention measurements.

When preparing the saturated soil sample for the Hyprop2 device, boreholes that were 0.5 cm in diameter and 1.25 cm and 3.75 cm deep, were made in the saturated soil sample. In the case of the silt loam, the soil extracted from the boreholes was set

aside for water retention measurements using a water activity meter (see section 2.7 below). The two mini tensiometers on the Hyprop2 device were then lowered into the boreholes. The combined Hyprop2 and soil core was then vertically rotated to expose the open end of the soil to the atmosphere and placed upon an electronic balance. Capillary pressure head measurements were collected as the moisture evaporated from the soil, and water was drawn from the tensiometers. As data were collected the changes in weight were recorded as volumetric water content (θ) and $\log_{10}$ capillary pressure head (h) in pF units from the tensiometers. These data points were used in conjunction with Meter Hyprop-Fit software to produce high-resolution soil water retention curves (Peters and Durner, 2008; Peters et al., 2015)

The Hyprop fitting software, Shypfit2.0, uses a modified version of the evaporation method (Schindler et al., 2010) to produce a $\theta(h)$ curve. The evaporation method measures pressure head at two separate depths in the soil. This method created two pressure head measurements for every recorded water content. To adjust for this, the geometric mean of the two pressure head measurements is taken so that each water content value is associated with a mean pressure head at a given time as detailed in Equation [11]:

$$h = \sqrt{(h_{1,} \cdot h_{2,})} \tag{11}$$

In Equation [11] h is the geometric mean of the pressure heads, h_1 is the pressure head measured from the first tensiometer at a given time, and h_2 is the pressure head measured from the second tensiometer at a given time (Pertassek et al., 2015).

The evaporation method is modified to account for the non-linear water content distribution in some soil samples near saturation. At the beginning of the evaporation

process, small but systematic errors are associated with soil samples that are coarse-textured or have well-structured secondary pore systems. The bias in the estimated retention function is caused by the uneven distribution of water at hydrostatic equilibrium. Correcting non-linear water content distribution is also vital to accurately determine the unsaturated hydraulic conductivity. An unsaturated hydraulic conductivity prediction based on an incorrect retention function can significantly vary from the true function (Peters and Durner, 2006). This error is avoided by using the integral evaluation of the measurement, as shown in Equation [12]:

$$\bar{\theta}(b) = \frac{1}{h_{lb} - h_{ub}} \int_{h_{lb}}^{h_{ub}} \theta(b,h)dh \quad (12)$$

Equation [12] is used to determine the corrected mean water content, $(\bar{\theta})$, where $\theta(b,h)$ is the parametric retention function, b is the parameter vector, h_{lb} is the pressure head at the lower boundary of the soil column and h_{ub} is the pressure head at the upper boundary of the soil column (Peters and Durner, 2008).

Equation [1], the van Genuchten equation, was the function used for curve fitting the $\theta(h)$ data. The equation includes four parameters. The first parameter, the saturated water content, θ_s, was a known value for every soil core. θ_s was calculated from each sample's bulk density using an assumed specific gravity of 2.65. The other three parameters α, $n\left(=\frac{1}{1-m}\right)$, and θ_r were best estimates obtained by fitting the van Genuncten equation to the data using Shypfit2.0 software (see Section 2.12). The fitting parameter α represents the inverse of the air entry point of the soil. The α values were found to be log-normally distributed and so they were $\log_{10}$-transformed prior to statistical analysis. The fitting parameter θ_r represents the residual water content; the

water content remaining at the end of the drying cycle. A more detailed description of the van Genuchten equation is available in section 1.3.3.2

2.6 Unsaturated Hydraulic Conductivity

Unsaturated hydraulic conductivity parameters were calculated using Shiftfit2.0 software from $K(\theta)$ data gathered by the Hyprop2 device. The Hyprop2 device provides measurements of the water flux at the center of the soil sample and the mean gradient of the hydraulic head. These parameters are required inputs for the Darcy-Buckingham Equation, Equation [9] from section 1.3.3.4 (Pertassek et al., 2015).

The water flux at the center of the soil core for a given time is approximated using Equation [13].

$$q = \frac{L}{2}\frac{\theta_i - \theta_{i-1}}{\Delta t} \tag{13}$$

The parameter L is the core length and θ is the water content. The water content at the center of the sample is measured at two points in time, θ_i and θ_{i-1}.The variable Δt represents time as half of the evaporation rate (Pertassek et al., 2015).

The average gradient of the hydraulic head at the center of the sample is evaluated using equation [14]:

$$\Delta h = \frac{\bar{h}_1 - \bar{h}_2}{z_2 - z_1} - 1 \tag{14}$$

The variables $\bar{h}_1$ and $\bar{h}_2$ represent mean pressure head at two separate depths. The variables $z_1$and z_2 characterize the two separate depths of the tensiometers associated with the Hyprop2 device (Pertassek et al., 2015).

Using the Darcy-Buckingham relationship given in Equation [9], the water flux at the center of the soil sample is divided by the average gradient of the hydraulic head to determine unsaturated hydraulic conductivity.

The unsaturated hydraulic conductivity data were fitted using Equation [10], the capillary conductivity function from the Mualem pore bundle model (Mualem, 1976). The Shypfit2.0 program was used and the fitting was done simultaneously with the water retention fitting, yielding with single estimate of n (see Section 2.13). Analyses were then conducted on τ and the estimated K_{sat}, the two unique parameters estimated by fitting the unsaturated hydraulic conductivity curve (see Section 2.12).

2.7 Water Activity Meter

For fine-textured soils, the Hyprop2 device cannot measure the full range of soil capillary pressure heads needed to form a full soil water retention curve. For such soils, the dry range of the measurement can be measured using a water activity meter (Campbell et al., 2017). Therefore, water activity meter measurements were performed on the Hamblen silt loam soil.

Approximately 1 g of soil was sub-sampled from the center of each of the water-saturated silt loam cores. The moist soil was then uniformly spread into a circular sample container. The samples were exposed to the atmosphere for approximate 1-hour intervals. Following each drying period, samples were capped to stop atmospheric evaporation and allowed to equilibrate. The samples were then individually placed in a Novasina Labmaster-a_w (Novasina-Ag, Lachen, Switzerland) to measure the activity of the soil water. After the measurement was recorded, each sample was capped and then weighed to measure soil moisture content. The process was repeated until there were

no changes in the water content over time. The soil samples were then oven-dried at 105 ℃ for 24 hr. The oven dry weights were used, along with the soil bulk density values, to determine volumetric water contents (θ).

The water activity measurements were converted from water activity (a_w), the measure of the water vapor pressure of a substance over the vapor pressure of water, to total water potential. The total potential measurements were first corrected for calibration error. A best-fit line was plotted to measured calibration points determined from salt standards. The equation of the best-fit line was used to correct all of the measured total potential values.

The Novasina Labmaster- a_w includes both matric and osmotic potentials when measuring total potential. Total potential is dominated by the osmotic potential in the wet range leading to erroneous measurements of matric potential. To correct for this error, the osmotic potential was calculated and removed from the total potential as follows:

$$\psi_m = \psi_t - \psi_o \left(\frac{\theta}{\theta_s}\right) \quad (15)$$

In Equation [15], ψ_m is the matric potential, ψ_t is the total potential, and ψ_o is the osmotic potential. The variable θ is the volumetric water content and θ_s is the volumetric water content at saturation. The matric potential measurements were then converted to pF values, i.e., the base ten logarithm of capillary pressure head in cm. Together the θ and pF measurements were used to determine the soil water retention curve near residual water content.

2.8. Above Ground Biomass

The shoot biomass was removed from the cores prior to measuring the soil hydraulic properties. It was oven-dried for three days at 60 ˚C and then weighed.

2.9 Below Ground Biomass

The presence of mycorrhizal fungi in the inoculated cores was confirmed using microscopy, as seen in Figure 5. For this process a sub-section of mycorrhizal root was clipped from the exposed bottom of the soil core. The root sub section was taken from the bottom of the soil core, rather than the center, to ensure the physical integrity of the extracellular mycorrhizal hyphae.

Below ground biomass was separated from the soil medium through root floating using DI water. The roots were gently picked from the soil and untangled. Then the root nodes were removed. The total root mass was weighed. A sub-sample of the processed roots was set aside for root scanning and analysis. The roots, including the sub-sample used for root scanning, were then oven-dried for three days at 60˚C.

2.10 Total Biomass

Total biomass was calculated as the sum of the oven dry weight from the calculated above ground and below ground biomass.

2.11 Root Scanning

A sub-sample of clean roots was scanned. The sub-sample size was determined by scanning the entire root mass of one sample. To uniformly scan the root volume, each scanning tray was filled to the same extent. The scanning trays were filled to

capacity while not allowing for overlap of root material or extension passed the dimensions of the scanner.

The root volume ratio (R_v) is the ratio of total root volume to the total volume of soil. R_v was determined from the total root volume of each scan. The data were log-normally distributed, so the base-ten logarithm ($\log_{10}$) of R_v was determined and the mean $\log_{10} R_v$ value (population mean) calculated from those results. The standard deviation of the population mean was determined. The sample number needed was calculated using Equation [16]:

$$n_a = \left(\frac{t_{\alpha,n-1} s}{\Delta}\right)^2 - n \tag{16}$$

Where n_a is the number of scans required to be 95% $((1-\alpha)\ x\ 100\%)$ sure of obtaining a sample mean within 5% (Δ) of the population mean. The variable $t_{a,n-1}$ is the two-tailed t-statistic for a significance level of α at $n-1$ degrees of freedom. The variable s is the standard deviation of the population mean (Davis, 2002). It was found that when log-normally distributed, the sample number needed to estimate the true mean within 95% was four scans.

The sub-sampled roots were selected at random from the total mass of clean and processed roots. Roots were uniformly placed on a tray, and that tray was placed on a scanner. The root scans were analyzed using WinRHIZO root scanning software. The scanned roots were then oven-dried for three days at 60℃ and weighed. The sub-sampled roots were added to the total root biomass weight. Total root volume was estimated through a ratio comparing the weight of the scanned roots to the unscanned roots.

2.12 Predictive Models

Predictive models were developed to investigate the influence of roots on the soil water retention curve. The predictive models utilized the R_v values calculated from the scanned root volume. The models are dependent upon varying assumptions about the effects of roots on porosity. As depicted in Table 4, Root-Model 1 assumed that roots reduce porosity and is from the work of Ng (2016) and Assouline (2006). Root-Model 2 assumed that roots reduce macroporosity (ϕ_{macro}) and is derived from the work of Ng (2016) and Assouline and Or (2014). Root-Model 3 assumed that roots increase macroporosity and is derived from Ng (2016) and Assouline and Or (2014). Root-Model 4 assumed roots increase porosity and is from the work of Ng (2016), and Assouline (2006).

2.13 Data Analysis

Equations [1] and [9] from section 1.3.3 were fitted to the water retention and unsaturated hydraulic conductivity data sets simultaneously using the Shypfit2.0 software package. This program uses a non-linear regression algorithm to minimize the sum of the weighted square residuals between the model predictions and actual data (Pertassek et al., 2015). The root mean square error, RMSE was calculated to determine the goodness of fit between the model and measured data for $\theta(h)$ and $K(\theta)$. The RMSE was calculated using Equation [16]:

$$RMSE = \sqrt{\frac{1}{k}\sum_{i=1}^{k}[y - \hat{y}]^2} \quad (16)$$

In Equation [16], the variables y and $\hat{y}$ are the measured and model-predicted values, and k is the number of observations. The RMSE was calculated for both the measured

and predicted values of the soil water retention curve as well as the measured and predicted values of the saturated hydraulic conductivity curve.

Analyses of Variance, ANOVA, were conducted to analyze differences in the various fitted and measured parameters within and between the datasets. This analysis also determined differences between the treatment means using Tukey's honestly significant difference (HSD) test. ANOVA's were conducted on saturated hydraulic conductivity, unsaturated hydraulic conductivity parameters, soil water retention parameters, and plant growth parameters. The analyses were conducted using the SAS statistical software (SAS Institute Inc., 2012) with statistical significance always assessed at the $p < 0.05$ level.

RESULTS

3.1 Plant Growth Parameters

The shoot and root biomass were harvested from the soil samples at the end of the growing period. The shoot and root biomass were dried and weighed to calculate total biomass. The scaled root volume, determined from the dried root weight, was used to calculate R_v. The R_v values were analyzed as $\log_{10} R_v$ to align with their log-normal distribution and the sample estimation method outlined in section 2.11.

3.1.1 Plant Growth Parameters for Flint Sand

The total biomass for the Flint sand treatments was statistically analyzed using a two-way ANOVA. There was an experimental effect but no interaction between treatment and experiment. The biomass from the separate growth periods was combined so that the experimental effect was averaged across both experiments. A Tukey's HSD test showed that the fertilizer rooted and mycorrhizal rooted treatments were significantly different from the rooted treatment, as seen in Figure 6 found in Appendix 2-Figures. Additionally, the mycorrhizal rooted treatment had much less variation among samples than the fertilizer rooted and rooted treatments.

A two-way ANOVA and a Tukey's HSD test were run on the $\log_{10} R_v$ values. The ANOVA did not show an interaction or experimental effect within the data at the 95% confidence interval. As such, the data from both experiments were combined and a significant treatment effect on the $\log_{10} R_v$ values was found. Tukey's HSD test showed that the rooted and mycorrhizal rooted treatments were significantly different, as can be

seen in Figure 7 found in Appendix 2-Figures, while the fertilizer rooted treatment was not significantly different from either of these treatments.

3.1.2 Plant Growth Parameters for Hamblen Silt Loam

A one-way ANOVA was conducted on the silt loam samples grown from November to January. The ANOVA and accompanying Tukey's HSD test showed that the above-ground biomass from the fall growth period was not statistically significant between treatments at the 95% confidence interval, as seen in Figure 8 found in Appendix 2-Figures. However, the mean total biomass value for the mycorrhizal rooted treatment was 2.56 g, over ten times the mean value, 0.24 g, for the rooted treatment. Total biomass displayed a trend whereby the variation of the rooted treatment resulted in a much narrower distribution than the distribution of the mycorrhizal rooted treatment.

A one-way ANOVA and Tukey's HSD test were run on the $\log_{10} R_v$ values. These analyses showed that the R_v values were statistically different at the 95% confidence interval. The mean $\log_{10} R_v$ values for the mycorrhizal treatment were statistically greater than the values for the rooted treatment, as seen in Figure 9 found in Appendix 2-Figures.

3.2 Saturated Hydraulic Conductivity

K_{sat} was measured with a permeameter using the constant head method. This method relied on gravitational differences in hydraulic head to determine K_{sat} (Scott, 2000). K_{sat} was calculated with Meter K_{sat} Permeameter Software (Meter Co, Munich, Germany) via an application of Darcy's Law as shown in Equation [8]. The constant head method and Darcy's law are detailed in section 2.4. The measured K_{sat} values

were $\log_{10}$-transformed prior to analysis because this property is generally considered to be log-normally distributed.

3.2.1 Flint Sand Measured K_{sat}

Three replicate measurements of K_{sat} were taken on each Flint sand soil core. The base-ten logarithm ($\log_{10}$) of each replicate K_{sat} value was calculated. The replicate values were then averaged to determine the mean $\log_{10} K_{sat}$ of each sample. These values were statistically compared using a two-way ANOVA, as seen in Figure 10, found in Appendix 2-Figures. The ANOVA was statistically significant and showed a significant effect between treatment and experiment but no interaction. Thus, the values from both experimental periods were combined and run in the same ANOVA. There were statistical differences between treatments at the 95% confidence interval. A Tukey's HSD test showed the data had two statistically different treatments: the control treatment was statistically different from the rooted treatment. The other treatments (mycorrhizal control, fertilizer rooted, and mycorrhizal rooted), were not significantly different from either of these two treatments.

3.2.2 Hamblen Silt Loam Measured K_{sat}

One K_{sat} measurement was taken for each natural soil sample with three replicate samples per treatment. The $\log_{10} K_{sat}$ was calculated for each measurement. These values were then statistically compared using a one-way ANOVA, as seen in Figure 11, found in Appendix 2-Figures. There were no statistically significant differences between treatments at the 95% confidence interval. Although not statistically significant, the $\log_{10} K_{sat}$ values do show a trend, as seen in Figure 11. The control

treatment had the smallest variation amongst sample results, followed by the rooted treatment, the mycorrhizal rooted treatment, and then the mycorrhizal control treatment.

3.3 RMSE Values from Curve Fitting the Soil Water Retention and Unsaturated Hydraulic Conductivity Data

The root mean square error, RMSE, values were determined by the Shypfit2.0 software using Equation [1] for the soil water retention curve $\theta(h)$ (SWRC) and Equation [10] for the unsaturated hydraulic conductivity curve $K(\theta)$ (Peters and Durner, 2015). The fitting was done simultaneously, yielding separate RMSE's for the water retention and unsaturated conductivity curves. The RMSE values for the Flint sand ranged from 0.0018 to 0.0105 for the $\theta(h)$ curves and between 0.0673 and 0.3719 for the $K(\theta)$ curves. The RMSE values for the silt loam ranged from 0.0034 to 0.0163 for the $\theta(h)$ curves and between 0.1105 and 0.2358 for the $K(\theta)$ curves. The complete listing of RMSE values is in Table 7 found in Appendix 1-Tables.

3.3.1 Fitted $\theta(h)$ and $K(\theta)$ Curves with Median RMSE Values for Flint Sand

The RMSE values for $\theta(h)$ curves were calculated for the Flint sand treatments. The median RMSE value for the curves fitted to the $\theta(h)$ data was 0.0038. The fit of the median RMSE for $\theta(h)$ is shown in Figure 12, found in Appendix 2-Figures. The curve-fit shown in Figure 12 represents the case for which one-half of the curve-fits were better, and the other half of the curve-fits were worse for this soil.

The RMSE values for the fitted $K(\theta)$ curves were calculated for the Flint sand treatments. The median RMSE value for the model curve-fitted to $K(\theta)$ data was 0.2872. The fit of the median RMSE for $K(\theta)$ is shown in Figure 13, found in Appendix

2-Figures. The fitted curve shown in Figure 13 represents the case for which one-half of the fitted curves had a better fit, and one-half of fitted curves had a worse fit. In general, these median fit curves show that Equations [1] and [10] provided good fits to the experimental datasets, with the observed and predicted values for the SWRC closer than those for the unsaturated hydraulic conductivity curve.

3.3.2 Fitted $\theta(h)$ and $K(\theta)$ Curves with Median RMSE Values for Hamblen Silt Loam

The RMSE values for the curve-fitted $\theta(h)$ and $K(\theta)$ data were calculated for the Hamblen Silt Loam treatments. The median RMSE value for the curve fitted to $\theta(h)$ data was 0.0095. The fit corresponding to the median RMSE for $\theta(h)$ is shown in Figure 14 found in Appendix 2-Figures. The median RMSE value from the curves fit to $K(\theta)$ data was 0.1479. The fit associated with the median RMSE is shown in Figure 16, found in Appendix 2-Figures. Figures 14 and 15 represent typical fits, i.e., the RMSE for which one-half of the curves had a better fit and one-half of the curves had a poorer fit. Again, the goodness of fit was reasonable, with Equation [1] providing a better match to the data than Equation [10].

3.4 Soil Water Retention Curve Parameters

SWRC parameters were obtained by fitting a hydraulic function to the $\theta(h)$ data collected using the evaporation method. The van Genuchten equation (van Genuchten, 1980), Equation [1], was used, and its parameters were estimated using the Shypfit2.0 software (Peters and Durner, 2015). The saturated water content (θ_s) was included in the fits as a known (measured) parameter, while the other parameters in Equation [1]

(α, n, and θ_r) were estimated. The α values were found to be log-normally distributed, and so they were $\log_{10}$-transformed prior to conducting the ANOVA's.

3.4.1 Flint Sand $\theta(h)$ Parameters

Statistically significant differences between treatments were found for the saturated water content (θ_s) at a 95% confidence interval using a two-way ANOVA. The ANOVA did not show an interaction between treatment and experiment, however, there was an experimental effect. Hence, mean values were averaged over both growth periods. As seen in Figure 16, the control treatment had the lowest mean θ_s value, sequentially followed by the mycorrhizal control, rooted, fertilizer rooted, and mycorrhizal rooted treatments. A Tukey's HSD test was run on these data. The treatments were sorted into three Tukey groups. Figure 16, in Appendix 2-Figures, displays significant differences between the control and mycorrhizal control; the rooted and fertilizer rooted; and the mycorrhizal rooted treatments.

The $\log_{10}\alpha$ values were analyzed using a two-way ANOVA. The model was not significant at the 95% confidence interval. As a result, there were no statistically significant differences between treatments based on Tukey's HSD test (Figure 17 found in Appendix 2-Figures). However, the amount of variation among the $\log_{10}\alpha$ values for the planted treatments was qualitatively higher than for the unplanted treatments, as can be seen in Figure 17.

The fitting parameter n had statistically significant differences between treatments when compared using a two-way ANOVA at the 95% confidence interval. The ANOVA did not show an experiment effect or a significant interaction between treatment and experiment. As seen in Figure 18, in Appendix 2-Figures, the mean

values for the n parameter (averaged over both experiments) followed a trend where the control treatment had the highest mean value, and the mycorrhizal rooted treatment had the lowest mean value. When analyzed with a Tukey's HSD test, the data were separated into three groups, as presented in Figure 18. As the only value in the first Tukey group, the control treatment had the highest value for the n parameter. The second group had lower values and consisted of the mycorrhizal control and rooted treatments. The fertilizer treatment had slightly lower values and shared characteristics with both the mycorrhizal control and rooted treatment as well as the third Tukey group. The third Tukey group, which had the lowest values, was the mycorrhizal rooted group.

The residual water content (θ_r) was tested with a two-way ANOVA and did not have any significant differences between the treatments at the 95% confidence interval as shown in Figure 19; found in Appendix 2-Figures. There were no apparent visual trends in these data.

3.4.2 Hamblen Silt Loam $\theta(h)$ Parameters

The θ_s parameter did not show any statistical differences between treatments at the 95% confidence interval. Although not statistically significant, the control treatment had the least variation among samples within the treatment. The mycorrhizal control, rooted, fertilizer rooted, and mycorrhizal rooted treatments had a noticeably greater variation in their distributions, as seen in Figure 20, found in Appendix 2-Figures.

The $\log_{10}\alpha$ values were analyzed using a one-way ANOVA. As seen in Figure 21 found in Appendix 2-Figures, the $\log_{10}\alpha$ values did not have statistically significant differences at the 95% confidence interval. Although not statistically significant, the $\log_{10}\alpha$ values do show a recognizable visual trend: the lowest mean $\log_{10}\alpha$ value

belonged to the control treatment, followed sequentially by the mycorrhizal control, rooted, fertilizer rooted, and mycorrhizal rooted treatments (Figure 21).

The fitting parameter n did not have any statistically significant differences between treatments at the 95% confidence interval when compared using a one-way ANOVA and Tukey's HSD test, as seen in Figure 22 found in Appendix 2-Figures. Although not statistically significant, the n parameter does show a qualitative trend that is meaningful. The unplanted treatments had higher mean n values and greater variation than the planted treatments, as seen in Figure 22.

The θ_r curve fitting parameter for the Hamblen silt loam soil was estimated as zero for all samples. This was because the water activity measurements taken near zero were included in an effort to constrain the dry end of the SWRC. As a result, the θ_r values were excluded from statistical analysis for this soil type.

3.5 Predictive Models for the Soil Water Retention Curve

Four predictive models were selected to represent the range of behavior possible in root permeated Flint sand and Hamblen silt loam, as seen in Figures 23 and 24 in Appendix 2-Figures. For the predictive models, Rooted-model 1 assumed that roots reduced porosity; Rooted-model 2 assumed that roots reduced macroporosity; Rooted-model 3 assumed that roots increased macroporosity, and Rooted-model 4 assumed roots increased porosity.

Model-4 for describing the impact of roots on the SWRC was the predictive model that best predicted the $\theta(h)$ curves for the rooted treatments. Rooted-model 4 used fitting parameters from the average of the unrooted treatments as well as the largest measured R_v value from the root permeated treatments. The highest R_v value

was used to show the greatest difference between the control treatments and the predictive model.

The forward predictions of Rooted-model 4 were compared to actual $\theta(h)$ data from the Flint sand and Hamblen silt loam soils, as seen in Figures 25 and 26 in Appendix 2-Figures. A comparison between the parameters for Rooted-model 4 and the curves fit to the real $\theta(h)$ data from the Flint sand and Hamblen silt loam soils is listed Table 10. Rooted-model 4 was plotted against data for the unrooted and fertilizer rooted treatments. The fertilizer rooted treatment from the Flint sand soil was used for comparison purposes to better align with the influence of naturally-occurring nutrients on the rooted treatment from the silt loam soil. Rooted-model 4 suggests that the Flint sand rooted treatment increased total porosity, and slightly decreased the air entry value (i.e., increasing α), by shifting the rooted SWRC to the left as compared to the unrooted control SWRC.

For the Hamblen silt loam, the presence of roots and roots with mycorrhizal fungi had no significant influence on the $\theta(h)$ parameters as compared to the controls. The minimal impact of roots on the SWRC's for this soil was reflected in the performance of the predictive models. Rooted-model 4 was plotted against the measured $\theta(h)$ data for the unrooted and rooted treatments from the Hamblen silt loam soil (Figure 26), and there was no identifiable effect of the presence of roots in either the measured data or the forward predictions.

3.6 Unsaturated Hydraulic Conductivity Curve Parameters

The fitting software Shiftfit2.0 recommends tying the fitting of the $\theta(h)$ and $K(\theta)$ curves to improve soil hydraulic estimations of the $K(\theta)$ curve (Pertassek et al., 2015).

This approach was followed. Initially, the $K(\theta)$ data were fitted using the measured K_{sat} values. However, these values resulted in poor overall fits. Therefore, K_{sat} was treated as a fitting parameter, along with τ, when fitting the $K(\theta)$ data in conjunction with the fitting parameters for the SWRC.

3.6.1 Flint Sand $K(\theta)$ Parameters

The mean values and standard deviations of the estimated $\log_{10} K_{sat}$ values are listed in Table 11, found in Appendix 1-Tables. The estimated $\log_{10} K_{sat}$ values were statistically analyzed using a two-way ANOVA and Tukey's HSD test. The mean $\log_{10} K_{sat}$ values did not have any significant differences amongst treatments at the 95% confidence interval. Similarly, when tested with a two-way ANOVA and Tukey's HSD test, τ did not exhibit any significant differences amongst treatments at the 95% confidence interval, as shown in Figure 27 in Appendix 2-Figures. No clear trends were visible in the means or distributions of the τ values for Flint sand.

3.6.2 Hamblen Silt Loam $K(\theta)$ Parameters

The $\log_{10} K_{sat}$ values for the unsaturated hydraulic conductivity function, Equation [10], were estimated from the evaporation method. The mean values and accompanying standard deviation of the estimated $\log_{10} K_{sat}$ are listed in Table 9, found in Appendix 1-Tables. These values did not follow a trend, and when analyzed with a one-way ANOVA, no significant differences were found between treatments.

The curve fitting parameter τ was also tested with a one-way ANOVA. There was no significant difference between the treatments at the 95% confidence interval, as shown in Figure 27 found in Appendix 2-Figures. Although not statistically significant,

the variation of sample values across treatments showed an apparent trend. The unplanted treatments had a greater variation among samples and, therefore, wider a distribution than the planted treatments. The mycorrhizal rooted samples had the narrowest variation among treatments.

DISCUSSION

4.1 Plant Growth Parameters

The relationship between biological material and soil hydraulic properties was studied through the quantification of plant biomass. Plant biomass was measured in a laboratory environment; shoot biomass was dried and weighed, and root biomass was scanned, dried, and weighed to estimate root volume as well as total biomass. The results from the total biomass and root volume ratio (R_v) were statistically analyzed using ANOVA and comparison of means tests.

4.1.1 Total Biomass

The total biomass is the sum of the weighed shoot biomass and root biomass. For Flint sand, the total biomass was averaged over the two growth periods ranging from April to June and August to October. When analyzed with an ANOVA, there was a statistically significant difference between treatments. A Tukey's HSD test showed there was a difference between the rooted treatment and the fertilizer rooted and mycorrhizal rooted treatments grown in the Flint sand soil. The nonmycorrhizal plants had less above-ground biomass resulting in less total biomass. The rooted treatment had less biomass than the fertilizer rooted and mycorrhizal rooted treatments. The presence of mycorrhizal fungi increased plant growth, equivalent to the addition of fertilizer and significantly more than the untreated plants. As mutualistic symbionts, mycorrhizal fungi have been shown to increase primary elongation and radial expansion of roots by accessing nutrients that the plant roots could not acquire otherwise (Hetrick, 1991). Greater nutrient access likely allowed the mycorrhizal and fertilized plants to grow more

above-ground biomass. Contrarily, the nutrient-stressed plants tended to grow finer thinner roots with more lateral offshoots and root hairs as supported by (López-Bucio et al., 2003).

The total biomass for the silt loam was harvested from samples grown from November to January. The silt loam soil was naturally nutrient-rich due to its organic composition. As such, the fertilizer treatment was not included in the experimental setup. The results for the comparison of means between the rooted and mycorrhizal rooted treatments for the silt loam soil were not statistically significant at the 95% confidence interval. Although not statistically significant, the results from the silt loam soil mirror those of the Flint sand. The mean value of the rooted treatment was much less than the mean value for the mycorrhizal rooted treatment. The mycorrhizal rooted treatment had more variation in results and, therefore, a wider distribution of total dry weights than the rooted treatment. Some of the mycorrhizal rooted samples did not grow as consistently as the other samples in this treatment, thereby increasing variation and extending the distribution. Variablity in mycorrhizal inoculation could have influenced the growth and caused the uneven distribution of dry weights. Although inconsistent, the presence of inoculated mycorrhizal fungi increased the above-ground biomass when compared to the untreated samples. The mutualistic relationship between mycorrhizal fungi and roots has been shown to help plants gain additional nutrients in already nutrient-rich soil (Van Der Heijden et al., 2006).

In both the Flint sand and the Hamblen silt loam, the presence of mycorrhizal fungi enabled plants to grow more biomass than the non-mycorrhizal treated samples. In the nutrient-free soil, the mycorrhizal fungi performed as well as the fertilized

treatment. In the nutrient-rich organic soil, the presence of mycorrhizal fungi increased the distribution of biomass growth, with some cores achieving much better growth than others. The statistical analysis of plant biomass supported the first hypothesis that the biomass of plants with mycorrhizae fungi would be greater than the biomass of plants without mycorrhizae fungi. The effect of mycorrhizal fungi on total biomass growth has potentially far-reaching implications for enhancing sustainable agriculture practices and decreasing our reliance on supplementary fertilizer applications.

4.1.2 Root Volume Ratio (R_v)

The root volume ratio (R_v) is the ratio of total root volume to the total volume of soil. The void ratio of a root permeated soil is calculated from the input parameter R_v. The void ratio is applied in some $\theta(h)$ models to better capture the effect of roots on soil water retention (Ng et al., 2016).

The treatment means of the $\log_{10} R_v$ values for Flint sand and Hamblen silt loam were statistically different at the 95% confidence level. For the Flint sand the highest $\log_{10} R_v$ values were for the mycorrhizal rooted treatment followed by the fertilizer rooted and rooted treatments. When analyzed with a Tukey's HSD test, the rooted and mycorrhizal rooted treatments were significantly different and in separate Tukey groups. The fertilizer treatment, the intermediate value, shared characteristics with the rooted treatment, and the mycorrhizal rooted treatment.

The $\log_{10} R_v$ values for the Hamblen silt loam were also analyzed with an ANOVA and a Tukey's HSD test. These tests revealed two statistically different groupings: rooted (the lower values) and mycorrhizal rooted (the higher values). The mycorrhizal rooted treatment had the highest $\log_{10} R_v$ values across both soil types.

The presence of mycorrhizal fungi increased total root growth, thereby increasing the root volume ratio in both soil types. These results also supported the first hypothesis, in that the presence of mycorrhizal fungi promoted overall growth and resulted in a greater R_v than in the rooted treatment alone.

As R_v is a primary component in calculating void ratio; the results imply that the mycorrhizal roots filled more total pore space than the untreated roots. The ability of mycorrhizal fungi to access nutrients may have caused the inoculated roots to focus growth on primary elongation and radial expansion (Hetrick, 1991). This led to visually longer (in the vertical direction) and radially-thicker roots associated with the mycorrhizae-inoculated plants. The longer and thicker roots rearranged soil aggregates as the roots radially expanded into available macropores.

4.2 Impact of Plant Roots and Mycorrhizal Fungi on Soil Hydraulic Properties

Soil hydraulic properties were measured in a laboratory environment to experimentally investigate the impact of plant roots and mycorrhizal fungi on soil water relations. The research found that the impact of roots and mycorrhizal fungi on soil hydraulic properties was soil dependent.

The Flint sand soil had statistically significant treatment effects for K_{sat} and for the SWRC parameters θ_s and n from the van Genuchten equation detailed in Equation [1] (van Genuchten, 1980). The constant head flow experiments conducted on Flint sand verified previous research (Barley, 1954; Leung et al., 2015a; Scanlan and Hinz, 2010) that the presence of living roots decreased K_{sat} in comparison to the unplanted treatment. The significant differences among the θ_s and n van Genuchten equation parameters indicated that the shape of the SWRC differed between the unplanted and

planted treatments. Although not statistically significant at the 95% confidence level, the results for the fitted $K(\theta)$ curve provided insight into the impact of vegetation on unsaturated flow in sandy soil.

The Hamblen silt loam soil had no significant treatment effects at the 95% confidence level. However, the results from this soil showed qualitative trends suggesting an influence of plant roots and mycorrhizal fungi on soil hydraulic properties. The presence of roots and mycorrhizal fungi increased the variation of sample results within treatments. Although less clearly defined than the Flint sand soil, the results from the natural soil samples do show the influence of roots and mycorrhizal fungi on soil hydraulic properties.

4.2.1 Saturated Hydraulic Conductivity, K_{sat}

The saturated hydraulic conductivity, K_{sat}, is a measure of the rate of water conductance through a saturated medium. It was hypothesized that the presence of roots and mycorrhizal fungi would partially fill macropores and therefore decrease the saturated hydraulic conductivity of the soil. This hypothesis was tested through a statistical comparison of treatment means with an ANOVA. This analysis demonstrated how the presence and absence of mycorrhizal fungi, in conjunction with plant roots, impacted K_{sat}.

It was found that the $\log_{10} K_{sat}$ measurements for the Flint sand soil supported the premise of our hypothesis, i.e., the presence of roots resulted in statistically lower mean $\log_{10} K_{sat}$ values in comparison to the other treatments.

Although not statistically significant the K_{sat} results for the natural silt loam soil offered insight into the intricate relationships between soil, vegetation, and K_{sat}. For the

Hamblen silt loam soil the $\log_{10} K_{sat}$ measurements from the mycorrhizal and root-permeated treatments resulted in greater variation among the replicate sample cores. As a result, the measurements for this soil did not support the hypothesis of a reduction in mean saturated hydraulic conductivity due to the presence of roots and mycorrhizal.

The disparity in the K_{sat} results between the two soil types were likely due to the different textures and nutrient statuses of the two soil types. The K_{sat} values for the Hamblen silt loam were between 2 and 4 orders of magnitude lower than those for the Flint sand. The Hamblen soil loam soil was repacked and had few macropores and low inherent conductivity, whereas the coarse-grained Flint sand had many macropores and was highly conductive. As a result, roots and fungal hyphae were able to readily fill these macropores and reduce the saturated hydraulic conductivity of the Flint sand. With the silt loam soil, the presence of roots and mycorrhizal fungi simply increased the variation of the treated samples.

The impact of roots on K_{sat} is soil dependent and is influenced by how roots change soil structure as they grow. As a root develops, the root tip of the growing root is forced into similarly-sized soil pores. Over time, the growing root swells and causes a shift in the arrangement of soil particles (Hillel, 2004). This process either increases soil porosity and thereby reduces bulk density or causes soil pores to become plugged, thereby reducing porosity. The statistically lower K_{sat} values for the rooted treatment in the Flint sand soil suggested that the roots reduced macroporosity via pore plugging (Sedgley and Barley, 1954).

The growth pattern of roots is nutrient-dependent. Nutrient deficiency causes the growth of plant roots to change from primary root elongation to the formation of lateral

roots and root hairs (López-Bucio et al., 2003). In order to access limited nutrients, the roots in the nutrient-deficient Flint sand treatment had to increase the growth of lateral roots and root hairs. The greater lateral growth observed with the rooted treatment likely also increased pore blocking in comparison to fertilizer rooted and mycorrhizal rooted treatments. The pore-blocking effect was not seen in the fertilizer treatment due to the addition of supplementary nutrients. Additionally, the pore blocking effect was not seen in the mycorrhizal rooted treatment due to the ability of mycorrhizal to access additional nutrients not available to the nonmycorrhizal treatment (Figure 10).

The lack of statistical significance between treatments in the Hamblen silt loam was likely due to the increased availability of nutrients in the fine-textured soil. With access to available nutrients, the rooted treatment from the silt loam soil did not have to sacrifice primary root elongation for lateral root growth. The lack of substantial pore plugging resulted in little difference between the planted treatments and unplanted treatments in this soil.

4.2.3 RMSE from Fitting SWRC and Unsaturated Hydraulic Conductivity

The root mean square error (RMSE) is a measure of the average deviation between the fitted model and measured data. There was no statistical difference between the fit of the RMSE values by treatment. However, the RMSE values for Flint sand indicated a more accurate fit than the RMSE values for the Hamblen silt loam.

The fits with the median RMSE values for $\theta(h)$ and $K(\theta)$ for the Flint sand and Hamblen, silt loam were selected for detailed scrutiny. In the Flint sand, the van Genuchten model tended to underestimate θ_s values and over predict θ_r values. In the silt loam soil, the van Genuchten model failed to capture the shape of the break in the

SWRC, related inversely to α, while underpredicting θ_s values. Additionally, the fit of the $\theta(h)$ curve for the silt loam soil was impacted by the water activity measurements which resulted in estimated θ_r values of zero. The slight contrast between the fitted curve and the actual data could be due to the simultaneous fitting of curves to the $\theta(h)$ and $K(\theta)$ data by the Shiftfit2.0 software. Although the curve-fit applied to $K(\theta)$ data improved when tied to the fit of the $\theta(h)$, it resulted in slightly poorer fits for $\theta(h)$ data.

4.2.4 SWRC Parameters

The SWRC characterized the static hydraulic properties of the Flint sand and Hamblen silt loam soils by providing a measure of water availability. The shape of the SWRC is dependent upon the relationship between soil porosity and vegetation, which influences water retention (Ni et al., 2018). The third hypothesis stated that the presence of roots and mycorrhizal fungi would change the shape of the SWRC near saturation. The hypothesis was tested through a statistical comparison of group means with an ANOVA and a Tukey's HSD test. Analysis of the θ_s, α, n, and θ_r parameters from the van Genuchten equation, Equation [1], demonstrated how the presence and absence of mycorrhizal fungi, in conjunction with plant roots, impacted soil water retention.

The water content of the sample at saturation (θ_s) was experimentally determined using the sample bulk density and an assumed specific gravity of 2.65 for the Flint sand and silt loam soils. When analyzed with a Tukey's HSD test, the mean θ_s values for the three rooted treatments in the Flint sand were found to be statistically different from the two control treatments. The presence of roots, fertilizer + roots, and mycorrhizae + roots all increased θ_s in Flint sand soil relative to the controls with no roots. The mean θ_s

values for the silt loam treatments were not statistically different at the 95% confidence interval. Although not a statistically significant result, the presence of roots and mycorrhizal fungi in silt loam soil appeared to increase the variability of the θ_s results.

Assuming complete water saturation (i.e., no trapped air), the θ_s is equivalent to the porosity, which is inversely related to the dry bulk density. Therefore, roots impacted the porosity and soil structure as they grew in the Flint sand. As roots filled pore spaces, they radially expanded. In consolidated porous media, the growing roots would clog the open pore space and cause a reduction in porosity and θ_s. In the unconsolidated Flint sand, however, the growing roots caused a shift in the arrangement of grains within the rhizosphere. Root pressure likely created an increase in the pore space around the roots. The growing roots thus caused a decrease in bulk density as the soil volume expanded. Rather than decreasing θ_s due to porosity loss, the roots actually decreased bulk density and increased θ_s in root permeated soil. The same effect was not seen in the Hamblen silt loam due to the inherently high porosity of this soil.

The variable α is a shape parameter that is inversely related to the air entry point of the soil. The α parameter controls the break in the SWRC, a point at which water content starts to decline rapidly with increasing pressure head. The α parameter, when analyzed as the $\log_{10}$ of α was not statistically significant at the 95% confidence interval for either the Flint sand or silt loam soil. Overall, the presence of roots and mycorrhizal fungi did not influence mean $\log_{10}$ α values. The lack of statistical significance for α in either soil is surprising as some predictive models for root permeated soil rely on α as the primary indicator for root influence in soils (see section 3.5). Although not statistically significant, there is visual evidence for the Flint sand of a slight shift in the

SWRC to the left, which is indicative of a lower air-entry value and a slightly higher α value (Figure 17).

The n parameter controls the slope of the SWRC. The slope of the curve represents the pore-size distribution. Higher n values denote steeper slopes and narrower pore-size distributions, while lower n values indicate more gradual slopes and broader pore-size distributions (Bodner et al., 2014; Rachman et al., 2004).

There were statistically significant differences in n amongst the treatments at the 95% confidence interval for the Flint sand when analyzed with an ANOVA and a Tukey's HSD test. The unrooted controls had the highest n values and, consequently, the steepest slopes. Slope steepness decreased in the mycorrhizal control, rooted, fertilizer rooted, and mycorrhizal rooted treatments, indicating that roots and fungal hyphae expanded the pore-size distribution.

When analyzed with a one-way ANOVA, the n values for the Hamblen silt loam were not statistically significant at the 95% confidence interval. Although not statistically significant, the mean n values for this soil did share a similar trend to the mean values for the Flint sand treatments. The mean n values for the unplanted treatments were qualitatively higher than the mean n-values for the planted treatments, suggesting that the presence of roots and mycorrhizal fungi also contributed to a broadening of the pore-size distribution in comparison to the control treatment for the silt loam soil.

The trends discussed above for the Flint sand and, to a lesser extent, the Hamblen silt loam, support the third hypothesis. The presence of roots and roots with mycorrhizal fungi increased the porosity and decreased the n parameter and thereby changed the shape of the soil water retention curve close to saturation when compared

to bare soil. The n parameter, in particular, was highly influenced by root-induced changes in pore-size distribution. As roots grew in the Flint sand, the pore-size distribution became broader, with increases in the numbers of both larger and smaller pores. The presence of roots also caused an increase in the overall porosity, as seen in the results.

Mycorrhizal fungi caused a broadening of the pore-size distribution through the promotion of enhanced root growth, as outlined above. This is consistent with the work of (Hosseini et al., 2016), who showed statistically lower n values for their fungal endophyte treatment, when compared to the other treatments. Interestingly, the present study appears to be relatively novel in finding a strong effect of roots and mycorrhizae on the porosity and slope of the SWRC. Most previous studies have reported strong statistical differences amongst α values, and we did not see this effect.

The residual water content (θ_r) is the amount of water remaining in the soil at very high capillary pressure heads. As explained previously, the θ_r parameter was only analyzed for the Flint sand soil. The θ_r parameter for the sit loam soil was estimated as zero due to the influence of the additional water activity measurements to the SWRC. For Flint sand, the θ_r parameter showed no significant differences between treatments at the 95% confidence interval. Tellingly, information on θ_r is rarely reported in the literature; in one of the few studies to investigate the effects of roots on residual water content, Leung (2015b) found that θ_r was consistent across root-permeated and bare soil, supporting our observation of lack of statistical significance for this parameter.

4.2.4 SWRC Predictive Models

Rooted-model 4 mirrored the measured $\theta(h)$ data from the rooted fertilizer treatment indicating that the presence of roots increased total porosity in the Flint sand soil. The predictive model and rooted data for the Flint sand were visually offset from the data for the unrooted bare soil. The presence of roots caused the rooted data and predictive model to have a higher θ_s than the unrooted data. The rooted data and predictive model also had their break in the curve, inversely related to α, slightly before the unrooted data. The predictive model clearly reflects the impact of roots on initially low porosity soil. In the Flint sand, roots increased porosity while simultaneously clogging pore spaces and preventing preferential water flow.

The predictive models for the Hamblen silt loam were less useful forecasters of the impact of roots on the SWRC soil since there were only minimal differences between treatments due to roots. The higher porosity associated with silt loam soil resulted in R_v having little impact on the model predictions. All forward prediction models were visually similar, with rooted-model 4 slightly greater than the control and rooted-model 3 slightly less than the control. When compared to real data for the unrooted and root permeated treatments, the forward prediction, rooted-model 4, slightly underestimated θ_s. The predictive model also slightly underestimated the break in the curve, which was inversely related to α. However, these differences were minimal, and the main message is that neither the data nor the model predictions indicted any significant impact of roots on the SWRC of this high porosity soil.

4.2.5 Unsaturated Hydraulic Conductivity Parameters

The unsaturated hydraulic conductivity function used by the fitting software Shypfit2.0 was Equation [10] (Mualem, 1976). The fitting parameter τ, an empirical fitting parameter for pore tortuosity and pore connectivity, was estimated as well as an estimated saturated hydraulic conductivity K_{sat} (Pertassek et al., 2015). Neither the estimated K_{sat} or τ parameter from the unsaturated hydraulic conductivity fits resulted in any statistically significant differences between the treatments at the 95% confidence interval for either the Flint sand or Hamblen silt loam.

These results contradicted the fourth hypothesis, which stated that root and mycorrhizal hyphae derived changes in pore connectivity would increase the unsaturated hydraulic conductivity of the soil. Due to Poiseuille's law, larger pore spaces conduct more water than smaller pore spaces (Scott, 2000). The larger preferential flow paths were the first to be lost under partially-saturated conditions leaving behind the smaller pores for water conductance. The presence of roots was expected to decrease the amount of open preferential flow paths via pore-clogging and therefore skew open pore spaces toward smaller pore radii. The impact of this process, however, was not reflected in the results.

Instead, the rooted and mycorrhizal rooted treatments were undifferentiable from the control treatment. As the root permeated soils desaturated, there was no increase in unsaturated flow through smaller pore spaces. In the Flint sand, the radially expanding roots simultaneously increased macroporosity while inducing pore-clogging. Interestingly, while pore-clogging influenced other parameters, such as measured K_{sat} and n, there was no effect on $K(\theta)$. The lack of statistical significance in the silt loam

was predictable; as a fine-textured soil, the presence of roots and mycorrhizal fungi generally show less impact on soil structure overall (Lehmann et al., 2017). The lack of statistical significance also likely reflects the variability of $K(\theta)$ often found in nature.

CONCLUSIONS, LIMITATIONS, AND SUGGESTIONS FOR FUTURE RESEARCH

This research aspired to investigate the influence of roots and mycorrhizal fungi on the flow and retention of water in soil through the statistical comparison of hydraulic parameters. The influence of vegetation on soil hydraulic parameters was explored through the application of laboratory experiments and quantification of plant biomass and root volume ratios (R_v). Using this approach, statistically significant relationships were found between biological parameters and soil hydraulic properties.

Plant biomass was measured by weighing the total biomass after oven drying. The amount of roots present in the soil was obtained by measuring the root volume and calculating R_v. Physical measurements in a laboratory environment were conducted to measure K_{sat}, $\theta(h)$, and $K(\theta)$. Forward predictive models were developed from the calculated R_v values and the hypothesized impacts of roots on the soil water retention parameters.

In both soil types, the presence of roots with mycorrhizal fungi increased total biomass. This increase in biomass was reflected in the mean R_v values, which were statistically higher for the mycorrhizal rooted treatment than for the rooted treatment in both Flint sand and Hamblen silt loam. The impact of the significantly higher R_v values was reflected in the predictive models for Flint sand, where root-model 4 (increased porosity) gave the best representation of the SWRC curve for rooted soil. The R_v values for the Hamblen silt loam were not large enough to influence the forward models' predictions due to the high initial porosity of this soil. In other words, Root-Model 4 was successful in predicting the impact of roots on the SWRC for the relatively low porosity

Flint sand, but was unable to identify any effect of roots on the SWRC on high porosity soil. Both sets of predictions were supported by the experimental data.

In the Flint sand, roots increased porosity while simultaneously clogging pore spaces and preventing preferential water flow. This effect of plant roots on porosity was reflected in the shape of the SWRC where the presence of roots increased θ_s and decreased n. The presence of roots inoculated with mycorrhizal fungi further accentuated these effects in the Flint sand. The growth of roots in nutrient deficient soil was reflected in the root architecture. With limited nutrients, the rooted treatment from the Flint sand had a statistically lower K_{sat} due to the root blockage of preferential flow paths. This decrease in K_{sat} was not reflected in the fertilizer rooted and mycorrhizal rooted treatments due to greater nutrient access, which likely influenced root morphology and the extent of pore plugging.

The influence of roots on soil hydraulic properties was not reflected in the Hamblen silt loam results, as none of the treatments were statistically different from each other. Although not statistically significant, the SWRC results for this soil were consistent with prior studies involving high porosity, natural soils. The present study appears to be one of the first to compare $K(\theta)$ parameters between bare, rooted, and mycorrhizal rooted soils. However, evidence showed that neither roots nor roots with mycorrhizal fungi had any pronounced influence on unsaturated flow parameters in either Flint sand or Hamblen silt loam under the conditions of these experiments.

In most cases, the presence of mycorrhizal fungi furthered the impact of roots on the SWRC for the low porosity soil. Mycorrhizal fungi accentuated the influence of roots on key soil hydraulic parameters. The presence of mycorrhizal fungi promoted overall

growth and resulted in greater total biomass and R_v. The presence of roots and roots with mycorrhizal fungi changed the shape of the SWRC for Flint sand in comparison to roots, with mycorrhizal fungi moving the curve upward by increasing macroporosity and changing the pore-size distribution thereby decreasing the slope. In Flint sand, roots with mycorrhizal fungi had a greater influence on hydraulic properties than roots alone.

This research has several limitations worth devoting more time and research into investigating. Due to the nature of the relatively short growth periods, the effect of roots and mycorrhizal fungi on soil hydraulic properties was limited by time. Literature has shown that the effect of roots on pore plugging is time-dependent with the aging and death of roots opening root-created macropores and increasing saturated flow via preferential flow paths (Leung et al., 2015b; Ng et al., 2016; Scholl et al., 2014).

Additionally, the research is limited by the lack of soil diversity, and replication in the case of the Hamblen silt loam. Soil water retention curves are temporally and spatially variable with a different curve required for not only different soil types, but also different soil horizons, and under wetting versus drying conditions. Extension of this research to a wider range of soil types and including hysteresis would be valuable. Increased replication would increase the ability of the statistical analyses to identify significant treatment effects.

This study investigated the impact of mycorrhizal fungi and switchgrass on soil hydraulic properties; however, there is potential for different mycorrhizal-plant associates to have alternate results. Outside of a controlled environment, multiple sub-species of mycorrhizal fungi can associate with a plant simultaneously. Separate species have been known to compete for access to resources and mutualistic plant

assimilates. Therefore, a multi-mycorrhizal association could affect hyphal-impact on soil hydraulic properties differently, and is worth investigating.

Additional research is needed to grasp the full impact of roots with mycorrhizal fungi on soil hydraulic properties. Research into multiple plant-fungal associates in various soil types would give the best representation of mycorrhizal fungi on soil hydraulic properties. Further research into the hydraulic properties of mycorrhizal-plant associates grown in disturbed and undisturbed natural soil conditions is also warranted. A long-term study into different plant and fungal associates in multiple soil types with increased replication would give the best representation of the impacts of roots and mycorrhizal fungi on soil hydraulic properties.

LIST OF REFERENCES

Akhzari D. (2015) Response ofGlycyrrhiza glabraL. to Arbuscular Mycorrhizal Fungi and Water Stress. Journal of Essential Oil Bearing Plants 18:992-1002. DOI: 10.1080/0972060x.2014.890085.

Aravena J.E., Berli M., Ruiz S., Suárez F., Ghezzehei T.A., Tyler S.W. (2014) Quantifying coupled deformation and water flow in the rhizosphere using X-ray microtomography and numerical simulations. Plant and Soil 376:95-110. DOI: 10.1007/s11104-013-1946-z.

Aravena J.N.E., Berli M., Ghezzehei T.A., Tyler S.W. (2011) Effects of Root-Induced Compaction on Rhizosphere Hydraulic Properties - X-ray Microtomography Imaging and Numerical Simulations. Environmental Science & Technology 45:425-431. DOI: 10.1021/es102566j.

Assouline S. (2006) Modeling the Relationship between Soil Bulk Density and the Water Retention Curve. Vadose zone journal : VZJ. 5:554-563. DOI: 10.2136/vzj2005.0083.

Assouline S., Or D. (2014) The concept of field capacity revisited: Defining intrinsic static and dynamic criteria for soil internal drainage dynamics. Water Resources Research 50:4787-4802. DOI: 10.1002/2014wr015475.

Augé R.M., Stodola A.J.W., Tims J.E., Saxton A.M. (2001) Moisture retention properties of a mycorrhizal soil. Plant and Soil 230:87-97. DOI: 10.1023/A:1004891210871.

Augé R.M., Sylvia D.M., Park S., Buttery B.R., Saxton A.M., Moore J.L., Cho K. (2004) Partitioning mycorrhizal influence on water relations of Phaseolus vulgaris into soil and plant components. Canadian Journal Bottany 82:503-514. DOI: 10.1139/b04-020.

Barley K.P. (1954) Effects of Root Growth and Decay on The Permeability of a Synthetic Sandy Loam. Soil Science 78:205-210. DOI: 10.1097/00010694-195409000-00005.

Besserer A., Puech-Pagès V., Kiefer P., Gomez-Roldan V., Jauneau A., Roy S., Portais J.-C., Roux C., Bécard G., Séjalon-Delmas N. (2006) Strigolactones Stimulate Arbuscular Mycorrhizal Fungi by Activating Mitochondria. PLoS Biology 4:e226. DOI: 10.1371/journal.pbio.0040226.

Bitterlich M., Franken P., Graefe J. (2018) Arbuscular Mycorrhiza Improves Substrate Hydraulic Conductivity in the Plant Available Moisture Range Under Root Growth Exclusion. Frontiers in Plant Science 9. DOI: 10.3389/fpls.2018.00301.

Bodner G., Leitner D., Kaul H.P. (2014) Coarse and fine root plants affect pore size distributions differently. Plant and Soil 380:133-151. DOI: 10.1007/s11104-014-2079-8.

Brito I., de Mario C., Goss M.J. (2009) Techniques for Arbuscular Mycorrhiza Inoculum Reduction Symbiotic Fungi. Soil Biology 18:307-318. DOI: 10.1007/978-3-540-95894-9_19

Campbell G.S., Campbell C.S., Rivera L., D.R. C., B. C.L., Chambers C. (2017) How to generate a soil moisture characteristic using the WP4C, Meter Environment Knowledge Base Meter Group Munich, Germany

Carminati A., Moradi A.B., Vetterlein D., Vontobel P., Lehmann E., Weller U., Vogel H.-J., Oswald S.E. (2010) Dynamics of soil water content in the rhizosphere. Plant and Soil 332:163-176. DOI: 10.1007/s11104-010-0283-8.

Czarnes S., Hallett P.D., Bengough A.G., Young I.M. (2000) Root- and microbial-derived mucilages affect soil structure and water transport. European Journal of Soil Science 51:435-443. DOI: 10.1046/j.1365-2389.2000.00327.x.

Daly K.R., Mooney S.J., Bennett M.J., Crout N.M.J., Roose T., Tracy S.R. (2015) Assessing the influence of the rhizosphere on soil hydraulic properties using X-ray computed tomography and numerical modelling. Journal of Experimental Botany 66:2305-2314. DOI: 10.1093/jxb/eru509.

Dane J.H., Topp G.C. (2002) Methods of Soil Analysis: Part 4, Physical Method Soil Science Society of America, Madison, WI.

Davis J.C. (2002) Statistics and Data Analysis in Geology. 3rd ed. Wiley and Sons, New York.

Daynes C.N., Field D.J., Saleeba J.A., Cole M.A., McGee P.A. (2013) Development and stabilisation of soil structure via interactions between organic matter, arbuscular mycorrhizal fungi and plant roots. Soil biology & biochemistry. 57:683-694. DOI: 10.1016/j.soilbio.2012.09.020.

Dexter A.R. (1987) Compression of soil around roots. Plant and Soil 97:401-406. DOI: 10.1007/bf02383230.

Dhiman I., Bilheux H., DeCarlo K., Painter S.L., Santodonato L., Warren J.M. (2018) Quantifying root water extraction after drought recovery using sub-mm in situ empirical data. Plant and Soil 424:73-89. DOI: 10.1007/s11104-017-3408-5.

Durner W. (1994) Hydraulic conductivity estimation for soils with heterogeneous pore structure. Water Resources Research 30:211-223. DOI: 10.1029/93wr02676.

Feddes R., Hoff H., Bruen M., Dawson T. (2001) Modeling root water uptake in hydrological and climate models. Bulletin of the American Meteorological Society 82:2797-2809. DOI: 10.1175/1520-0477(2001)0822.3.CO;2.

Gallipoli D., Wheeler S.J., Karstunen M. (2003) Modelling the variation of degree of saturation in a deformable unsaturated soil. Géotechnique 53:105-112. DOI: 10.1680/geot.2003.53.1.105.

Gehring C.A. (2017) Introduction: Mycorrhizas and Soil Structure, Moisture, and Salinity, in: N. Johnson, et al. (Eds.), Mycorrhizal Mediation of Soil, Elsevier Inc. pp. 235-240.

Guha A., Han J., Cummings C.R., McLennan D.A., Warren J.M. (2018) Differential ecophysiological responses and resilience to heat wave events in four co-occurring temperate tree species. Environmental Research Letters 13. DOI: 10.1088/1748-9326/aabcd8.

Hallett P., Feeney D., Bengough A., Rillig M., Scrimgeour C., Young I. (2009) Disentangling the impact of AM fungi versus roots on soil structure and water transport. Plant and Soil 314:183-196. DOI: 10.1007/s11104-008-9717-y.

Hetrick B.A.D. (1991) Mycorrhizas and root architecture. Experientia 47:355-362. DOI: 10.1007/bf01972077.

Hillel D. (2004) Introduction to environmental soil physics Elsevier Academic Press, Amsterdam.

Hosseini F., Mosaddeghi M.R., Hajabbasi M.A., Sabzalian M.R. (2016) Role of fungal endophyte of tall fescue (Epichloë coenophiala) on water availability, wilting point and integral energy in texturally-different soils. Agricultural Water Management 163:197-211. DOI: 10.1016/j.agwat.2015.09.024.

Jarvis S., Woodward S., Alexander I.J., Taylor A.F. (2013) Regional scale gradients of climate and nitrogen deposition drive variation in ectomycorrhizal fungal communities associated with native Scots pineane. Glob Chang Biol 19:1688-96. DOI: 10.1111/gcb.12178.

Johnson M.S., Lehmann J. (2006) Double-funneling of trees: Stemflow and root-induced preferential flow. Écoscience 13:324-333. DOI: 10.2980/i1195-6860-13-3-324.1.

Jotisankasa A., Sirirattanachat T. (2017) Effects of grass roots on soil-water retention curve and permeability function. Canadian Geotechnical Journal 54:1612-1622. DOI: 10.1139/cgj-2016-0281.

Kang M., Bilheux H.Z., Voisin S., Cheng C.L., Perfect E., Horita J., Warren J.M. (2013) Water calibration measurements for neutron radiography: Application to water content quantification in porous media. Nuclear instruments & methods in physics research. 708:24-31. DOI: 10.1016/j.nima.2012.12.112.

Kosugi K.I. (1996) Lognormal Distribution Model for Unsaturated Soil Hydraulic Properties. Water Resources Research 32:2697-2703. DOI: 10.1029/96wr01776.

Lehmann A., Leifheit E.F., Rillig M.C. (2017) Mycorrhizas and Soil Aggregation, in: N. C. Johnson, et al. (Eds.), Mycorrhizal Mediation of Soil Fertility, Structure, and Carbon Storage Elsevier pp. 526.

Leung A.K., Garg A., Coo J.L., Ng C.W.W., Hau B.C.H. (2015a) Effects of the roots of Cynodon dactylon and Schefflera heptaphyllaon water infiltration rate and soil hydraulic conductivity. Hydrological Processes 29:3342-3354. DOI: 10.1002/hyp.10452.

Leung A.K., Garg A., Ng C.W.W. (2015b) Effects of plant roots on soil-water retention and induced suction in vegetated soil. Engineering Geology 193:183-197. DOI: https://doi.org/10.1016/j.enggeo.2015.04.017.

López-Bucio J., Cruz-RamíRez A., Herrera-Estrella L. (2003) The role of nutrient availability in regulating root architecture. Current Opinion in Plant Biology 6:280-287. DOI: 10.1016/s1369-5266(03)00035-9.

Moradi A.B., Carminati A., Vetterlein D., Vontobel P., Lehmann E., Weller U., Hopmans J.W., Vogel H.-J., Oswald S.E. (2011) Three-dimensional visualization and quantification of water content in the rhizosphere. New Phytologist 192:653-663. DOI: 10.1111/j.1469-8137.2011.03826.x.

Mualem Y. (1976) A new model for predicting the hydraulic conductivity of unsaturated porous media. Water Resources Research 12:513-522. DOI: 10.1029/wr012i003p00513.

Ng C.W.W., Ni J.J., Leung A.K., Wang Z.J. (2016) A new and simple water retention model for root-permeated soils. Géotechnique Letters 6:106-111. DOI: 10.1680/jgele.15.00187.

Ni J.J., Leung A.K., Ng C.W.W. (2018) Modelling effects of root growth and decay on soil water retention and permeability. Canadian Geotechnical Journal 56:1049-1055. DOI: 10.1139/cgj-2018-0402.

Oswald S.E., Menon M., Carminati A., Vontobel P., Lehmann E., Schulin R. (2008) Quantitative Imaging of Infiltration, Root Growth, and Root Water Uptake via Neutron Radiography. Vadose Zone Journal 7:1035-1047. DOI: 10.2136/vzj2007.0156.
Pertassek T., Peters A., Durner W. (2015) HYPROP-FIT Software User's Manual, V.3.0,, in: M. G. AG (Ed.), Mettlacher Str. 8, 81379 München, Germ any. pp. 66.
Peters A., Durner W. (2006) Improved estimation of soil water retention characteristics from hydrostatic column experiments. Water Resources Research 42:n/a-n/a. DOI: 10.1029/2006WR004952.
Peters A., Durner W. (2008) Simplified evaporation method for determining soil hydraulic properties. Journal of Hydrology 356:147-162. DOI: 10.1016/j.jhydrol.2008.04.016.
Peters A., Durner W. (2015) SHYPFIT 2.0 User's Manual Institut für Ökologie, Technische Universität Berlin, Germany
Peters A., Iden S.C., Durner W. (2015) Revisiting the simplified evaporation method: Identification of hydraulic functions considering vapor, film and corner flow. Journal of Hydrology 527:531-542. DOI: 10.1016/j.jhydrol.2015.05.020.
Petersson H., Messing I., Steen E. (1987) Influence of root mass on saturated hydraulic conductivity in arid soils of central Tunisia. Arid Soil Research and Rehabilitation 1:149-160. DOI: 10.1080/15324988709381140.
Powis V.B., Whalley W.R., Bird N.R.A., Leeds-Harrison P.B. (2003) Some mechanisms responsible for the alteration of soil hydraulic properties by root activity in: H. M. Moore, et al. (Eds.), Land Reclamation-Extending Boundaries: Proceedings of the 7th Internation Conference, Runcorn, UK, 13-16 May Swets and Zeitlinger, Lisse pp. 404.
Querejeta J.I. (2017) Soil Water Retention and Availability as Influenced by Mycorrhizal Symbiosis, in: N. C. Johnson, et al. (Eds.), Mycorrhizal Mediation of Soil: Fertility Structure and Carbon Storage Elsevier. pp. 299-317.
Rachman A., Anderson S.H., Gantzer C.J., Alberts E.E. (2004) Soil Hydraulic Properties Influenced by Stiff-Stemmed Grass Hedge Systems. Soil Science Society of America Journal 68:1386-1393. DOI: 10.2136/sssaj2004.1386.
Robinson D.A., Hopmans J.W., Filipovic V., Van Der Ploeg M., Lebron I., Jones S.B., Reinsch S., Jarvis N., Tuller M. (2019) Global environmental changes impact soil hydraulic functions through biophysical feedbacks. Global Change Biology 25:1895-1904. DOI: 10.1111/gcb.14626.
Samaei F., Asghari S., Aliasgharzad N. (2015) The effects of two arbuscular mycorrhizal fungi on some physical properties of a sandy loam soil and nutrients uptake by spring barley. Journal of Soil Environment 1:1-9.
Scanlan C. (2009) Processes and Effects of Root Induced Changes to Soil Hydraulic Properties School of Earth and Environment, University of Western Australia
Scanlan C., Hinz C. (2010) Insight into the processes and effects of rootinduced changes to soil hydraulic properties, Proceedings of the 19th World Congress of Soil Science, Soil Solutions For a Changing World.
Schindler U., Durner W., Von Unold G., Müller L. (2010) Evaporation Method for Measuring Unsaturated Hydraulic Properties of Soils: Extending the

Measurement Range. Soil Science Society of America Journal 74:1071-1083. DOI: 10.2136/sssaj2008.0358.
Scholl P., Leitner D., Kammerer G., Loiskandl W., Kaul H.P., Bodner G. (2014) Root induced changes of effective 1D hydraulic properties in a soil column. Plant and Soil 381:193-213. DOI: 10.1007/s11104-014-2121-x.
Scott H.D. (2000) Soil physics : agricultural and environmental applications. 1st ed. ed. Wiley-Blackwell, Iowa State University Press, Ames, IA.
Sedgley R.H., Barley K.P. (1954) Effects of root growth and decay on the permeability of a synthetic sandy loam. Soil Science 78:205-210.
Sedgley R.H., Barley K.P. (1958) Effects of root growth and decay on the capillary conductivity of a sandy loam at low soil-moisture tension. Soil Science 86:175-179. DOI: 10.1097/00010694-195810000-00002
Seneviratne S.I., Corti T., Davin E.L., Hirschi M., Jaeger E.B., Lehner I., Orlowsky B., Teuling A.J. (2010) Investigating soil moisture–climate interactions in a changing climate: A review. Earth Science Reviews 99:125-161.
N.R.C.S. (2019) Soil Survey of Roane County, Tennessee, in: U. S. D. o. Agriculture (Ed.).
Shao W., Ni J., Leung A.K., Su Y., Ng C.W.W. (2017) Analysis of plant root–induced preferential flow and pore-water pressure variation by a dual-permeability model. Canadian Geotechnical Journal 54:1537-1552. DOI: 10.1139/cgj-2016-0629.
Thomas R.S., Dakessian S., Ames R.N., Brown M.S., Bethlenfalvay G.J. (1986) Aggregation of a Silty Clay Loam Soil by Mycorrhizal Onion Roots. Soil Science Society of America Journal 50:1494-1499. DOI: 10.2136/sssaj1986.03615995005000060023x.
Tuli A., Hopmans J.W., Rolston D.E., Moldrup P. (2005) Comparison of Air and Water Permeability between Disturbed and Undisturbed Soils. Soil Science Society of America Journal 69:1361-1371. DOI: 10.2136/sssaj2004.0332.
US Silica Company (2010) Material Safety Data Sheet-Silica Sand and Ground Silica, US Silica Company.
Van Der Heijden M.G.A., Streitwolf-Engel R., Riedl R., Siegrist S., Neudecker A., Ineichen K., Boller T., Wiemken A., Sanders I.R. (2006) The mycorrhizal contribution to plant productivity, plant nutrition and soil structure in experimental grassland. New Phytologist 172:739-752. DOI: 10.1111/j.1469-8137.2006.01862.x.
van Genuchten M.T. (1980) A Closed-form Equation for Predicting the Hydraulic Conductivity of Unsaturated Soils1. Soil Science Society of America Journal 44:892-898. DOI: 10.2136/sssaj1980.03615995004400050002x.
Verma S., Varma A., Rexer K.-H., Hassel A., Kost G., Sarbhoy A., Bisen P., Bütehorn B., Franken P. (1998) Piriformospora indica, gen. et sp. nov., a New Root-Colonizing Fungus. Mycologia 90:896-903. DOI: 10.2307/3761331.
Weiß M., Waller F., Zuccaro A., Selosse M.A. (2016) Sebacinales – one thousand and one interactions with land plants. New Phytologist 211:20-40. DOI: 10.1111/nph.13977.
Whalley W.R., Riseley B., Leeds-Harrison P.B., Bird N.R.A., Leech P.K., Adderley W.P. (2005) Structural differences between bulk and rhizosphere soil. European Journal of Soil Science 56:353-360. DOI: 10.1111/j.1365-2389.2004.00670.x.

Yan W.M., Zhang G. (2015) Soil-water characteristics of compacted sandy and cemented soils with and without vegetation. Canadian Geotechnical Journal 52:1331-1344. DOI: 10.1139/cgj-2014-0334.
Zhuang J., Flury M., Jin Y. (2003) Colloid-facilitated Cs transport through water-saturated Hanford sediment and Ottawa sand. Environmental science & technology 37:4905-4911. DOI: 10.1021/es0264504.

APPENDIX 1 - TABLES

Table 1: Pressure head and pore-size distribution parameters for various $\theta(h)$ models.

Model		Pressure head parameters	Pore-size distribution parameters
van Genuchten (1980),	Eq. (1)	α	n, m
Kosugi (1996),	Eq. (2)	h_m	σ
Gallipoli et al. (2003),	Eq. (3)	ψ, ω	n, m
Daynes et al. (2003),	Eq. (4)	χ	β
Augé et al. (2001, 2004),	Eq. (5)	λ	μ, δ
Durner et al. (1994),	Eq. (6)	α	n

Table 2: Selected physical and chemical soil properties of Flint sand and Hamblen silt loam.

Soil	Texture	Organic Matter ($wt\ \%$)	pH	Specific Gravity	CEC $(cmolc/kg)$
Flint Sand	Sand	0*	6.0 – 8.0[a]	2.65[a]	0.6[b]
Hamblen Silt Loam	Silty clay loam	0.2 - 1.0[c]	5.0 - 7.0[c]	2.65*	3.7 - 7.6[c]

[a] US Silica Company
[b] Zhuang et al. 2003
[c] Soil Survey of Roane County Tennessee, 2019
* Assumed Value

Table 3: Average greenhouse climatic conditions (Guha et al., 2018).

	Air Temperature (ºC)	Relative Humidity (%)	Photosynthetically Active Radiation (µmol m^{-2} s^{-1})
Day	24	35	500
Night	18	41	0

Table 4: Predictive models for root-influenced SWRC parameters.

Model	θ_s in presence of roots	α in presence of roots	References
Root Model 1	$(\theta_s)_{root} = \theta_s - R_v$	$\alpha_{root} = \alpha\left(\frac{1-(\theta_s)_{root}}{1-\theta_s}\right)^{3.72}$	Ng et al. 2016, Assouline et al. 2006
Root Model 2	$(\theta_s)_{root} = \theta_s - R_v$	$\alpha_{root} = \alpha\frac{(\phi_{macro} - R_v)^2}{\phi_{macro}{}^2}$	Ng et al. 2016, Assouline & Or 2014
Root Model 3	$(\theta_s)_{root} = \frac{\theta_s + R_v}{1+R_v}$	$\alpha_{root} = \alpha\frac{\left(\frac{\phi_{macro}+R_v}{1+R_v}\right)^2}{\phi_{macro}{}^2}$	Ng et al. 2016, Assouline & Or 2014
Root Model 4	$(\theta_s)_{root} = \frac{\theta_s + R_v}{1+R_v}$	$\alpha_{root} = \alpha\left(\frac{1-(\theta_s)_{root}}{1-\theta_s}\right)^{-3.72}$	Ng et al. 2016, Assouline et al. 2006

θ_s = saturated water content
θ_r = residual water content
R_v = root volume ratio
α = inverse of air entry point
ϕ_{macro} = macroporosity

Table 5: Plant Biomass and R_v values for the individual cores.

Growth Period	Soil Type	Treatment	Shoot Mass (g)	Root Mass (g)	Total Mass (g)	R_v
APR-JUN	FS	FRT	0.54	0.56	1.10	0.0293
APR-JUN	FS	FRT	0.47	0.38	0.85	0.0066
APR-JUN	FS	FRT	0.67	0.63	1.30	0.0127
APR-JUN	FS	RTS	0.36	0.46	0.82	0.0031
APR-JUN	FS	RTS	0.29	0.14	0.43	0.0088
APR-JUN	FS	RTS	0.27	0.26	0.53	0.0083
APR-JUN	FS	RTS+MYC	1.10	0.90	2.00	0.0236
APR-JUN	FS	RTS+MYC	0.89	1.17	2.06	0.0188
APR-JUN	FS	RTS+MYC	0.63	0.54	1.17	0.0237
AUG-OCT	FS	FRT	1.52	0.48	2.00	0.0084
AUG-OCT	FS	FRT	1.64	0.38	2.02	0.0058
AUG-OCT	FS	FRT	1.17	0.43	1.60	0.0088
AUG-OCT	FS	RTS	0.75	0.31	1.06	0.0075
AUG-OCT	FS	RTS	0.97	0.37	1.34	0.0051
AUG-OCT	FS	RTS	0.65	0.29	0.94	0.0084
AUG-OCT	FS	RTS+MYC	1.24	0.64	1.88	0.0112
AUG-OCT	FS	RTS+MYC	1.15	0.67	1.82	0.0207
AUG-OCT	FS	RTS+MYC	1.13	0.69	1.82	0.0149
NOV-JAN	HSL	RTS	0.21	0.03	0.24	0.0030
NOV-JAN	HSL	RTS	0.20	0.07	0.27	0.0012
NOV-JAN	HSL	RTS	0.14	0.06	0.20	0.0020
NOV_JAN	HSL	RTS+MYC	2.97	0.95	3.92	0.0169
NOV-JAN	HSL	RTS+MYC	0.42	0.16	0.58	0.0053
NOV-JAN	HSL	RTS+MYC	2.29	0.88	3.17	0.0187

APR-JUN = April-June AUG-OCT = August-October NOV-JAN = November-January
FS = Flint Sand HSL = Hamblen Silt Loam FRT = Fertilizer Rooted
RTS = Rooted RTS + MYC = Mycorrhizal Rooted

Table 6: Measured K_{sat} values for the individual cores determined by the constant head method.

Growth Period	Soil Type	Treatment	K_{sat} (m/s)
APR-JUN	FS	CON	7.39×10^{-4}
APR-JUN	FS	CON	2.20×10^{-4}
APR-JUN	FS	CON	3.91×10^{-4}
APR-JUN	FS	CON+MYC	2.67×10^{-4}
APR-JUN	FS	CON+MYC	3.97×10^{-5}
APR-JUN	FS	CON+MYC	9.16×10^{-5}
APR-JUN	FS	FRT	4.44×10^{-5}
APR-JUN	FS	FRT	1.21×10^{-4}
APR-JUN	FS	FRT	5.22×10^{-5}
APR-JUN	FS	RTS	9.89×10^{-5}
APR-JUN	FS	RTS	3.37×10^{-5}
APR-JUN	FS	RTS	9.62×10^{-5}
APR-JUN	FS	RTS+MYC	4.01×10^{-4}
APR-JUN	FS	RTS+MYC	1.36×10^{-4}
APR-JUN	FS	RTS+MYC	2.72×10^{-5}
AUG-OCT	FS	CON	2.45×10^{-4}
AUG-OCT	FS	CON	5.31×10^{-5}
AUG-OCT	FS	CON	7.28×10^{-5}
AUG-OCT	FS	CON+MYC	1.56×10^{-4}
AUG-OCT	FS	CON+MYC	6.09×10^{-5}
AUG-OCT	FS	CON+MYC	6.42×10^{-5}
AUG-OCT	FS	FRT	6.96×10^{-5}
AUG-OCT	FS	FRT	5.20×10^{-5}
AUG-OCT	FS	FRT	5.50×10^{-5}
AUG-OCT	FS	RTS	5.18×10^{-5}
AUG-OCT	FS	RTS	5.57×10^{-5}
AUG-OCT	FS	RTS	6.38×10^{-5}
AUG-OCT	FS	RTS+MYC	4.11×10^{-5}
AUG-OCT	FS	RTS+MYC	3.49×10^{-6}
AUG-OCT	FS	RTS+MYC	2.66×10^{-5}
NOV-JAN	HSL	CON	1.91×10^{-8}
NOV-JAN	HSL	CON	2.05×10^{-8}
NOV-JAN	HSL	CON	1.93×10^{-8}
NOV-JAN	HSL	CON+MYC	1.32×10^{-6}
NOV-JAN	HSL	CON+MYC	1.34×10^{-8}
NOV-JAN	HSL	CON+MYC	1.72×10^{-8}
NOV-JAN	HSL	RTS	2.35×10^{-8}
NOV-JAN	HSL	RTS	4.39×10^{-8}
NOV-JAN	HSL	RTS	1.36×10^{-8}
NOV-JAN	HSL	RTS+MYC	1.36×10^{-8}

Table 6 Continued

NOV-JAN	HSL	RTS+MYC	2.32×10^{-8}
NOV-JAN	HSL	RTS+MYC	2.99×10^{-7}

APR-JUN = April-June AUG-OCT = August-October NOV-JAN = November-January
FS = Flint Sand HSL = Hamblen Silt Loam CON+MYC = Mycorrhizal Control
CON = Control FRT = Fertilizer Rooted RTS = Rooted
RTS + MYC = Mycorrhizal Rooted

Table 7: RMSE values for Equations [1] and [10] fitted to the experimental data for each core simultaneously.

Soil Type	Treatment	RMSE θ(h)	RMSE K(θ)
FS	CON	0.0105	0.3189
FS	CON	0.0063	0.2431
FS	CON	0.0045	0.3057
FS	CON	0.0047	0.0673
FS	CON	0.0048	0.3653
FS	CON	0.0045	0.2787
FS	CON+MYC	0.0044	0.3313
FS	CON+MYC	0.0031	0.2135
FS	CON+MYC	0.0021	0.2880
FS	CON+MYC	0.0037	0.3021
FS	CON+MYC	0.0038	0.1597
FS	CON+MYC	0.0021	0.3272
FS	FRT	0.0055	0.2302
FS	FRT	0.0045	0.2853
FS	FRT	0.0050	0.2668
FS	FRT	0.0031	0.2333
FS	FRT	0.0027	0.2864
FS	FRT	0.0025	0.2397
FS	RTS	0.0035	0.2968
FS	RTS	0.0018	0.3295
FS	RTS	0.0027	0.3719
FS	RTS	0.0023	0.3034
FS	RTS	0.0045	0.2968
FS	RTS	0.0052	0.1920
FS	RTS+MYC	0.0034	0.2589
FS	RTS+MYC	0.0037	0.2563
FS	RTS+MYC	0.0029	0.3063
FS	RTS+MYC	0.0083	0.2844
FS	RTS+MYC	0.0046	0.3064
FS	RTS+MYC	0.0028	0.3140
HSL	CON	0.0087	0.1411
HSL	CON	0.0094	0.1731
HSL	CON	0.0100	0.1388
HSL	CON+MYC	0.0096	0.1123
HSL	CON+MYC	0.0106	0.1497
HSL	CON+MYC	0.0163	0.1105
HSL	RTS	0.0072	0.1460
HSL	RTS	0.0125	0.1803

Table 7 Continued

HSL	RTS	0.0132	0.2358
HSL	RTS+MYC	0.0076	0.1755
HSL	RTS+MYC	0.0070	0.1674
HSL	RTS+MYC	0.0034	0.1180

FS = Flint Sand HSL = Hamblen Silt Loam CON+MYC = Mycorrhizal Control
CON = Control FRT = Fertilizer Rooted RTS = Rooted
RTS + MYC = Mycorrhizal Rooted

Table 8: Summary of ANOVA results for the fitting parameters from Equation [1].

Soil Type	Parameter	Model R^2	Model F-value	Model p-value	Treatment F-Value	Treatment p-value
FS	θ_s	0.8356	24.39	<.0001	27.17	<.0001
FS	α	0.1523	1.120	0.3681	1.120	0.3681
FS	n	0.8164	27.79	<.0001	27.79	<.0001
FS	θ_r	0.1241	0.890	0.4869	0.890	0.4869
HSL	θ_s	0.0133	0.430	0.7365	0.430	0.7365
HSL	α	0.4225	1.950	0.2001	1.950	0.2001
HSL	n	0.5868	3.790	0.0586	3.790	0.0586

FS = Flint Sand HSL = Hamblen Silt Loam

Table 9: Soil hydraulic parameters estimated by fitting Equations [1] and [10] to the experimental data for the individual cores simultaneously.

Soil Type	Treatment	θ_s Measured (cm^3/cm^3)	α ($1/cm^3$)	n (-)	θ_r (cm^3/cm^3)	K_{sat} Estimated (m/s)	τ (-)
FS	CON	0.33	0.0497	14.30	0.03	1.68×10^{-6}	-1.41
FS	CON	0.36	0.0508	14.37	0.07	4.10×10^{-7}	-1.79
FS	CON	0.33	0.0503	12.01	0.04	2.05×10^{-7}	-1.85
FS	CON+MYC	0.38	0.0633	10.85	0.09	1.83×10^{-7}	-1.82
FS	CON+MYC	0.35	0.0511	9.82	0.07	4.17×10^{-7}	-1.42
FS	CON+MYC	0.36	0.0492	9.50	0.07	1.71×10^{-7}	-1.70
FS	FRT	0.38	0.0583	8.17	0.05	5.32×10^{-7}	-1.69
FS	FRT	0.37	0.0495	10.12	0.05	3.67×10^{-7}	-1.77
FS	FRT	0.38	0.0537	7.60	0.05	1.69×10^{-7}	-1.81
FS	RTS	0.38	0.0495	10.18	0.07	2.34×10^{-7}	-1.79
FS	RTS	0.36	0.0497	13.28	0.05	2.34×10^{-7}	-1.85
FS	RTS	0.40	0.0530	11.57	0.07	2.60×10^{-7}	-1.79
FS	RTS+MYC	0.40	0.0628	6.74	0.04	2.05×10^{-7}	-1.82
FS	RTS+MYC	0.40	0.0623	6.04	0.04	2.08×10^{-7}	-1.81
FS	RTS+MYC	0.41	0.0525	6.96	0.07	2.37×10^{-7}	-1.71
FS	CON	0.33	0.0519	12.92	0.00	3.30×10^{-7}	-1.83
FS	CON	0.33	0.0518	15.00	0.01	2.45×10^{-7}	-1.84
FS	CON	0.32	0.0516	12.80	0.00	2.78×10^{-7}	-1.83
FS	CON+MYC	0.35	0.0506	13.01	0.03	4.14×10^{-7}	-1.78
FS	CON+MYC	0.33	0.0509	11.00	0.02	2.74×10^{-7}	-1.77
FS	CON+MYC	0.32	0.0515	9.62	0.00	2.31×10^{-7}	-1.69
FS	FRT	0.38	0.0528	9.42	0.03	4.33×10^{-7}	-1.76
FS	FRT	0.37	0.0516	9.27	0.03	4.77×10^{-7}	-1.70
FS	FRT	0.37	0.0528	8.31	0.01	4.24×10^{-7}	-1.79
FS	RTS	0.36	0.0574	9.31	0.02	5.34×10^{-7}	-1.69
FS	RTS	0.38	0.0509	9.95	0.05	3.56×10^{-7}	-1.75
FS	RTS	0.36	0.0532	10.25	0.03	2.00×10^{-7}	-1.85
FS	RTS+MYC	0.38	0.0532	6.35	0.03	6.85×10^{-7}	-1.55
FS	RTS+MYC	0.39	0.0505	8.26	0.04	2.79×10^{-7}	-1.75
FS	RTS+MYC	0.38	0.0522	7.06	0.02	6.55×10^{-7}	-1.63
HSL	CON	0.57	0.0026	1.36	0.00	2.60×10^{-6}	-2.89
HSL	CON	0.58	0.0032	1.30	0.00	8.94×10^{-7}	-6.00
HSL	CON	0.57	0.0023	1.41	0.00	2.73×10^{-6}	3.16
HSL	CON+MYC	0.56	0.0036	1.29	0.00	1.69×10^{-6}	0.56
HSL	CON+MYC	0.57	0.0025	1.35	0.00	1.27×10^{-6}	-0.50
HSL	CON+MYC	0.59	0.0029	1.38	0.00	8.24×10^{-7}	-3.98

Table 9 Continued

HSL	RTS	0.55	0.0039	1.27	0.00	2.22×10^{-6}	-3.04
HSL	RTS	0.57	0.0036	1.29	0.00	2.33×10^{-6}	-3.83
HSL	RTS	0.58	0.0032	1.27	0.00	4.91×10^{-6}	-0.41
HSL	RTS+MYC	0.59	0.0052	1.27	0.00	1.66×10^{-6}	0.52
HSL	RTS+MYC	0.59	0.0031	1.26	0.00	1.55×10^{-6}	-1.51
HSL	RTS+MYC	0.57	0.0033	1.30	0.00	1.05×10^{-6}	-0.75

APR-JUN = April-June AUG-OCT = August-October NOV-JAN = November-January
FS = Flint Sand HSL = Hamblen Silt Loam CON+MYC = Mycorrhizal Control
CON = Control FRT = Fertilizer Rooted RTS = Rooted
RTS + MYC = Mycorrhizal Rooted

Table 10: Values of input parameters used for the forward predictions in Figure 25 and Figure 26.

Curve	Model	Parameters	Soil Type: Flint Sand	Soil Type: Hamblen Silt Loam
Unrooted	$\frac{\theta-\theta_r}{\theta_s-\theta_r}=[1+(\alpha h)^n]^{1-\frac{1}{n}}$	α	0.050	0.003
		θ_s	0.333	0.573
		θ_r	0.025	0
		n	13.57	1.36
Rooted-model 4	$\frac{\theta-\theta_r}{\theta_{s_{root}}-\theta_r}=[1+(\alpha_{root}h)^n]^{1-\frac{1}{n}}$	α_{root}	0.056	0.003
		$\theta_{s_{root}}$	0.353	0.574
		θ_r	0.25	0
		n	13.57	1.36
		R_v	0.03	0.003

Note: Parameters are averages of the individual parameter values for the control (unrooted) treatment and the largest R_v value from the rooted treatments.

Table 11: Mean estimated K_{sat} values and standard deviations from fitting Equation [10] the experimental $K(\theta)$ data.

Soil Type	Treatment	Estimated Mean K_{sat} (m/s)	Standard Deviation
FS	CON	5.61×10^{-7}	5.64×10^{-7}
FS	CON+MYC	2.90×10^{-7}	1.37×10^{-7}
FS	FRT	2.51×10^{-7}	4.71×10^{-8}
FS	RTS	3.78×10^{-7}	9.36×10^{-8}
FS	RTS+MYC	5.09×10^{-7}	1.51×10^{-7}
HSL	CON	2.08×10^{-6}	1.03×10^{-6}
HSL	CON+MYC	1.26×10^{-6}	4.33×10^{-7}
HSL	RTS	3.15×10^{-6}	1.52×10^{-6}
HSL	RTS+MYC	1.42×10^{-6}	3.24×10^{-7}

FS = Flint Sand HSL = Hamblen Silt Loam CON+MYC = Mycorrhizal Control
CON = Control FRT = Fertilizer Rooted RTS = Rooted
RTS + MYC = Mycorrhizal Rooted

APPENDIX 2 - FIGURES

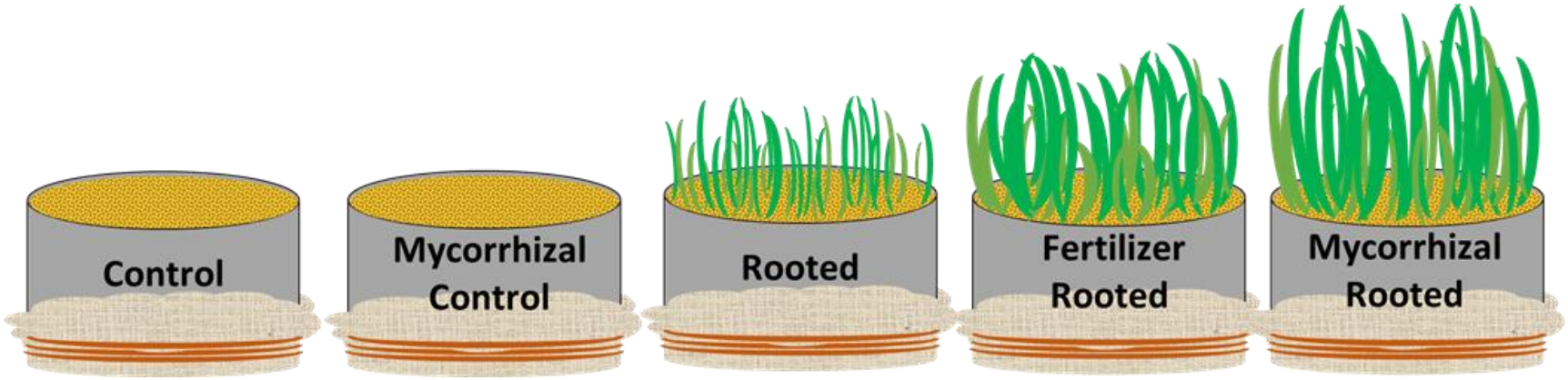

Figure 1: The experimental design for the Flint sand cores consisted of five treatments: control (CON), mycorrhizal control (CON+MYC), rooted (RTS), fertilizer rooted (FRT), and mycorrhizal rooted (RTS+MYC).

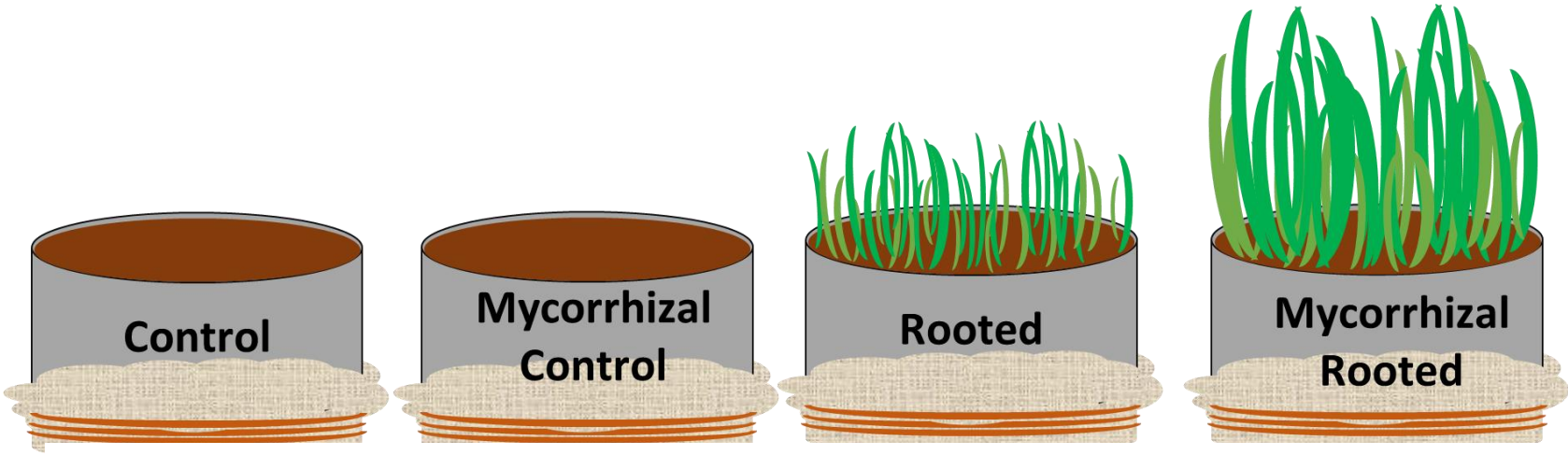

Figure 2: The experimental design for the Hamblen silt loam cores consisted of four treatments: control (CON), mycorrhizal control (CON+MYC), rooted (RTS) and mycorrhizal rooted (RTS+MYC).

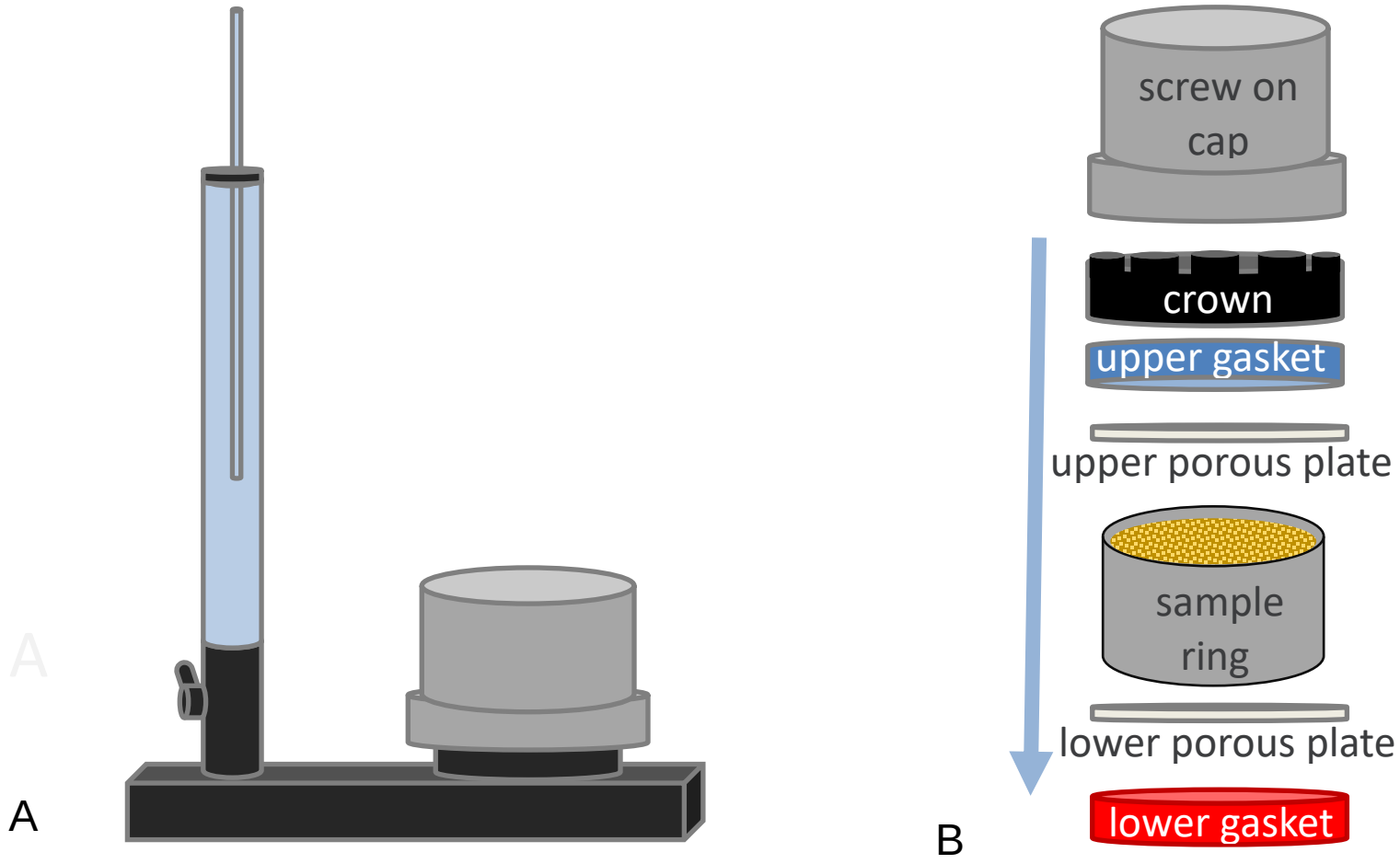

Figure 3: Illustration of a Meter K_{sat} permeameter (A) that was used in conjunction with the constant head method to measure the saturated hydraulic conductivity (K_{sat}) of the Flint sand and Hamblen silt loam soil cores. Soil samples were fitted with two porous plates attached by gaskets and firmly secured to the permeameter using a screw on cap (B).

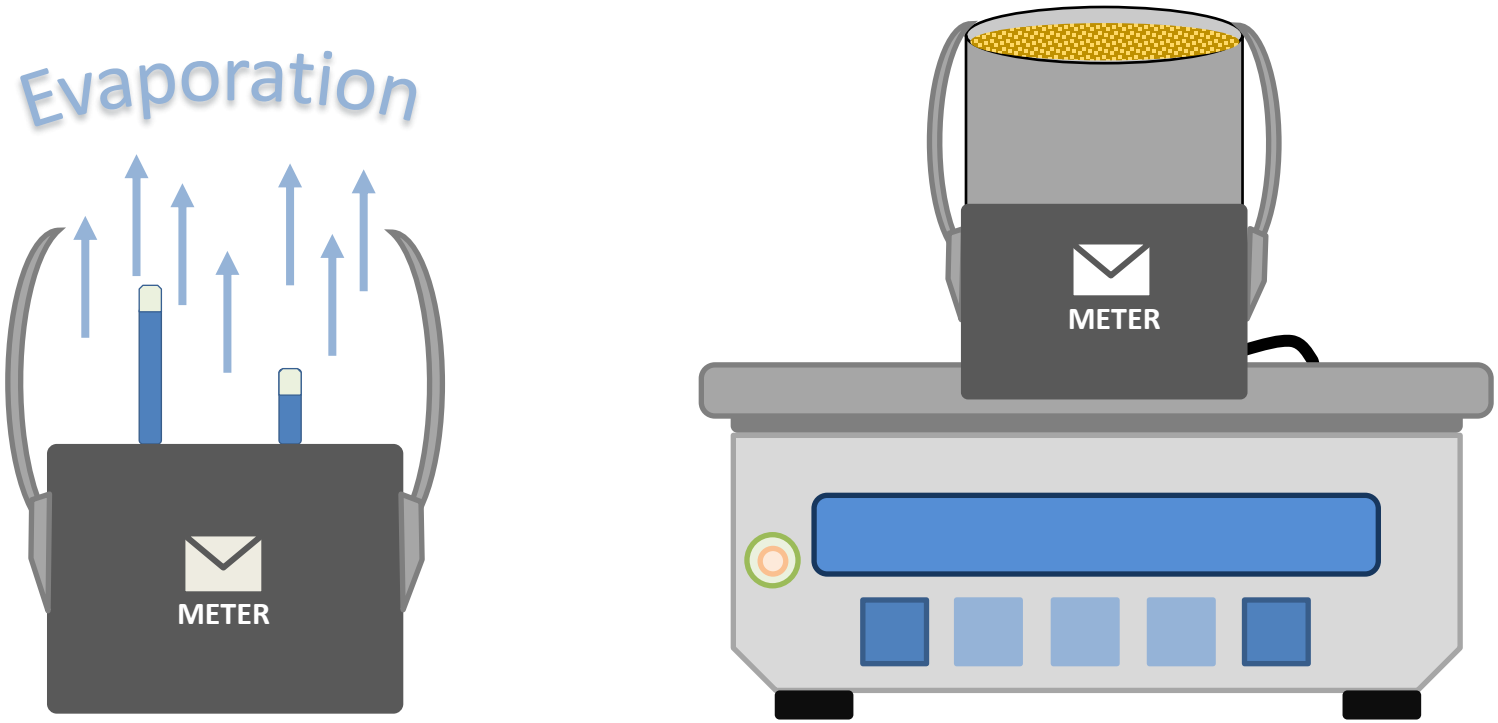

Figure 4: Illustration of a Meter Hyprop2 that device was used to measure $\theta(h)$ and $K(\theta)$. The device works by recording changes in pressure head (h) and volumetric water content (θ) due to evaporation. Evaporative loss was measured as weight in grams.

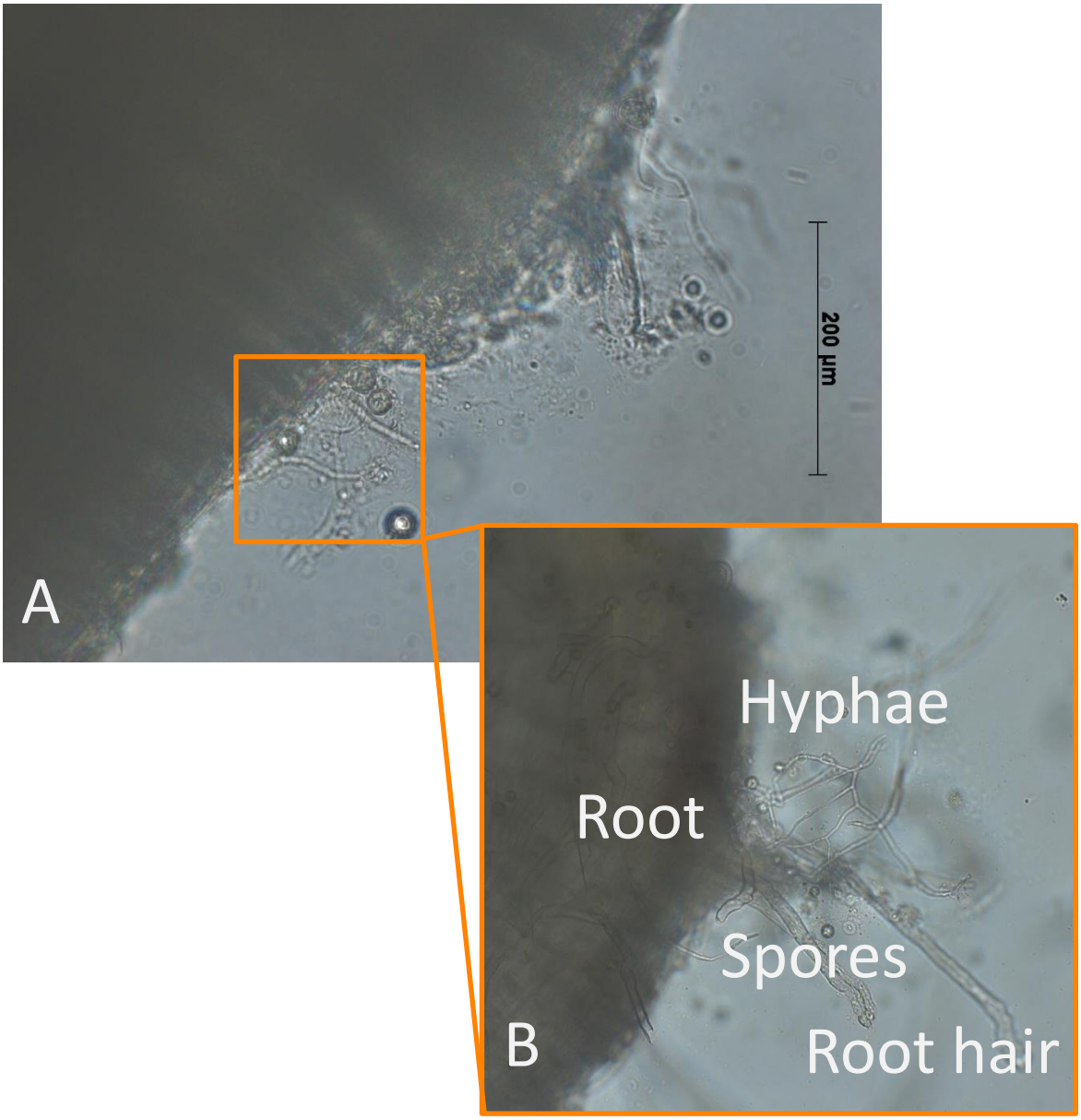

Figure 5: The presence of fungal hyphae in the inoculated treatments was confirmed using microscopy. (A) was taken under 40x magnification and shows a root with mycorrhizal hyphae and fungal spores. (B) closeup of a similar area at 20x magnification showing root physiology (root and associated root hairs) as distinguished from mycorrhizal physiology (fungal spores and fungal hyphae).

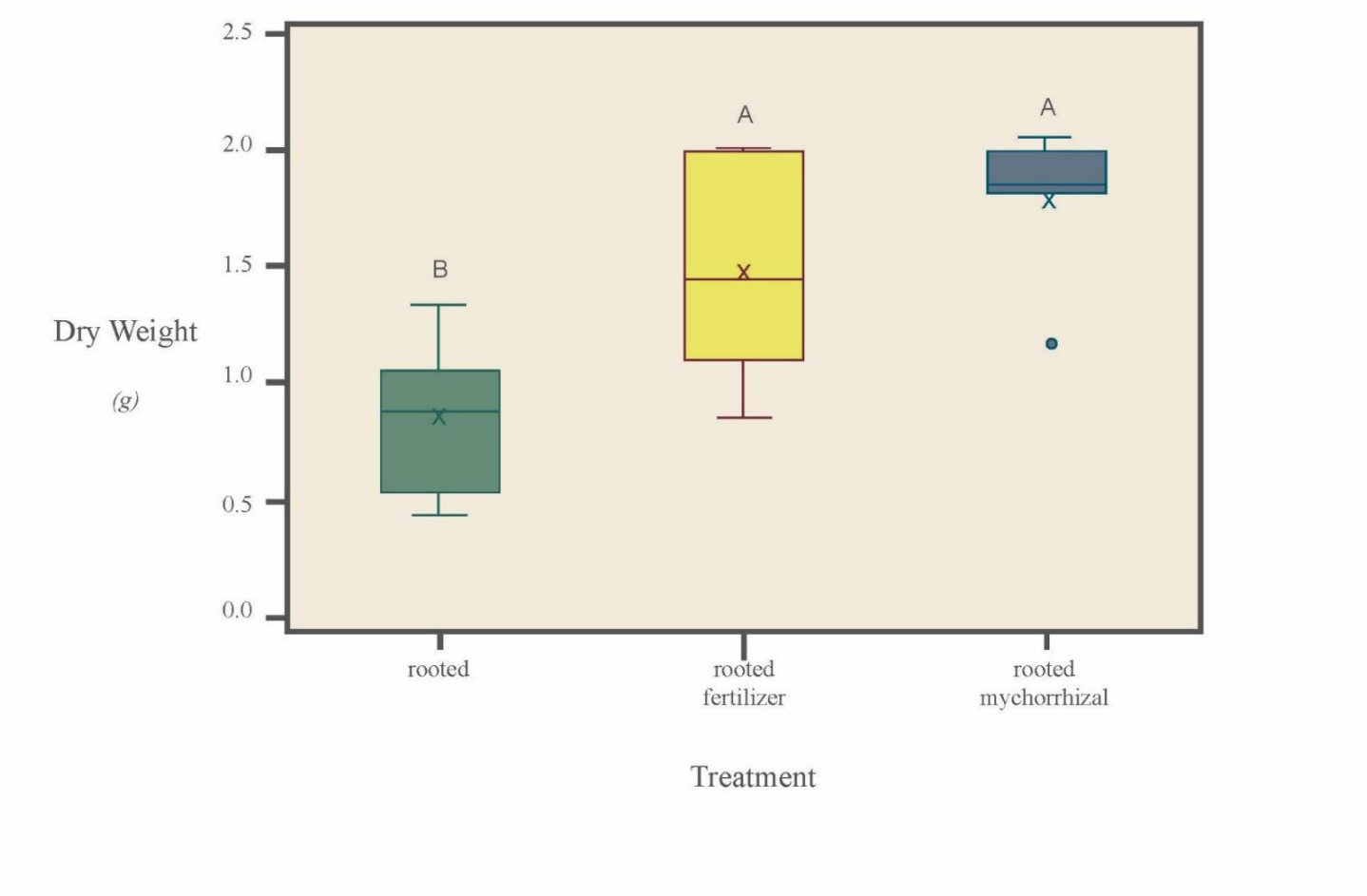

Figure 6: Boxplots and Tukey HSD letter groupings for total biomass. Results are from plants harvested from Flint sand cores grown from April to June 2019 and August to October 2019. The x-axis is the experimental treatment. The y-axis is the dry weight measured in grams. The median value is displayed as a horizontal line. The arithmetic mean is shown as an x symbol. Letters above the graphs display the Tukey letter grouping. Treatments that share a letter are not significantly different at $p < 0.05$.

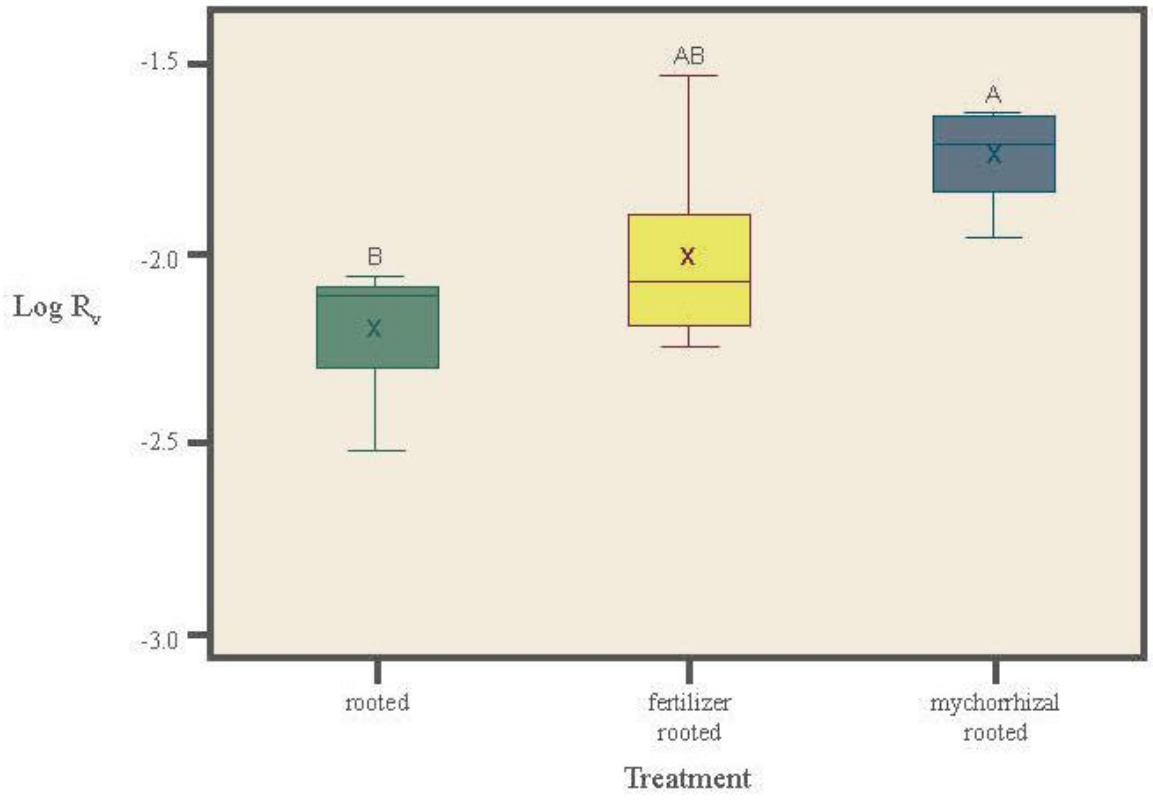

Figure 7: Boxplots with Tukey HSD letter groupings for the root volume ratio, R_v, for Flint sand. The x-axis is treatment. The y-axis is the base-ten logarithm of R_v. The median value is displayed as a horizontal line. The arithmetic mean is shown as an x symbol. Letters above the graphs display the Tukey letter grouping. Treatments that share a letter are not significantly different at $p < 0.05$.

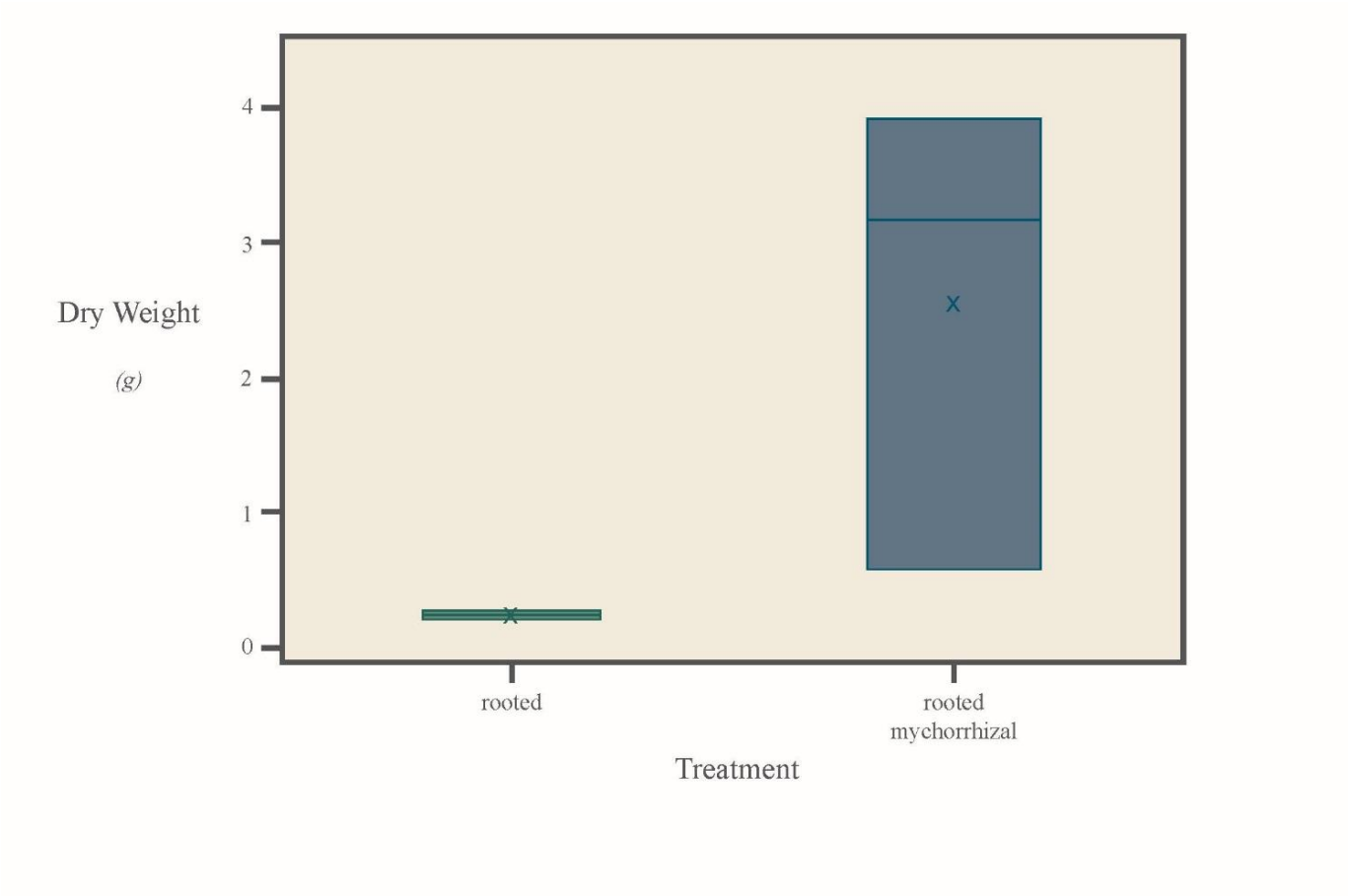

Figure 8: Boxplots for total biomass for the Hamblen silt loam soil. The y-axis is the dry weight measured in grams. The median value is displayed as a horizontal line. The arithmetic mean is shown as an x symbol. There were no statistically significant differences between the treatments at $p < 0.05$.

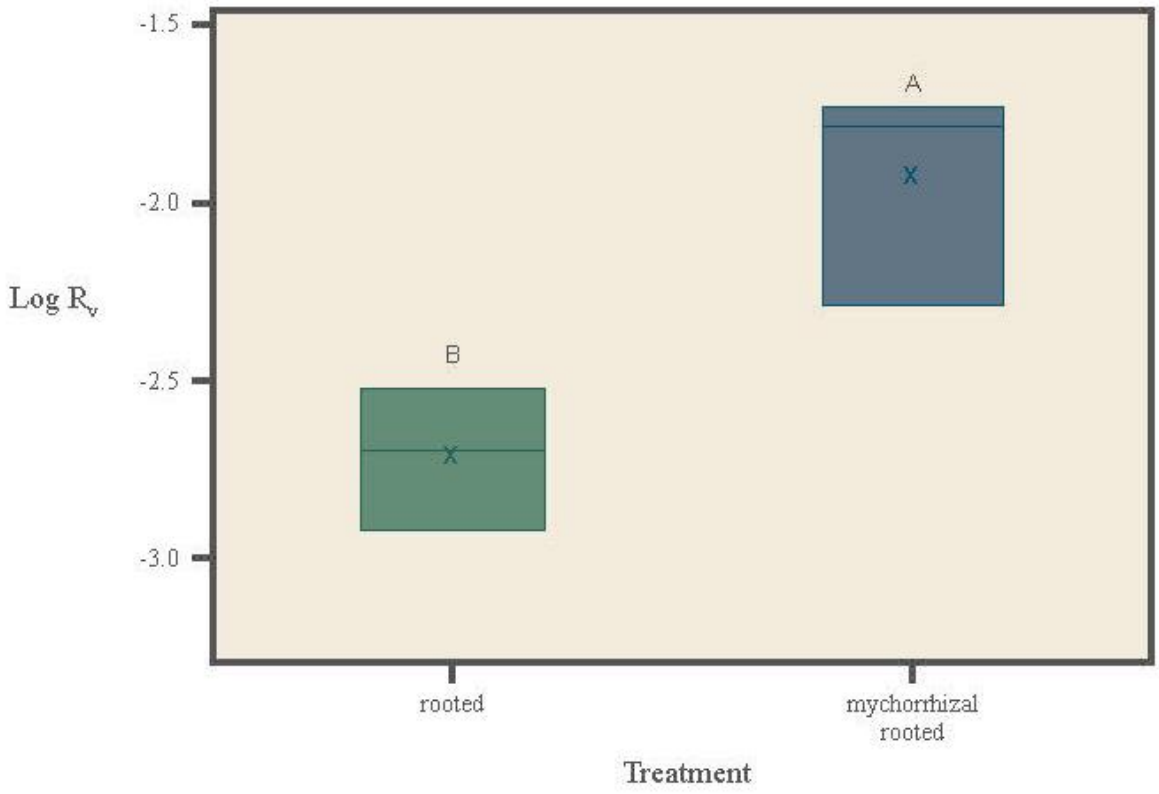

Figure 9: Boxplot with Tukey HSD letter grouping for the root volume ratio, R_v for Hamblen silt loam. The x-axis is treatment. The y-axis is the base-ten logarithm of R_v. The median value is displayed as a horizontal line. The arithmetic mean is shown as an x symbol. Letters above the graphs display the Tukey letter grouping. Treatments that share a letter are not significantly different at $p < 0.05$.

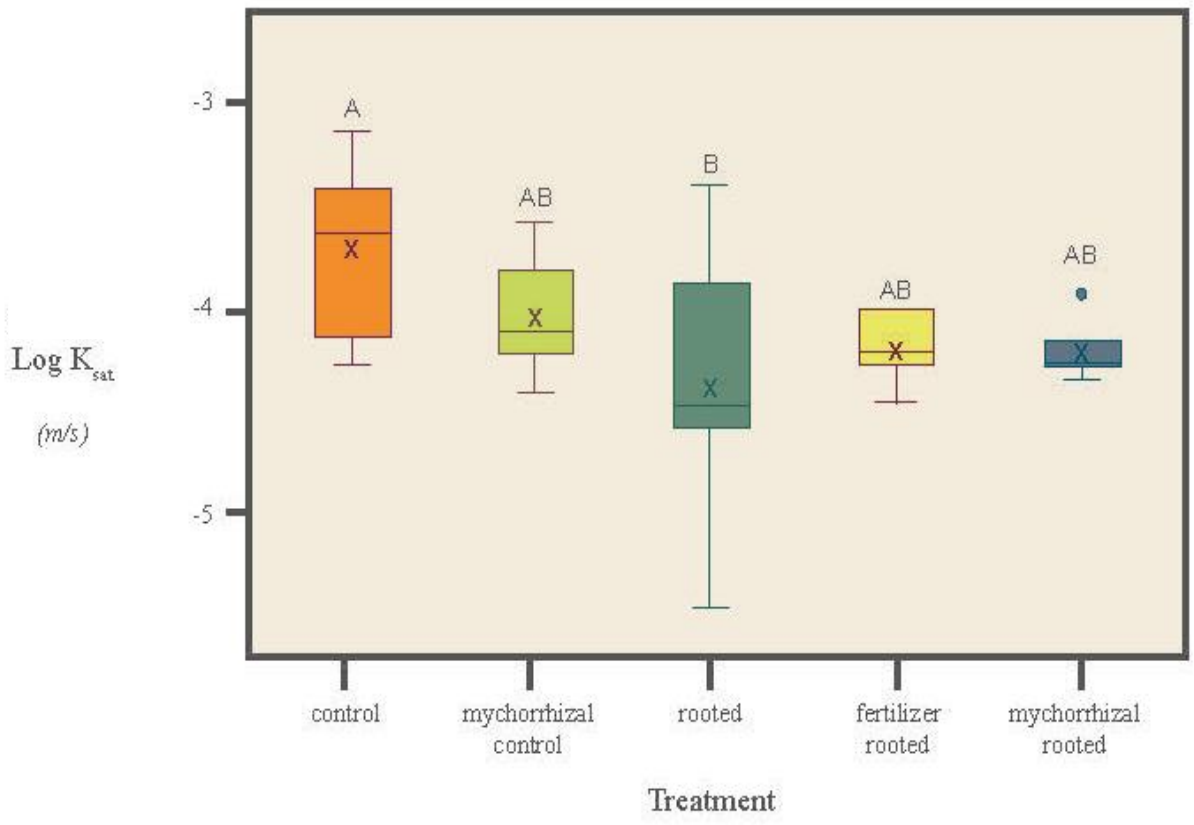

Figure 10: Boxplots and Tukey HSD letter groupings for the average $\log_{10} K_{sat}$ for Flint sand. The x-axis is the experimental treatment. The y-axis is the average base-ten logarithm of $\log_{10} K_{sat}$ measured in meters per second. The median value is displayed as a horizontal line. The arithmetic mean is shown as an x symbol. Outliers are represented as circles. Hinges represent the 25th and 75th percentiles of the distributions. Letters above the graphs display the Tukey letter grouping. Treatments that share a letter are not significantly different at $p < 0.05$.

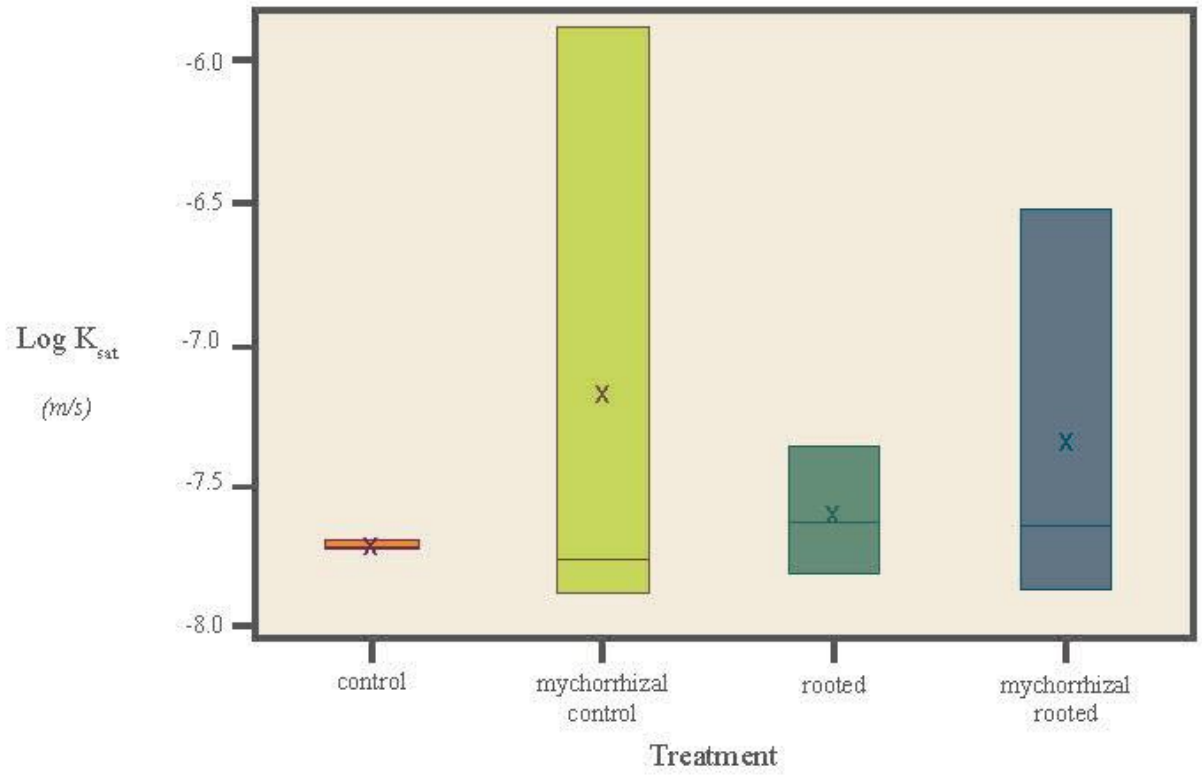

Figure 11: Boxplots of the $\log_{10} K_{sat}$ for Hamblen silt loam. The x-axis is the experimental treatment, while the y-axis is the base-ten logarithm of $\log_{10} K_{sat}$ measured in meters per second. The horizontal line represents the median value. The arithmetic mean is shown as an x symbol. There were no statistically significant differences between the treatments at $p < 0.05$.

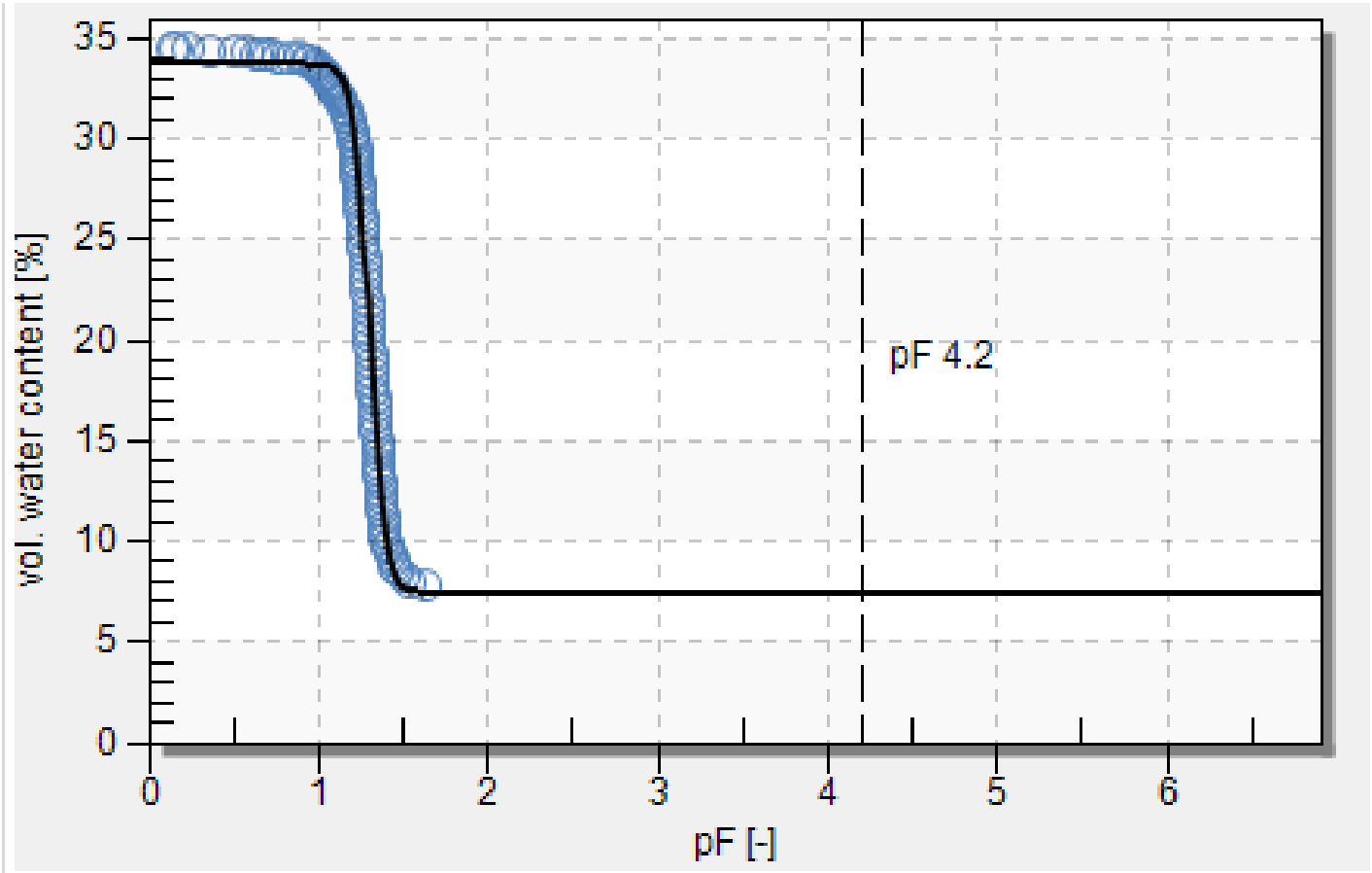

Figure 12: Flint sand soil water retention curve representing the median RMSE value for the curve fit (i.e., one half of the curves had a better fit and one half of the curves had a worse fit). The x-axis is the capillary pressure head measured as the base-ten logarithm of cm (pF). The y-axis is the volumetric water content measured in percent. Circles are data points; solid line is the fitted curve.

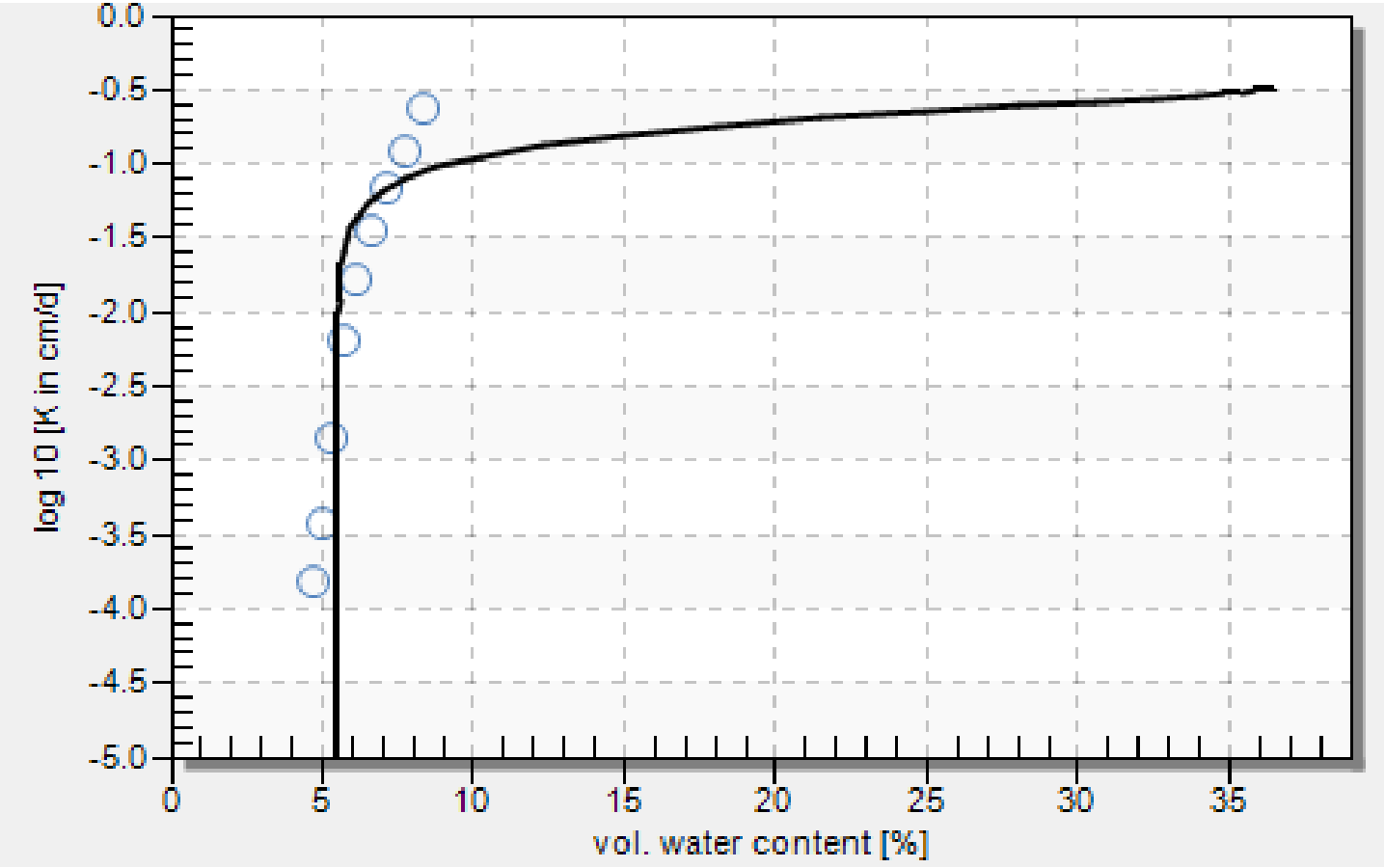

Figure 13: Flint sand unsaturated hydraulic conductivity curve representing the median RMSE value for the curve fit (i.e., one half of the curves had a better fit and one half of the curves had a worse fit). The x-axis is the volumetric water content measured in percent. The y-axis is the base-ten logarithm of hydraulic conductivity measured in cm per day. Circles are data points; solid line is the fitted curve.

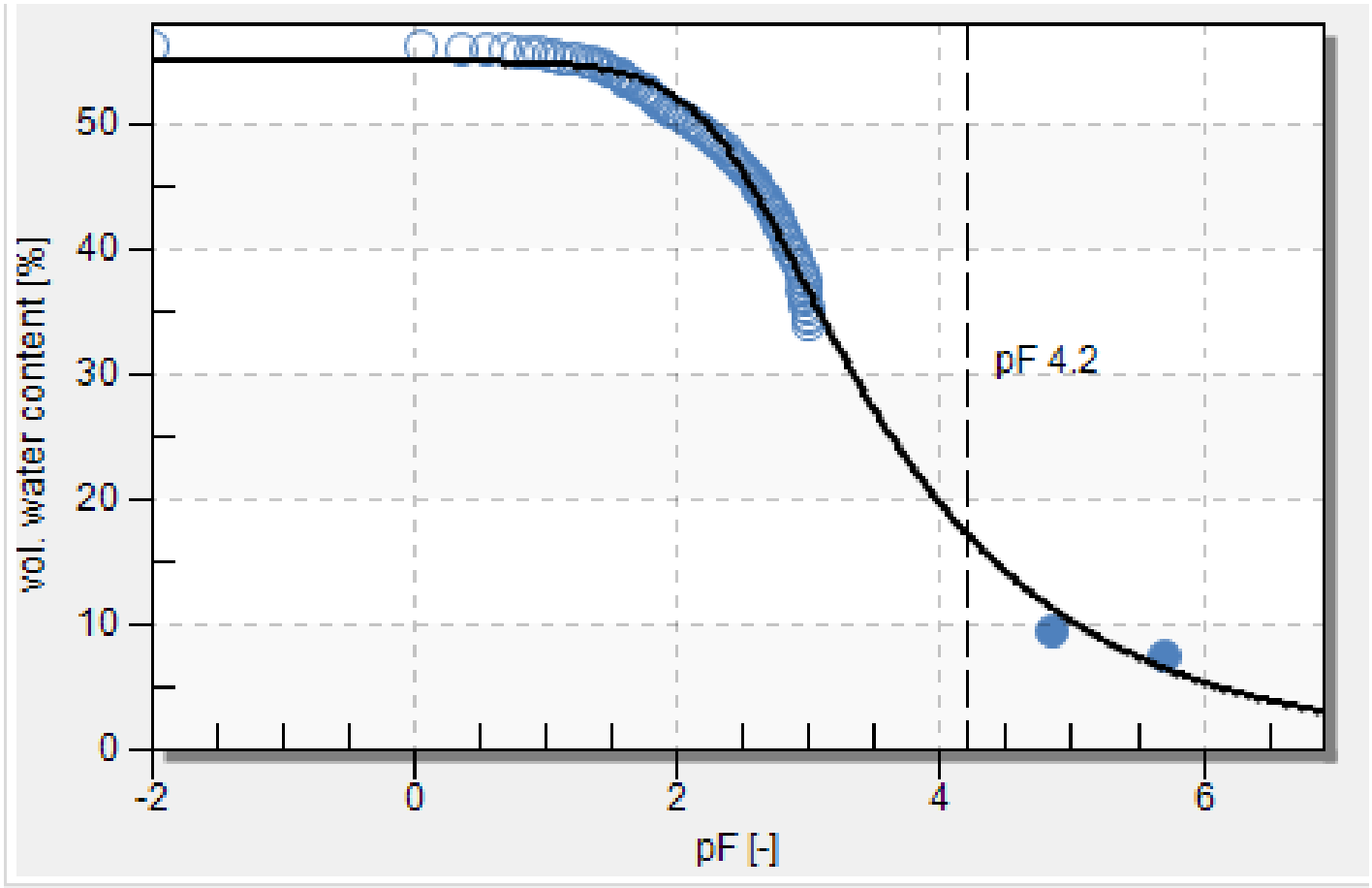

Figure 14: Hamblen silt loam soil water retention curve representing the median RMSE value for the curve fit (i.e., one half of the curves had a better fit and one half of the curves had worse fit). The x-axis is the capillary pressure head measured as the base-ten logarithm of cm (pF). The y-axis is the volumetric water content measured in percent. Circles are data points; solid line is the fitted curve.

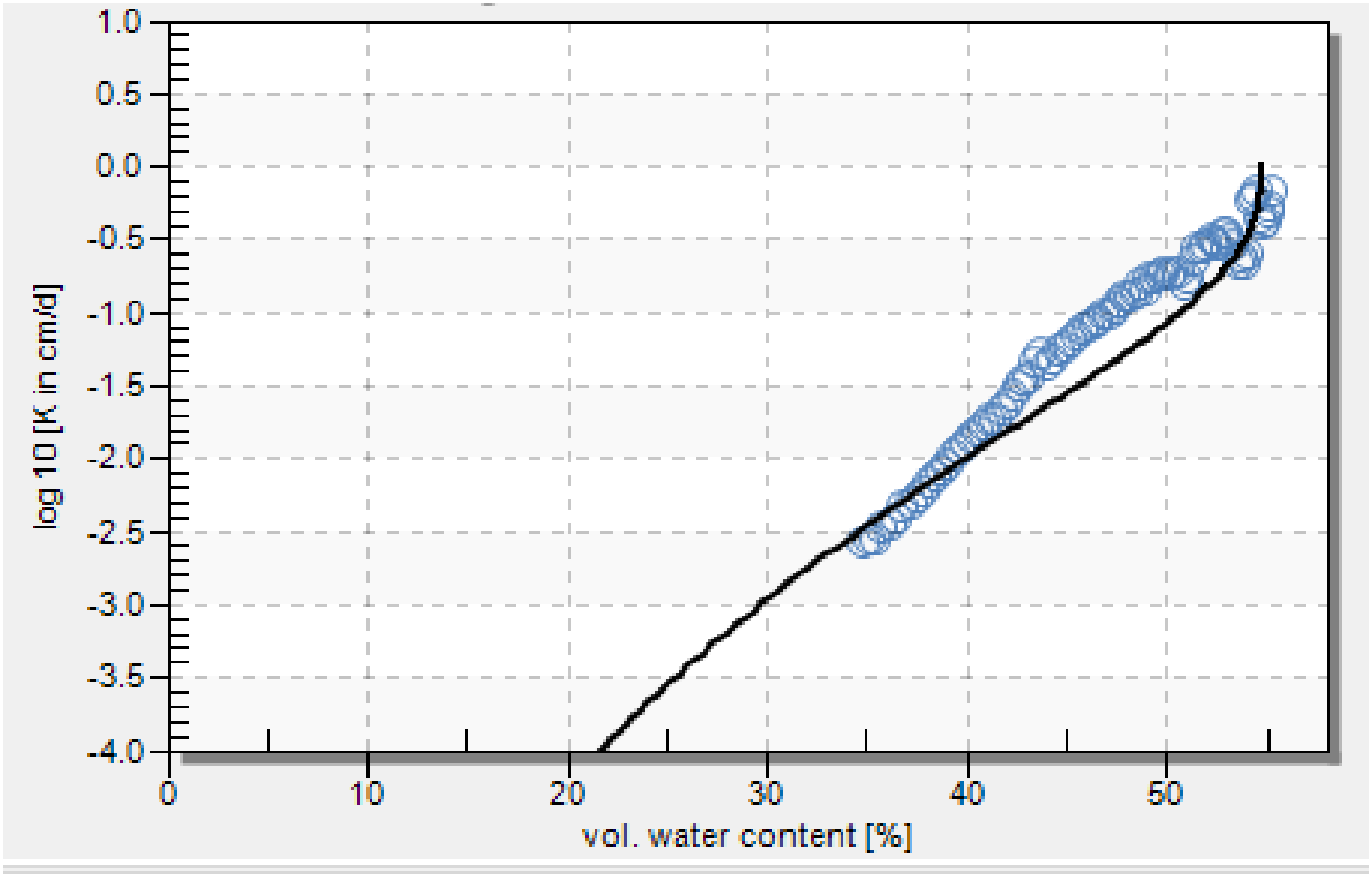

Figure 15: Hamblen silt loam unsaturated hydraulic conductivity curve representing the median RMSE value for the curve fit (i.e., one half of the curves had a better fit and one half of the curves had a worse fit). The x-axis is the volumetric water content measured in percent. The y-axis is the base-ten logarithm of hydraulic conductivity measured in cm per day. Circles are data points; solid line is the fitted curve.

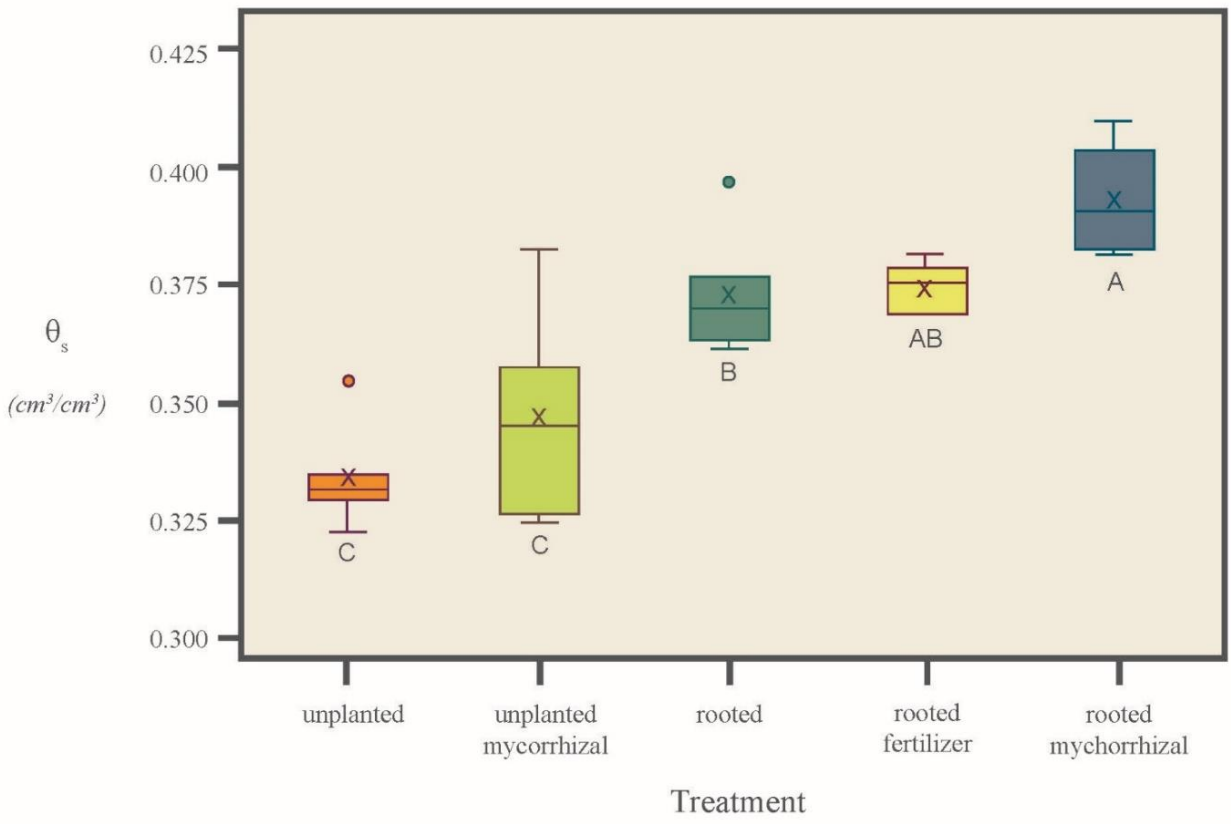

Figure 16: Boxplots and Tukey letter groupings for the $\theta(h)$ fitting parameter θ_s for Flint sand. The x-axis is the experimental treatment, while the y-axis is saturated water content (θ_s) measured in cm^3/cm^3. The median value is a horizontal line. The arithmetic mean is shown as an x symbol. The circles are outliers. Hinges represent the 25th and 75th percentiles of the distributions. Letters below the graphs display the Tukey letter grouping. Treatments that share a letter do not have a statistically significant difference at $p < 0.05$.

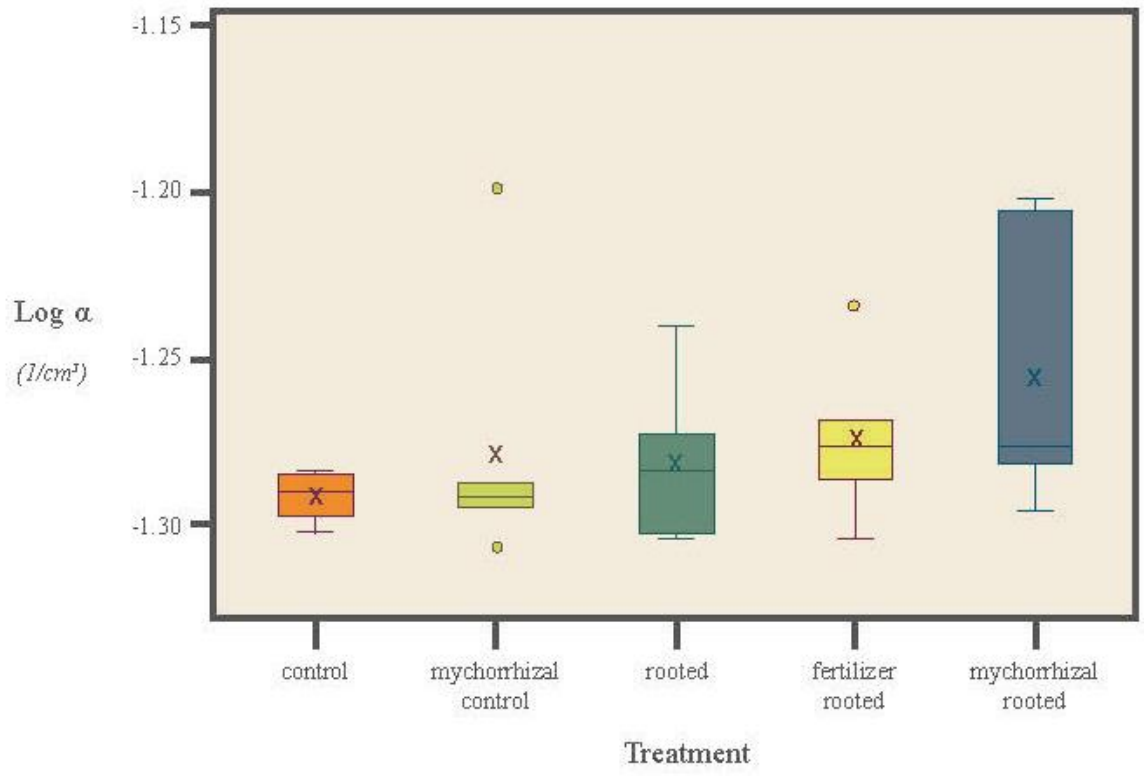

Figure 17: Boxplots of the soil water retention curve fitting parameter α for Flint sand. The x-axis is the experimental treatment. The y-axis is α, the inverse of the air entry point measured in 1/cm^3. The median value is displayed as a horizontal line. The arithmetic mean is shown as an x symbol. Outliers are represented as circles. Hinges represent the 25th and 75th percentiles of the distributions. There were no statistically significant differences between the treatments at $p < 0.05$.

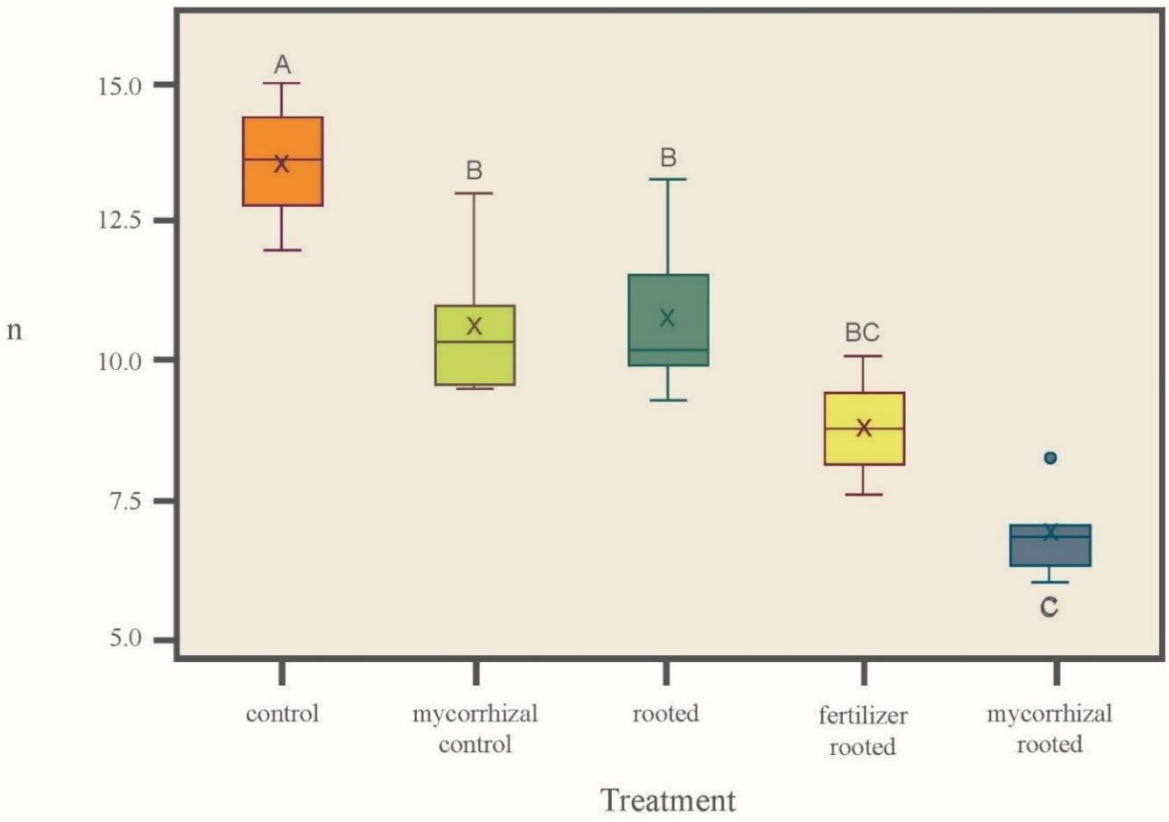

Figure 18: Boxplot and Tukey letter groupings for the soil water retention curve fitting parameter n for Flint sand. The x-axis is the experimental treatment. The y-axis is the fitting parameter n; a parameter related to the pore size distribution. The median value is displayed as a horizontal line. The arithmetic mean is shown as an x symbol. Outliers are represented as circles. Hinges represent the 25th and 75th percentiles of the distributions. Letters above the graphs display the Tukey letter grouping. Treatments that share a letter do not have a statistically significant difference at $p < 0.05$.

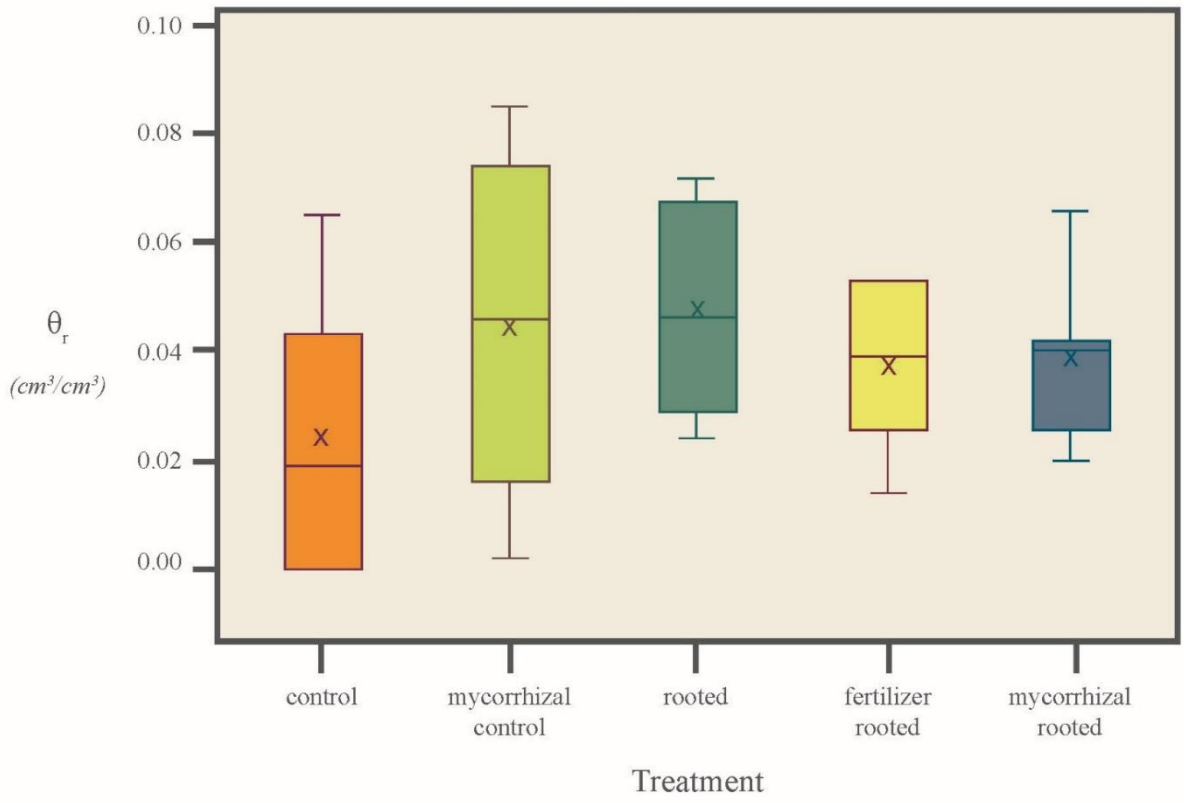

Figure 19: Boxplot of the soil water retention curve fitting parameter θ_r for Flint sand. The x-axis is the experimental treatment. The x-axis is treatment. The y-axis is the residual water content (θ_r) measured in cm^3/cm^3. The median value is displayed as a horizontal line. The arithmetic mean is shown as an x symbol. Hinges represent the 25th and 75th percentiles of the distributions. There were no statistically significant differences between the treatments at $p < 0.05$.

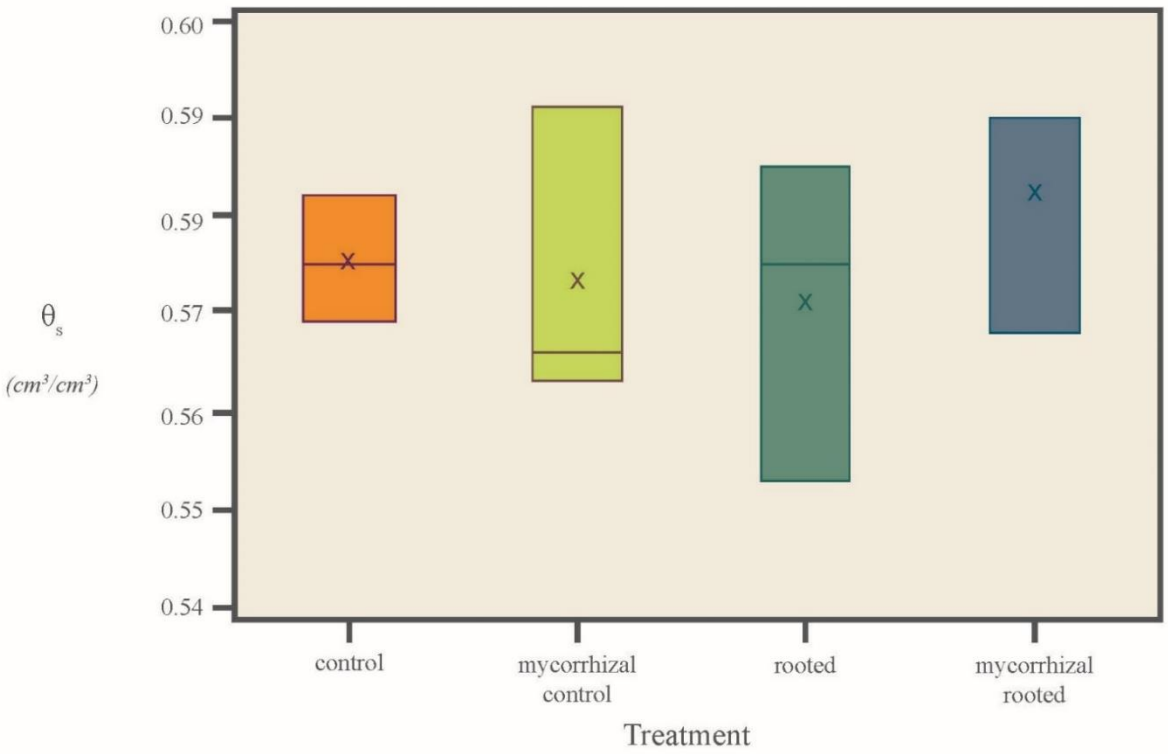

Figure 20: Boxplots of the soil water retention curve fitting parameter θ_s for silt loam soil. The x-axis is the experimental treatment. The y-axis is saturated water content (θ_s) measured in cm^3/cm^3. The median value is displayed as a horizontal line. The arithmetic mean is shown as an x symbol. There were no statistically significant differences between the treatments at $p < 0.05$.

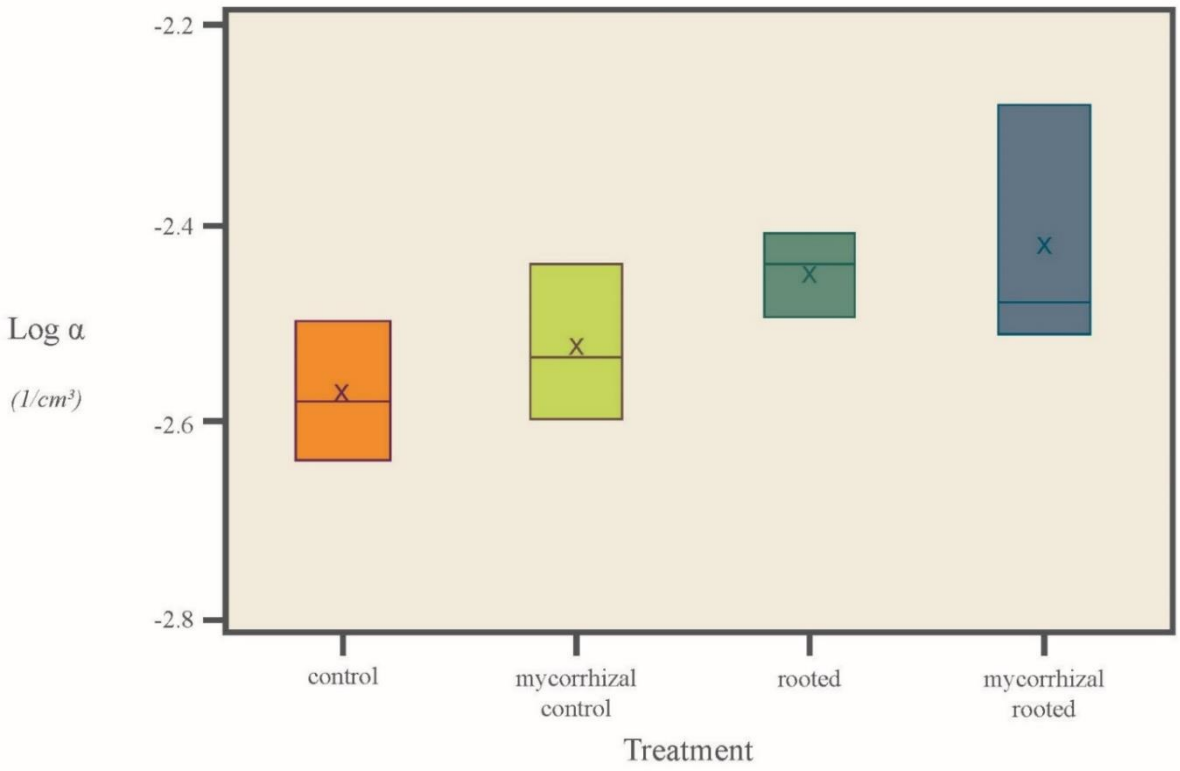

Figure 21: Boxplot of the log-tansformed soil water retention curve fitting parameter α for silt loam soil. The x-axis is the experimental treatment. The y-axis is α; the inverse of the air entry point measured in $1/cm^3$. The median value is displayed as a horizontal line. The arithmetic mean is shown as an x symbol. There were no statistically significant differences between the treatments at $p < 0.05$.

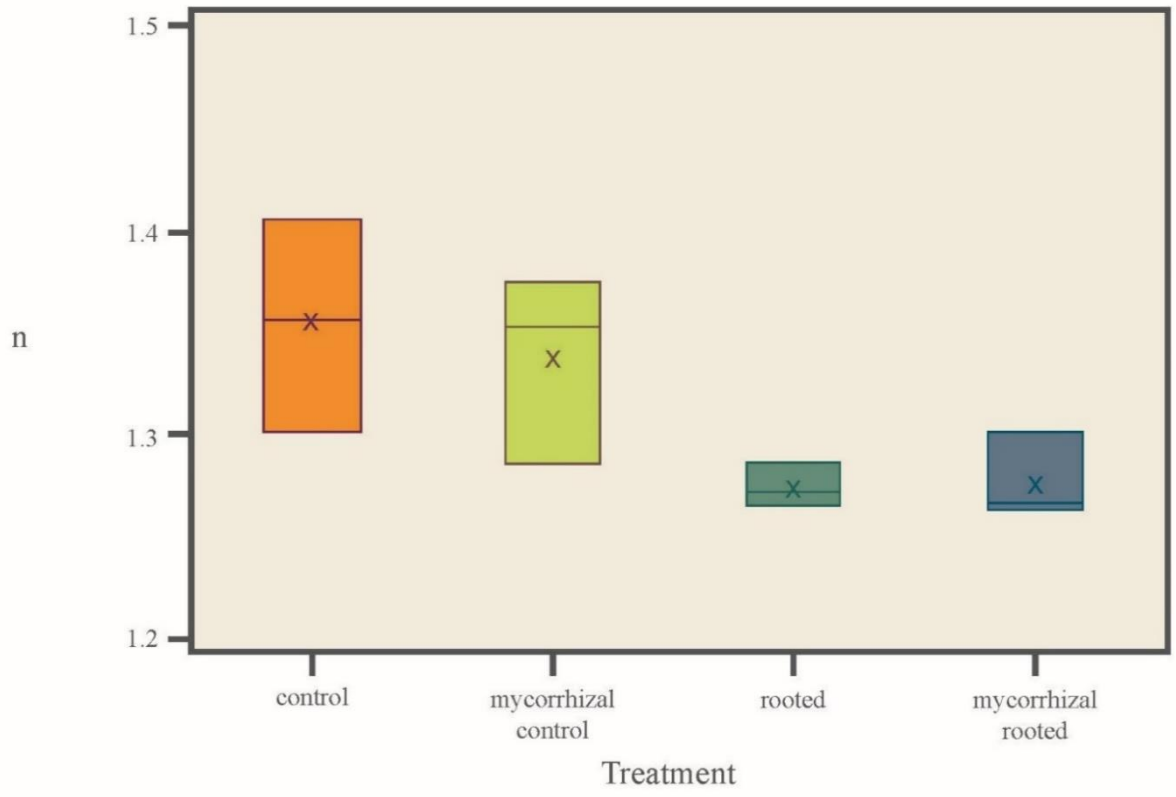

Figure 22: Boxplot of the soil water retention curve fitting parameter n for silt loam soil. The x-axis is the experimental treatment. The y-axis is the fitting parameter n; a parameter related to the pore size distribution. The median value is displayed as a horizontal line. The arithmetic mean is shown as an x symbol. There were no statistically significant differences between the treatments at $p < 0.05$.

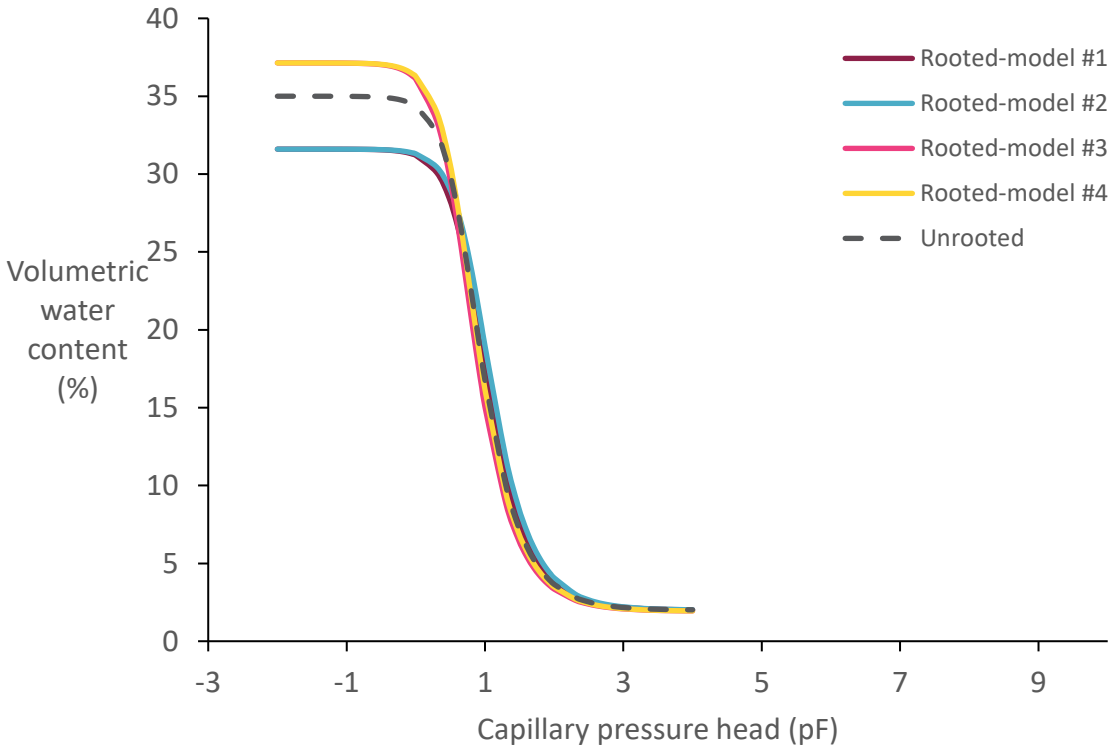

Figure 23: Proposed forward prediction models expressed as volumetric water content for sandy soil. Rooted-model 1 assumed that roots reduced porosity. Rooted-model 2 assumed that roots reduced macroporosity. Rooted-model 3 assumed that roots increased macroporosity. Rooted-model 4 assumed roots increased porosity. The y-axis is volumetric water content expressed as a percentage. The x-axis is the pressure head expressed as the base-ten logarithm of cm (pF). Forward predictions were generated from standard θ_s, θ_r, α, and n parameters from the van Genuchten equation as well as a calculated R_v value.

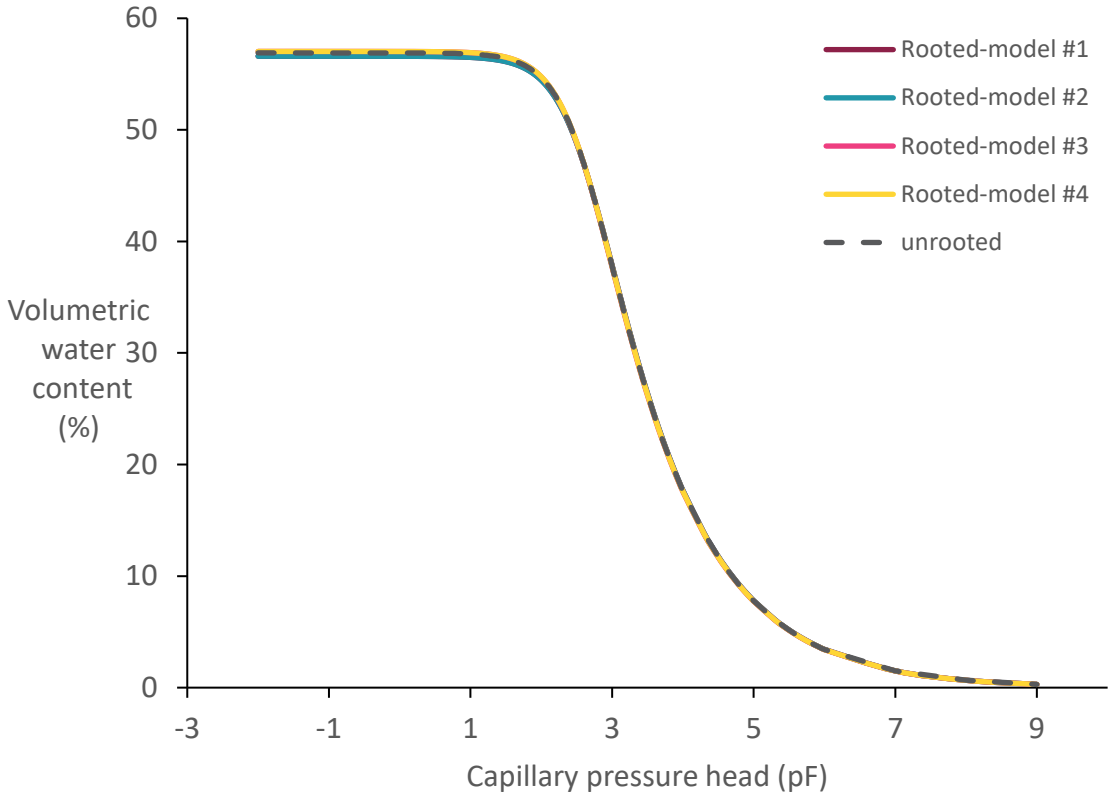

Figure 24: Proposed forward prediction models expressed as volumetric water content for Hamblen silt loam soil. For the silt loam soil, no visible difference was apparent between the models. The models were calculated so that Rooted-model 1 assumed that roots reduced porosity. Rooted-model 2 assumed that roots reduced macroporosity. Rooted-model 3 assumed that roots increased macroporosity. Rooted-model 4 assumed roots increased porosity. The y-axis is volumetric water content expressed as a percentage. The x-axis is the pressure head expressed as the base-ten logarithm of cm (pF). Forward predictions were generated from standard θ_s, θ_r, α, and n parameters from the van Genuchten equation as well as a calculated R_v value.

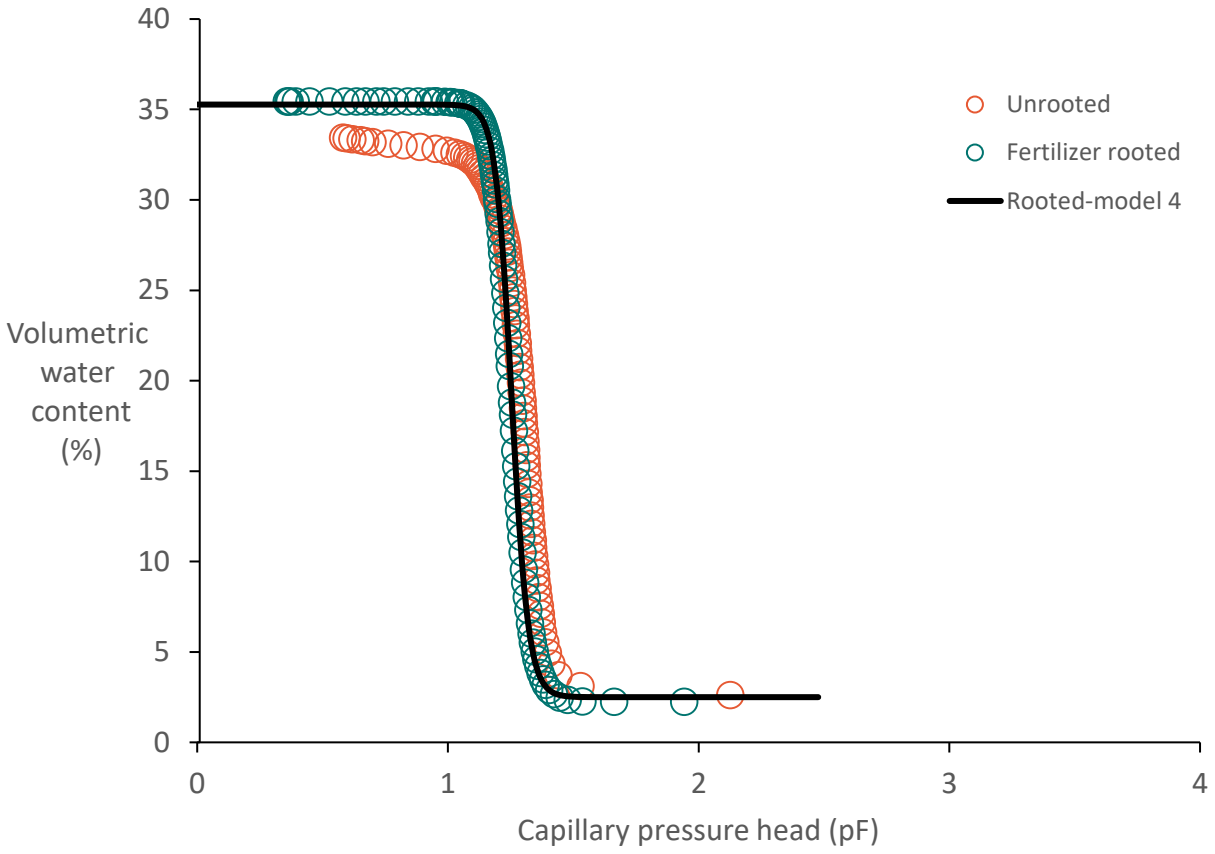

Figure 25: Forward prediction of Rooted-model 4 as compared to rooted and unrooted data for Flint sand. Unrooted and fertilizer rooted values were from single samples and chosen to show the greatest contrast between data sets. The y-axis is volumetric water content expressed as a percentage. The x-axis is the pressure head expressed as the base-ten logarithm of cm (pF). Forward predictions were generated from θ_s, θ_r, α, and n parameters from the fitting of the control data as well as the highest calculated R_v value from the fertilizer rooted treatment.

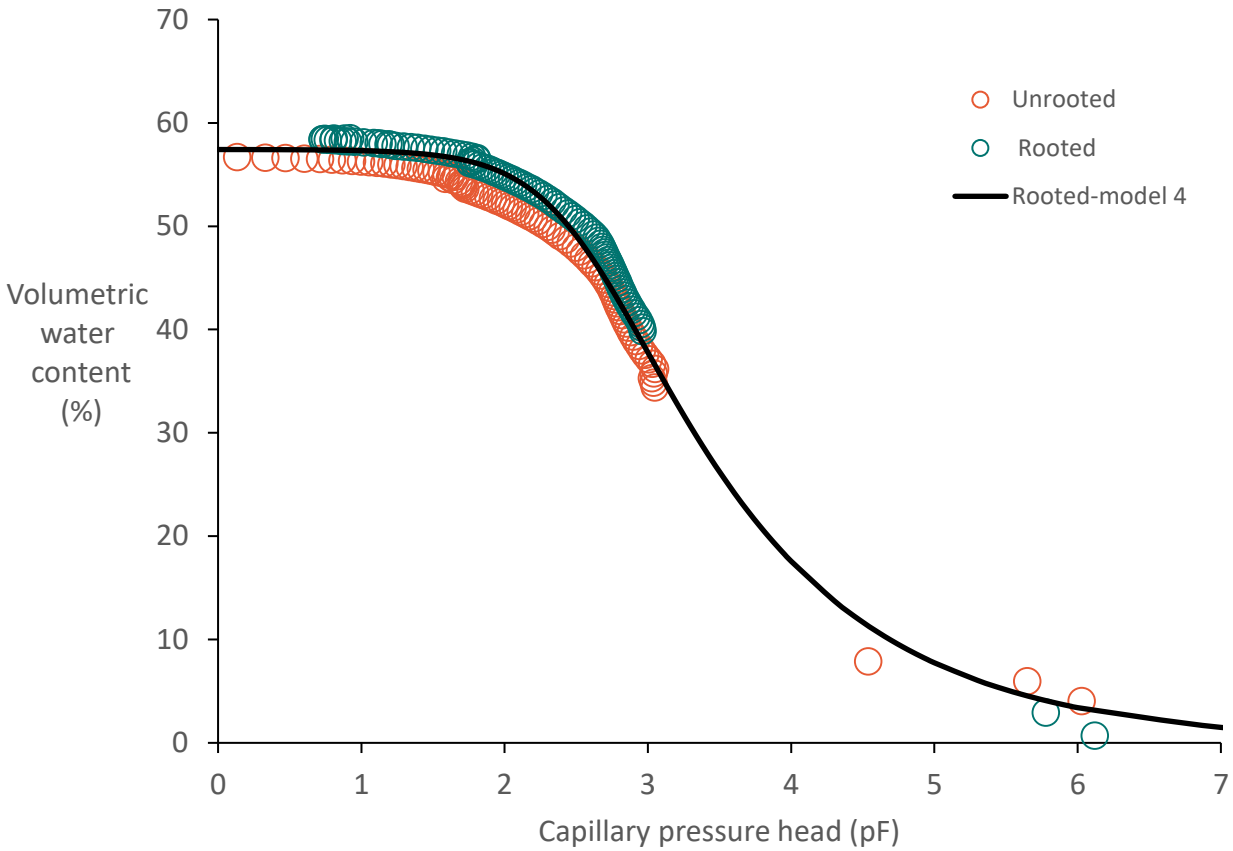

Figure 26: Forward prediction of Rooted-model 4 as compared to rooted and unrooted data for silt loam soil. Unrooted and rooted values were from single samples and chosen to show the greatest contrast between data sets. The y-axis is volumetric water content expressed as a percentage. The x-axis is the pressure head expressed as the base-ten logarithm of cm (pF). Forward predictions were generated from θ_s, θ_r, α, and n parameters from the fitting of the control data as well as the highest calculated R_v value from the rooted treatment.

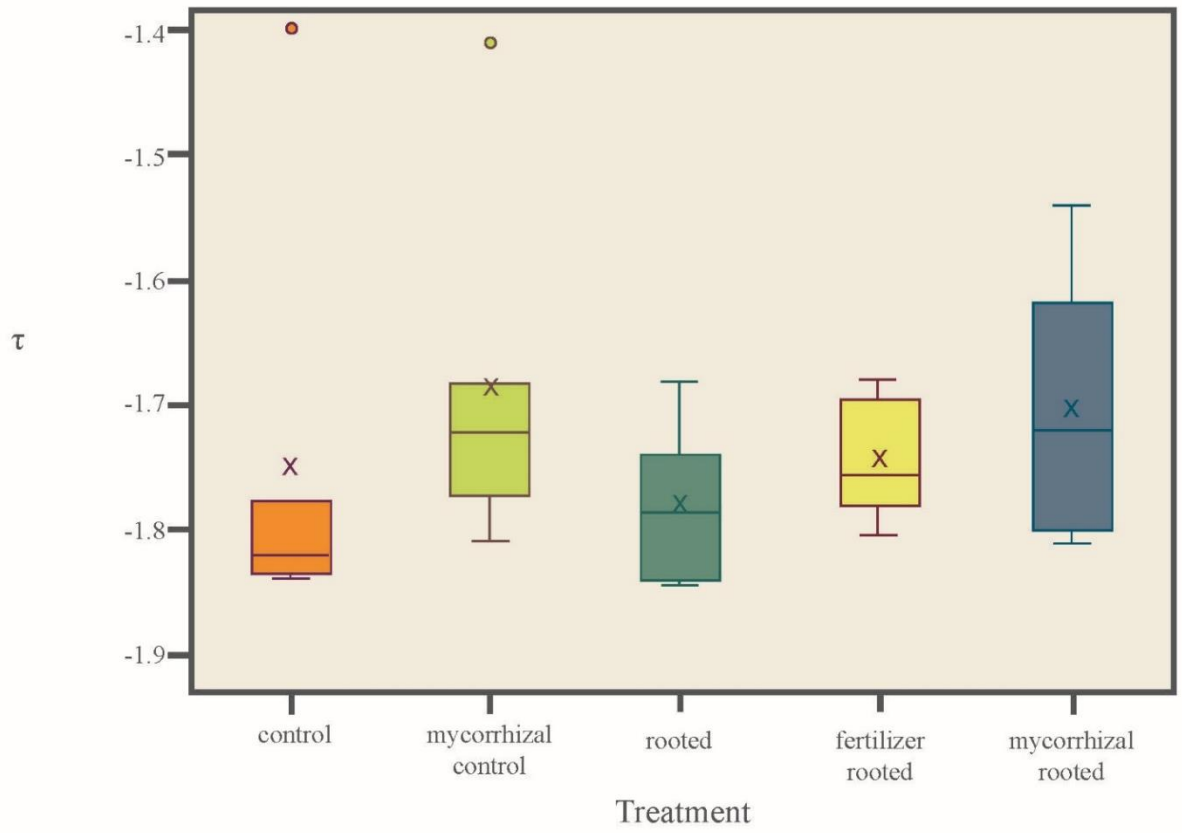

Figure 27: Boxplot for the unsaturated hydraulic conductivity curve fitting parameter τ for Flint sand. The x-axis is treatment. The y-axis is τ, an empirical parameter related to pore connectivity and tortuosity. The median value is displayed as a horizontal line. The arithmetic mean is shown as an x symbol. Outliers are represented as circles. Hinges represent the 25th and 75th percentiles of the distributions. There were no statistically significant differences between the treatments at $p < 0.05$.

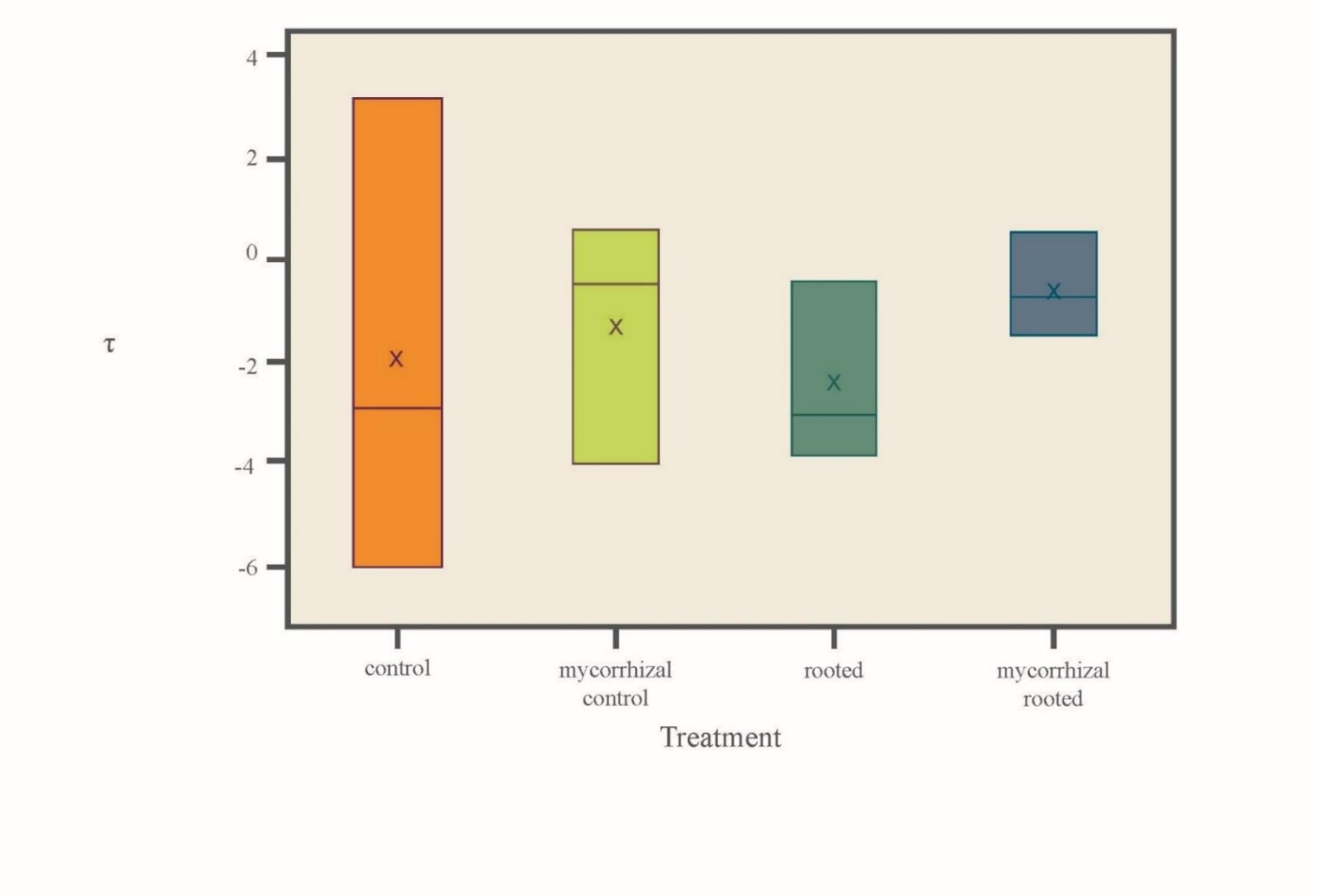

Figure 28: Boxplot for the unsaturated hydraulic conductivity curve fitting parameter τ for silt loam soil. The x-axis is treatment. The y-axis is τ, an empirical parameter related to pore connectivity and tortuosity. The median value is displayed as a horizontal line. The arithmetic mean is shown as an x symbol. There were no statistically significant differences between the treatments at $p < 0.05$.

VITA

Katelyn M. Marcacci was born to David and Jill Marcacci. She has two brothers: Henry and Michael. She attended Bishop England High School in Charleston, South Carolina, and graduated in 2013. She graduated from Clemson University in the Fall of 2017 with a Bachelor of Science degree in Geology. She was accepted into the University of Tennessee Earth and Planetary Science program in the Spring of 2018. While at UT, she studied plant-soil-water interactions under Dr. Ed Perfect and Dr. Jeff Warren. She completed her Master of Science degree in August 2020.